

**Structural analysis of the complex formed  
between the ansamycin antibiotic rifabutin and  
the BCL6 BTB-POZ domain**

Thesis submitted for the degree of  
Doctor of Philosophy  
at The University of Leicester

Sian E. Evans BSc MSc (Leicester)  
Departments of Cancer Studies and Molecular Medicine  
and Biochemistry  
University of Leicester

September 2014

*Dedicated to my little 'big' sis...x*

# **Structural analysis of the complex formed between the ansamycin antibiotic rifabutin and the BCL6 BTB-POZ domain.**

*Sian E. Evans*

## **Abstract**

BCL6 is a zinc finger transcriptional repressor that is over-expressed due to chromosomal translocations, or other abnormalities, in ~30-40% of the aggressive disease diffuse large B-cell lymphoma. BCL6 accomplishes its effects through the recruitment of co-repressors to the BTB-POZ domain of BCL6, which is a critical interaction for both a normal immune response and lymphomagenesis. Peptides or small molecule inhibitors, which prevent the association of the SMRT co-repressor with BCL6, abolish BCL6 function by attenuating its transcriptional repression. However, these agents are not yet suitable for clinical practice and there is a need to develop high-affinity and cell permeable BCL6 inhibitors.

In order to discover compounds, which have the potential to be developed into BCL6 inhibitors, a natural product library was screened, and it was found that the ansamycin antibiotic, rifamycin SV, had the ability to inhibit BCL6 transcriptional repression. NMR spectroscopy confirmed a direct interaction between rifamycin SV and the BTB-POZ domain of BCL6. In addition to rifamycin SV, NMR was used to screen other members of the ansamycin family for potential binding to BCL6. The rifamycin SV derivative, rifabutin, was also shown to interact with the BCL6 BTB-POZ domain.

A 2.3Å X-ray crystal structure of the BCL6-rifabutin complex revealed that rifabutin occupies a shallow pocket within the lateral groove, which is similar to that occupied by the SMRT binding peptide and 79-6, the previously described small molecule inhibitor. Further work employing artificial peptides showed the importance of interactions between specific residues of SMRT and the BCL6 BTB-POZ domain. The data presented in this thesis demonstrates a potentially druggable site on the BCL6 BTB-POZ domain and a unique approach to developing a structure activity relationship for a compound that will form the basis of a therapeutically useful BCL6 inhibitor

## Acknowledgements

First of all, I wish to thank to my supervisors Dr Simon Wagner and Professor John Schwabe for giving me this opportunity. I must also thank Dr Don Jones and Professor Karen Brown for their time as part of my Thesis committee. I would also like to extend my thanks to Louise Fairall and Ben Goult, who both went above and beyond during my PhD. From believing that an entire plate of crystals were actually protein, and not salt, for being a shoulder to cry on when things got tough, and for being the enthusiastic driving force behind my first, first author paper, I could not be prouder. I would also like to express my appreciation to Gregg Hudson and Peter Watson for their advice and support, and who were always happy to help. I would also like to thank all members of Professor John Schwabe's, and Dr Simon Wagner's laboratory and Cyril Dominguez for their support over the past few years.

I would especially like to thank Kath Clark and Christine Pullar for their invaluable support throughout my MSc and PhD. The time and energy both have spent helping me in these last few years does not go unnoticed.

The range of emotions that you endure throughout a PhD should not be underestimated. It has been a rollercoaster of ups and downs, fuelled by Starbucks, Costa and Cadbury's Boosts. This is my greatest achievement in life so far, and I couldn't have got through to the end if it wasn't for the amazing support and endless encouragement of the 'library crew', Lara Lewis, Eva (Mendez) Jordan and Alex Geddes. I must also thank Sharon, Kerrie and Sarah for helping me keep my head above water throughout the whole process. I also need to thank my sister Kim and my bum chum Rach 'Gay' for their love, amazing support and straight talking when things got tough, and saying things only a sister could get away with, in addition to the random texts to check that I am still alive!!

And finally, I would like to thank Paul, the one who has had to endure all of the emotions that come with a PhD, without actually doing one himself. Thanks for being there, for being the house 'pixie', and more importantly, thanks for not 'divorcing' me.

## **List of Contents**

<b>Abstract</b>	<b>iii</b>
<b>Acknowledgements</b>	<b>iv</b>
<b>List of Contents</b>	<b>v</b>
<b>Table of Contents</b>	<b>v</b>
<b>Table of Figures</b>	<b>viii</b>
<b>Table of Tables</b>	<b>x</b>
<b>Abbreviations</b>	<b>xi</b>
<b>Amino acid abbreviations and one letter codes</b>	<b>xiv</b>

## **Table of Contents**

<b>Chapter 1 - Introduction .....</b>	<b>1</b>
1.1 - Overview.....	1
1.2 - Human innate and adaptive immunity .....	1
1.3 - B-cell development and activation .....	2
1.4 - Role of BCL6 in germinal centre formation .....	2
1.5 - BCL6 gene and protein .....	6
1.6 - An overview of transcriptional regulation .....	10
1.7 - BCL6 mechanisms of transcriptional repression and its target genes.....	11
1.7.1 - Regulation of BCL6 expression in normal immunity .....	15
1.8 - Non-Hodgkin's lymphoma.....	16
1.8.1 - Risk factors for non-Hodgkin's lymphoma.....	16
1.8.2 - General overview of diffuse large B-cell lymphoma .....	17
1.9 - Why target the BCL6 BTB-POZ domain?.....	18
1.9.1 - BCL6 as a therapeutic target .....	20
1.10 - Aims .....	21
<b>Chapter 2 - Materials and Methods .....</b>	<b>22</b>
2.1 - Standard chemicals and reagents.....	22
2.2 - Buffers .....	22
2.2.1 - Protein purification .....	22
2.2.2 - 2TY Growth media for bacterial cell culture .....	23

2.2.3 - 2M9 Minimal media for use in NMR .....	23
2.2.4 - Fluorescence polarisation.....	24
2.2.5 - 2x SDS Sample buffer.....	24
<b>2.3 - Expression vectors.....</b>	<b>25</b>
2.3.1 - Oligonucleotides .....	26
<b>2.4 - Molecular Biology.....</b>	<b>26</b>
2.4.1 - Quantification of plasmid DNA .....	29
2.4.2 - Plasmid DNA sequencing .....	29
2.4.3 - Small scale purification of plasmid DNA .....	29
2.4.4 - Ethanol precipitation of DNA .....	29
<b>2.5 - Plasmid constructs.....</b>	<b>30</b>
2.5.1 - BCL6 BTB-POZ domain .....	30
2.5.2 - Peptide aptamers .....	30
<b>2.6 - Mammalian cell culture .....</b>	<b>30</b>
<b>2.7 - Protein expression and purification of bacterial culture .....</b>	<b>31</b>
2.7.1 - Bacterial culture .....	31
2.7.2 - Bacterial transformation.....	31
2.7.3 - Starter cultures and growth .....	31
2.7.4 - HIS-tagged protein purification .....	32
2.7.5 - Final stage of purification - separation of protein and affinity tag by gel filtration	33
2.7.6 - Analysis of protein purification by SDS-PAGE gel electrophoresis .....	33
2.7.7 - Protein Quantification .....	34
<b>2.8 - NMR Spectroscopy.....</b>	<b>34</b>
2.8.1 - Sample preparation .....	34
<b>2.9 - X-ray crystallography .....</b>	<b>35</b>
2.9.1 - Protein and compound preparation .....	35
2.9.2 - Non-divalent ion crystallisation plate .....	35
2.9.3 - Harvesting and cryo-cooling of crystals .....	35
2.9.4 - Data collection .....	36
<b>2.10 - Cell Titre Glo assay .....</b>	<b>36</b>
<b>2.11 - Fluorescence polarisation .....</b>	<b>36</b>
2.11.1 - Peptide synthesis .....	36
2.11.2 - Peptide coupling.....	36
2.11.3 - BODIPY labelled peptide purification.....	37
2.11.4 - Fluorescence polarisation reaction .....	37

<b>Chapter 3 - Screening potential small molecule inhibitors of the BCL6 BTB-POZ domain by NMR.....</b>	<b>38</b>
3.1 - <b>Introduction</b> .....	<b>38</b>
3.2 - <b>Results</b> .....	<b>39</b>
3.2.1 - Initial purification of the wild-type human BCL6 BTB-POZ domain.....	39
3.2.2 - Investigating the effects of different affinity tags to improve protein purification.	39
3.2.2.1 - Non-cleavable HIS tag .....	39
3.2.2.2 - GB1 solubility tag .....	40
3.2.3 - 2D ( <sup>1</sup> H- <sup>15</sup> N) TROSY of the BCL6 BTB-POZ domain.....	47
3.3 - <b>NMR studies of the interaction between BCL6 and peptide aptamers.</b> .....	<b>49</b>
3.4 - <b>Rifamycin SV interacts with the BCL6 BTB-POZ domain.</b> .....	<b>51</b>
3.5 - <b>Screening of rifamycin SV derivatives by NMR</b> .....	<b>53</b>
3.6 - <b>Investigating which residues of the BCL6 BTB-POZ domain are involved with rifamycin and rifabutin binding</b> .....	<b>57</b>
3.7 - <b>Discussion</b> .....	<b>59</b>
<b>Chapter 4 - Structure of BCL6 BTB-POZ domain in complex with rifabutin. ....</b>	<b>62</b>
4.1 - <b>Introduction</b> .....	<b>62</b>
4.2 - <b>Results</b> .....	<b>62</b>
4.2.1 - Initial crystallisation experiments .....	62
4.2.2 - Optimisation of crystallisation experiments.....	63
4.3 - <b>Structure determination</b> .....	<b>66</b>
4.3.1 - Harvesting crystals.....	66
4.3.2 - Data collection .....	66
4.3.3 - Data processing.....	69
4.3.4 - Model building and refinement.....	70
4.4 - <b>Structure of rifamycin SV in complex with the BCL6 BTB-POZ domain</b> .....	<b>71</b>
4.5 - <b>Structure of rifabutin in complex with the BCL6 BTB-POZ domain</b> .....	<b>75</b>
4.6 - <b>Rifabutin binds to the BTB-POZ domain in the same location as the co-repressor SMRT and the small molecule inhibitor, 79-6.</b> .....	<b>79</b>
4.7 - <b>Discussion</b> .....	<b>84</b>
<b>Chapter 5 - Are there specific effects of rifabutin on cellular function or co-repressor binding? .....</b>	<b>86</b>
5.1 - <b>Introduction</b> .....	<b>86</b>
5.2 - <b>Results</b> .....	<b>87</b>
5.2.1 - Investigating the effects of rifabutin and rifamycin SV on cell viability.....	87

5.2.2 - Development of a fluorescence polarisation assays to explore the ability of rifamycin SV and rifabutin to compete with SMRT for binding to BCL6.....	89
5.2.3 - Development of a substituted SMRT-BBD peptide.....	93
<b>5.3 - Discussion.....</b>	<b>98</b>
<b>Chapter 6 - Discussion and future work.....</b>	<b>102</b>
<b>Appendices 1: – Publications .....</b>	<b>108</b>
<b>References.....</b>	<b>117</b>

## **Table of Figures**

<b>Figure 1.1:</b> A schematic of the germinal centre.....	5
<b>Figure 1.2:</b> Schematic of the BCL6 protein.....	6
<b>Figure 1.3:</b> Surface representation of the BCL6 BTB-POZ domain in complex with the co-repressor SMRT.....	7
<b>Figure 1.4:</b> Sequence alignment of SMRT/NCOR2 and BCoR BCL6-binding domains (BBD).....	8
<b>Figure 1.5:</b> Crystal structure of the BCL6 BTB-POZ domain in complex with the co-repressor SMRT.....	12
<b>Figure 1.6:</b> BCL6 mediates transcriptional repression through distinct pathways.....	14
<b>Figure 1.7:</b> Potential ways to target BCL6 and abolish its transcriptional repression activity. ....	20
<b>Figure 2.1:</b> Vector maps based on the pET 30a+ backbone for bacterial protein expression provided by PROTEX at the University of Leicester. ....	25
<b>Figure 2.2:</b> Site directed mutagenesis .....	27
<b>Figure 3.1:</b> Purification of the wild-type BCL6 BTB-POZ domain expressed with a non-cleavable 6xHis affinity tag.....	41
<b>Figure 3.2:</b> Purification of the wild-type BCL6 BTB-POZ domain expressed with the GB1 solubility tag.....	42
<b>Figure 3.3:</b> 2D ( <sup>1</sup> H- <sup>15</sup> N) HSQC of the BCL6 BTB-POZ domain plus GB1.....	43
<b>Figure 3.4:</b> A chromatogram showing the A280nm protein trace of the BCL6 BTB-POZ domain produced by the de-salting column (Sephadex G-25 Fine).....	45
<b>Figure 3.5:</b> Protein purification and gel filtration of the BCL6 BTB-POZ domain. ....	46

<b>Figure 3.6:</b> 2D ( $^1\text{H}$ - $^{15}\text{N}$ ) TROSY of the BCL6 BTB-POZ domain (residues 7-128). ...	48
<b>Figure 3.7:</b> 2D ( $^1\text{H}$ - $^{15}\text{N}$ ) TROSY spectra of BCL6 in the presence of peptide aptamers L2-1 and L12-10. ....	50
<b>Figure 3.8:</b> Rifamycin SV binds to the BCL6 BTB-POZ domain.....	52
<b>Figure 3.9:</b> 2D ( $^1\text{H}$ - $^{15}\text{N}$ ) TROSY spectra for rifamycin SV derivatives (1). ....	54
<b>Figure 3.10:</b> 2D ( $^1\text{H}$ - $^{15}\text{N}$ ) TROSY-HSQC spectra for rifamycin SV derivatives (2). ...	55
<b>Figure 3.11:</b> Rifabutin binds directly to the BCL6 BTB-POZ domain. ....	56
<b>Figure 3.12:</b> Analysing the interaction between rifabutin and the BCL6 BTB-POZ domain .....	58
<b>Figure 4.1:</b> Examples of crystal forms for the BCL6 BTB-POZ domain grown in the presence of (A) rifabutin and (B) rifamycin SV. ....	64
<b>Figure 4.2:</b> Image of a BCL6 BTB-POZ domain crystal grown in the presence of rifamycin SV and the diffraction pattern produced. ....	67
<b>Figure 4.3:</b> Image of a BCL6 BTB-POZ domain crystal grown in the presence of rifabutin and the diffraction pattern produced. ....	68
<b>Figure 4.4:</b> Electron density of the BCL6 BTB-POZ domain crystallised in the presence of rifamycin SV. ....	73
<b>Figure 4.5:</b> BCL6 BTB-POZ domain crystallised in the presence of rifamycin SV. ....	74
<b>Figure 4.6:</b> Interaction of BCL6 with rifabutin. ....	77
<b>Figure 4.7:</b> Crystal packing of rifabutin in complex with the BCL6 BTB-POZ domain. ....	78
<b>Figure 4.8:</b> A comparison between SMRT, BCoR, 79-6 and rifabutin to the BCL6 BTB-POZ domain.....	81
<b>Figure 4.9:</b> Schematic diagrams of protein-ligand interactions generated from the 3D co-ordinates located within their respective PDB files.....	82
<b>Figure 4.10:</b> A comparison between the binding locations of rifabutin, SMRT and 79-6 on the BCL6 BTB-POZ domain. ....	83
<b>Figure 5.1:</b> Investigating the effects of rifamycin SV and rifabutin on cell viability....	88
<b>Figure 5.2:</b> Fluorescence polarisation assays used to investigate the ability of rifabutin and rifamycin SV to displace SMRT from the BCL6 BTB-POZ domain.....	92
<b>Figure 5.3:</b> Overlay of H1426 of SMRT and W509 of BCoR binding to the BTB-POZ domain of BCL6. ....	95
<b>Figure 5.4:</b> SMRT-BBD peptides replacing H1426 for an artificial amino acid.....	96

**Figure 5.5:** SMRT peptide containing artificial amino acids in place of H1426 to explore binding to the BCL6 BTB-POZ domain..... 97

## **Table of Tables**

<b>Table 2.1:</b> Buffers used for the purification of recombinant protein fused with a Ni-NTA affinity tag.....	22
<b>Table 2.2:</b> 2TY culture media and agar plate recipe.....	23
<b>Table 2.3:</b> 2M9 Minimal media for <sup>15</sup> N-labelled culture growth.....	23
<b>Table 2.4:</b> Fluorescence polarisation peptide coupling and reaction buffer. ....	24
<b>Table 2.5:</b> 2xSDS Sample Buffer.....	24
<b>Table 2.6:</b> A list of primers designed to produce various BCL6 BTB-POZ domain constructs including the triple surface cysteine mutant (C8Q, C67R and C84N). ....	28
<b>Table 2.7:</b> Primers designed to produce peptide aptamers .....	28
<b>Table 4.1:</b> Crystallisation hit conditions. ....	65
<b>Table 4.2:</b> Data collection and refinement statistics of the BCL6 BTB-POZ domain crystallised in the presence of rifamycin SV. ....	72
<b>Table 4.3:</b> Data collection and refinement statistics of the BCL6 BTB-POZ domain crystallised in the presence of rifabutin. ....	76
<b>Table 5.1:</b> Comparisons between the bindings of different lengths of the BBD peptides to BCL6.....	91

## **Abbreviations**

<b>aa</b>	Amino acid
<b>AID</b>	Activation induced deaminase
<b>APC</b>	Antigen-presenting cell
<b>Apt-48</b>	Aptamer 48
<b>ATR</b>	Ataxia telangiectasia and RAD3 related
<b>BACH2</b>	BTB and CNC homology 2
<b>BBD</b>	BCL6 binding domain
<b>BCL6</b>	B-cell lymphoma 6
<b>BCoR</b>	BCL6-interacting co-repressor
<b>BCR</b>	B-cell receptor
<b>BL</b>	Burkitt's lymphoma
<b>BLIMP-1</b>	B-lymphocyte induced maturation protein 1
<b>BPI</b>	BCL6 Peptide Inhibitor
<b>BSA</b>	Bovine serum albumin
<b>BTB/POZ</b>	Bric-a-brac, Tram track, Broad complex/Pox virus Zinc finger
<b>CB</b>	Centroblast
<b>CC</b>	Centrocytes
<b>CDKN1A</b>	Cyclin dependent kinase inhibitor 1A
<b>CHEK 1</b>	Checkpoint kinase 1
<b>CSR</b>	Class switch recombination
<b>CtBP</b>	C terminal binding protein 1
<b>D<sub>2</sub>O</b>	Deuterium oxide
<b>DLBCL</b>	Diffuse large B-cell lymphoma
<b>DMSO</b>	Dimethyl sulfoxide
<b>DMSO<sub>6</sub></b>	Dimethyl sulfoxide-d <sub>6</sub>
<b>DOX</b>	Doxycycline
<b>DTT</b>	Dithiothreitol
<b>EtOH</b>	Ethanol
<b>FDC</b>	Follicular dendritic cell
<b>FL</b>	Follicular lymphoma
<b>FP</b>	Fluorescence polarisation

<b>GAS</b>	Gamma activated sites
<b>GC</b>	Germinal centre
<b>GEP</b>	Gene expression profile
<b>GPS2</b>	G Protein Pathway Suppressor 2
<b>HAT</b>	Histone acetyl transferases
<b>HDAC</b>	Histone deacetylases
<b>HDACi</b>	Histone deacetylase inhibitor
<b>IL-4</b>	Interleukin-4
<b>IL-12</b>	Interleukin-12
<b>Ig</b>	Immunoglobulin
<b>LRF</b>	Leukemia/lymphoma-related factor
<b>NCoR</b>	Nuclear hormone receptor co-repressor
<b>NMR</b>	Nuclear magnetic resonance
<b>NuRD</b>	Nucleosome Remodelling Deacetylase
<b>MAD</b>	Multiple anomalous dispersion
<b>MHC II</b>	Major histocompatibility complex
<b>MIR</b>	Multiple isomorphous replacement
<b>MIZ-1</b>	Myc-interacting zinc finger protein 1
<b>MPD</b>	2-Methyl-2, 4-pentanediol
<b>MR</b>	Molecular replacement
<b>MTA3</b>	Metastasis associated 3
<b>OD<sub>600</sub></b>	Optical density at 600nm
<b>PBS</b>	Phosphate buffered saline
<b>PEG</b>	Poly-ethylene glycol
<b>PEST</b>	Proline, glutamic acid, serine and threonine
<b>PLZF</b>	Promyelocytic leukaemia zinc finger protein
<b>PRDM1</b>	PR Domain zinc finger protein 1
<b>RAG-1</b>	Recombination Activating Gene-1
<b>RAG-2</b>	Recombination Activating Gene-2
<b>RBT</b>	Rifabutin
<b>R-CHOP</b>	Rutiximab, Cyclophosphamide, Doxorubicin, Vincristine & Prednisone.
<b>RD2</b>	Repression domain 2
<b>RIF SV</b>	Rifamycin SV
<b>SDS</b>	Sodium Dodecyl Sulphate

<b>SHM</b>	Somatic Hypermutation
<b>STAT</b>	Signal Transduction and Activators of Transcription
<b>SQT</b>	Stefin-A Quadruple Mutant-Tracey
<b>SMRT</b>	Silencing Mediator of Retinoic acid and Thyroid hormone receptor
<b>TBL1</b>	Transducin $\beta$ -like Protein 1
<b>TBLR1</b>	TBL1-related protein
<b>TCEP</b>	Tris(2-Carboxyethyl)Phosphine)
<b>TE</b>	Tris, EDTA
<b>TEV</b>	Tobacco etch virus
<b>TROSY</b>	Transverse relaxation-optimised spectroscopy
<b>V(D)J</b>	Variable (Diversity) Joining
<b>ZF</b>	Zinc finger

## Amino acid abbreviations and one letter codes

Alanine	<b>A</b>	Ala	Leucine	<b>L</b>	Leu
Arginine	<b>R</b>	Arg	Lysine	<b>K</b>	Lys
Asparagine	<b>N</b>	Asn	Methionine	<b>M</b>	Met
Aspartic acid	<b>D</b>	Asp	Phenylalanine	<b>F</b>	Phe
Cysteine	<b>C</b>	Cys	Proline	<b>P</b>	Pro
Glutamine	<b>Q</b>	Gln	Serine	<b>S</b>	Ser
Glutamic acid	<b>E</b>	Glu	Threonine	<b>T</b>	Thr
Glycine	<b>G</b>	Gly	Tryptophan	<b>W</b>	Trp
Histidine	<b>H</b>	His	Tyrosine	<b>Y</b>	Tyr
Isoleucine	<b>I</b>	Ile	Valine	<b>V</b>	Val

# Chapter 1 - Introduction

## 1.1 - Overview

Lymphomas are malignant proliferations of mature lymphocytes, which are cells of the immune system responsible for adaptive immunity. Some proteins regulating the normal immune response are, therefore, important in lymphomagenesis. B-cell lymphoma 6 (*BCL6*) is a key oncogene involved in the normal immune system and in the development of diffuse-large B-cell lymphoma (DLBCL). The main goal of cancer therapy is to specifically target and kill cancer cells, whilst leaving normal cells unharmed. Conventional chemotherapy regimens are often associated with significant toxicities therefore; there is a need to develop targeted treatments and therapies. In this section, the function of *BCL6* within the immune system, its role in the development of DLBCL and ways in which *BCL6* can be targeted will be explored.

## 1.2 - Human innate and adaptive immunity

The human immune system is a multi-layered defence mechanism, responsible for protection against infections. The first layer of defence is the innate immune system, also known as the non-specific immune system (Chaplin 2010). The skin or mucous membranes e.g. in the lungs or intestine, provide a physical barrier component of protection to prevent micro-organisms from entering the human body. Within the human body, macrophages and neutrophils are responsible for the removal and destruction of antigens, including micro-organisms, by phagocytosis. Complement proteins are also an important component of innate immunity and help to protect against circulating micro-organisms (Markiewski *et al.* 2007; Sjöberg *et al.* 2009). Complex organisms can develop specific immunity to micro-organisms throughout life, and these immune responses are activated, upon re-exposure to the same antigen i.e. there is immune memory. These features of specificity and memory are characteristic of acquired immunity and require B- and T-cells. Macrophages and follicular dendritic cells (FDC), which are the professional antigen presenting cells, (APC), display antigen derived from the micro-organisms at the cell surface, in association with the major histocompatibility complex II (MHC II), to activate T-cells (Abbas *et al.* 2012). Naïve

T-cells recognising antigen in the context of MHC and responding to interleukin 4 (IL-4) and 12 (IL-12) released from the APC, differentiate to effector T-cells e.g. T-helper 1 and T-helper 2 cells. T-helper 2 cells secrete IL-4 and IL-5 leading to the activation of antigen specific B-cells within secondary lymphoid organs, such as lymph nodes. B-cells are responsible for antibody production, which is a crucial factor in neutralising circulating or extracellular micro-organisms. The transcription factor BCL6 plays a key role in B-cell development, and is crucial to the production of high affinity antibodies.

### **1.3 - B-cell development and activation**

Early B-cell development occurs in the bone marrow and is complete once a B-cell precursor (an immature B-cell) has productive rearrangements of the immunoglobulin (Ig) heavy and light chains, to produce a functional antibody molecule, which when associated with the B-cell surface is known as a B-cell receptor. An antibody molecule consists of two heavy and two light chains and rearrangement requires the recombination activating genes 1 and 2 (RAG-1 and RAG-2). B-cells are then selected on the basis of a functional B-cell receptor (BCR) and a lack of affinity for self. B-cells that possess a functional BCR become a mature naïve B-cell and leave the bone marrow, whereas B-cells that react with self or fail to produce a BCR undergo apoptosis (Goodnow *et al.* 1988). Mature B-cells traffic to the secondary lymphoid organs where they encounter T-cells (as described in section 1.2) and on activation, move to the primary B-cell follicles where they undergo intense proliferation to form a germinal centre (GC) (MacLennan 1994).

### **1.4 - Role of BCL6 in germinal centre formation**

GCs are transient structures that form in secondary lymphoid organs. The biological functions of GCs are to provide an environment where B-cells undergo genetic alterations within the Ig genes by a process known as somatic hypermutation (SHM), in order to produce high affinity antibodies. By light microscopy, GCs consist of two main compartments, a dark zone and a light zone. The dark zone comprises rapidly proliferating B-cells known as centroblasts (CB). SHM, which requires the activation induced deaminase (AID) enzyme to introduce base pair mutations into the antibody

genes, within the hyper-variable regions, takes place at this stage (Kuppers *et al.* 1993). CBs are then believed to migrate into the light zone where they become centrocytes (CC) (Liu *et al.* 1996). CCs then undergo selection through interactions with follicular dendritic cells (FDC)s and T-cells in the light zone. Those that produce a self-interacting or a low-affinity BCR for the antigen undergo apoptosis, but cells that have acquired high-affinity for the presenting antigen will differentiate into either a plasma cell or a memory B-cell and exit the GC (Liu *et al.* 1996; Epstein *et al.* 1999). Class switch recombination (CSR), a somatic recombination mechanism also requiring AID, which mediates isotype switching from IgM to IgG, IgA or IgE, thereby changing antibody effector function, also occurs at this stage (Klein & Dalla-Favera 2008).

B-cell lymphoma 6 (*BCL6*), a gene originally cloned from a chromosomal translocation in the human disease diffuse-large B-cell lymphoma (DLBCL), was found to be expressed in GC B-cells, but not in naïve B-cells or terminally differentiated plasma cells (Ye, Rao *et al.* 1993b; Ye, Lista *et al.* 1993a; Baron *et al.* 1993; Kerckaert *et al.* 1993; Bunting *et al.* 2013). The pivotal role of *BCL6* in GC formation was demonstrated in transgenic and knockout mice. Mice bearing homozygous disruptions of the *BCL6* locus were unable to form GCs, produce high-affinity antibodies and proceeded to develop an inflammatory response in multiple organs characterised by the infiltration of eosinophils (Fukuda *et al.* 1997; Dent *et al.* 1997; Ye *et al.* 1997). By contrast, mice that were engineered to constitutively express *BCL6* had enlarged GCs and progressed to develop a disease similar to human DLBCL (Cattoretti *et al.* 2005).

The function of *BCL6* has been investigated *in vitro*. Constitutive expression in a mouse cell line model of B-cell differentiation showed that *BCL6* allowed proliferation and repressed differentiation (Reljic *et al.* 2000) probably by repressing expression of B-lymphocyte induced maturation protein 1, (*BLIMP-1*), which is required for terminal B-cell differentiation (Tunyaplin *et al.* 2004). *BCL6* also attenuates the expression of genes involved in the DNA damage response, inhibits cell cycle arrest and cell death. For example, *BCL6* represses p53 (Phan *et al.* 2004), cyclin dependent kinase inhibitor 1A (*CDKN1A*) (Phan *et al.* 2005), ataxia telangiectasia and *RAD3* related (*ATR*) (Ranuncolo *et al.* 2007), and checkpoint kinase 1 (*CHEK 1*) (Ranuncolo *et al.* 2008), providing an environment which allows the rapid proliferation of B-cells whilst simultaneously attenuating DNA damage sensing proteins. This combination of

features may be important to allow the GC B-cells to tolerate genomic instability generated from SHM and CSR occurring during the production of high-affinity antibodies (Figure 1.1).

The expression of BCL6 is down regulated at the end of the GC reaction, to allow the expression of BLIMP-1, for terminal differentiation of B-cells into either an antibody secreting plasma cell or a memory B-cell. Malignant transformation of B-cells can be associated with both early and later stages of B-cell development. Constitutive expression of BCL6 within GC B-cells allows uncontrolled proliferation and prevents terminal differentiation, due to the continued repression of BLIMP-1. The continuous proliferation caused by BCL6 is believed to be a major reason for its importance in lymphomagenesis.

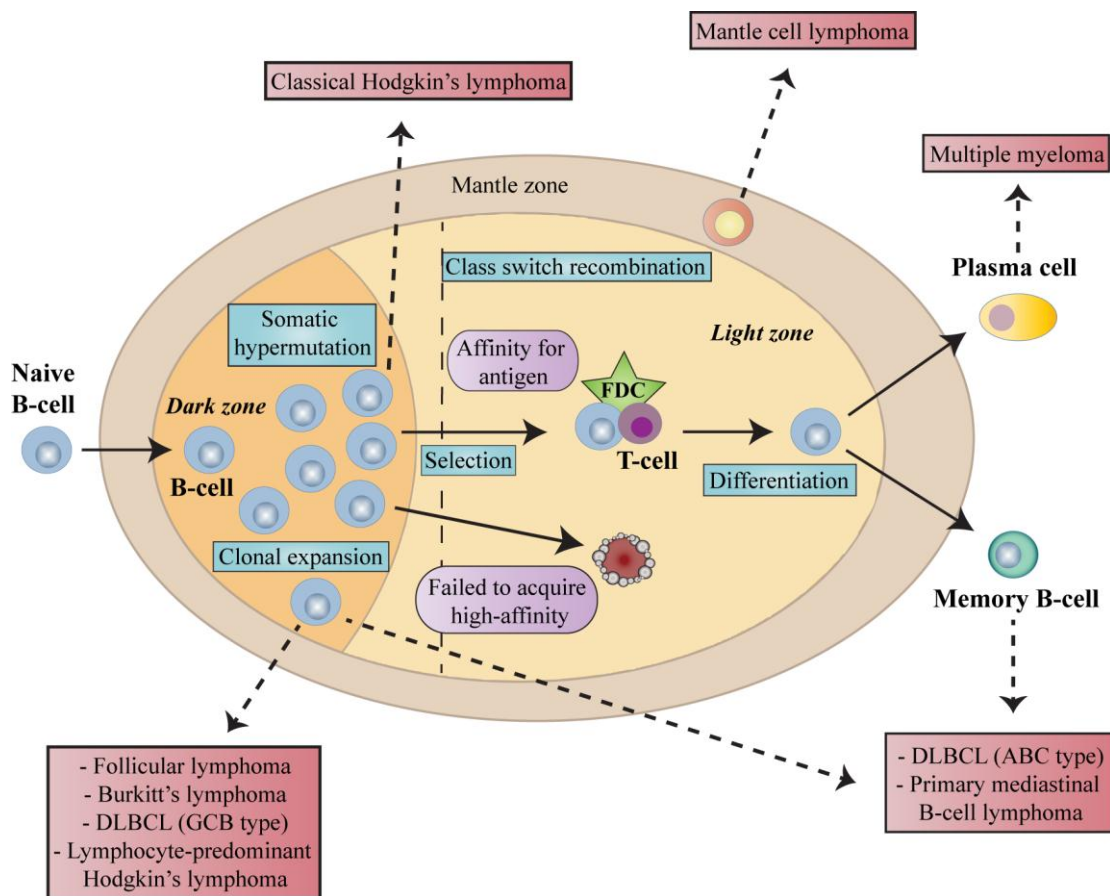


**Figure 1.1: A schematic of the germinal centre.**

Mature naïve B-cells move to primary B-cell follicles in secondary lymphoid organs such as the lymph nodes, where upon activation by T-cells undergo intense proliferation to form a germinal centre (GC). Naïve B-cells are replaced by rapidly proliferating B-cells and are displaced to the outside of the follicle where they form the mantle zone. The GC comprises of two main compartments, the dark zone and the light zone. The dark zone contains B-cells termed centroblasts (CB), which simultaneously undergo somatic hypermutation (SHM) and rapid proliferation. CBs then migrate to the light zone where they become centrocytes (CC). CCs then undergo selection through the interaction of follicular dendritic cells (FDC) and T-cells in addition to enduring class switch recombination (CSR). B-cells that have acquired affinity for the presenting antigen further differentiate into plasma cells or memory B-cells and exit the GC, those B-cells that have lack affinity or have acquired affinity for self undergo apoptosis. Red boxes illustrate examples of disease, which can arise from different stages of the GC reaction. Adapted from Küppers *et al.* 2005.

## 1.5 - BCL6 gene and protein

The *BCL6* gene, also known as BCL5 and LAZ3, was originally cloned in 1993, from a t(3;14) chromosomal translocation affecting band 3q27 associated with DLBCL (Offit *et al.* 1989; Bastard *et al.* 1992; Baron *et al.* 1993; Ye, Rao, *et al.* 1993b; Ye, Lista, *et al.* 1993a; Kerckaert *et al.* 1993). *BCL6* was subsequently found to be involved in chromosomal translocations in ~30-40% of DLBCL and 5-10% of follicular lymphoma (FL) (Coco *et al.* 1994; Ye *et al.* 1995; Butler *et al.* 2002). In DLBCL, *BCL6* is found to be constitutively expressed either due to chromosomal translocations fusing the *BCL6* coding region with heterologous promoters, or point mutations within the negative auto-regulatory circuit (Cattoretti *et al.* 2005).

*BCL6* is a 706 amino acid zinc finger transcription factor with a molecular weight of 95 kDa (Chang *et al.* 1996). It is a sequence specific transcriptional repressor encoding three distinct functional domains; an N-terminal BTB-POZ domain, a less well-defined central repression domain (RD2) and six *Krüppel*-like C<sub>2</sub>H<sub>2</sub> zinc fingers at the C-terminal (Figure 1.2).

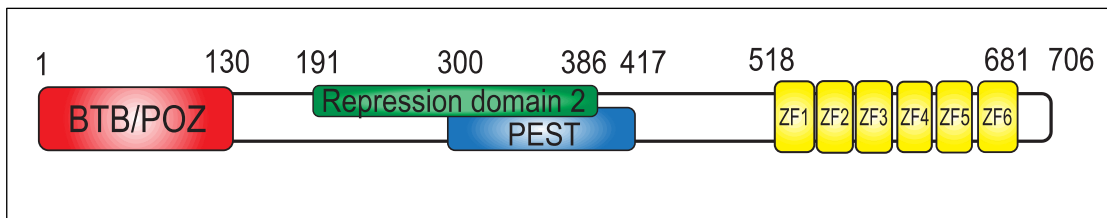


**Figure 1.2: Schematic of the BCL6 protein.**

*BCL6* encodes an N-terminal BTB-POZ domain (red) (1-130aa) known to mediate homodimerisation and heterodimerisation with other BTB-POZ domain containing proteins in addition to protein-protein interactions with co-repressors such as SMRT, NCoR and BCoR). A region known as the repression domain 2 (RD2) located at the centre of *BCL6* (green) (191-386aa), which also encodes a KKYK (K-lysine, Y-tyrosine) motif (375-379aa), overlapped with a PEST domain (blue) (300-417aa) to regulate *BCL6* protein stability and six *Krüppel*-like C<sub>2</sub>H<sub>2</sub> zinc fingers at the C-terminus (yellow) (518-541, 546-568, 574-596, 602-624, 630-652 and 658-681aa) for sequence specific DNA binding.

The BTB-POZ domain is a highly evolutionary conserved protein-protein interaction motif, consisting of around 130 amino acids, and is present in viruses and throughout eukaryotes (Bardwell & Treisman 1994; Albagli *et al.* 1995; Stogios *et al.* 2005; Perez-Torrado *et al.* 2006). The BTB-POZ domain was named after the *Drosophila* zinc finger transcription factors: Bric-à-brac, Tramtrack, and Broad Complex/Pox Virus Zinc Finger (Bardwell & Treisman 1994) and is present in 5-10% of all zinc finger proteins (Zollman *et al.* 1994; Ahmad *et al.* 1998). BCL6 forms a homodimer through interactions mediated by the BTB-POZ domain, but can also heterodimerise to other BTB-POZ containing proteins such as promyelocytic leukaemia zinc finger (PLZF) (Dhordain *et al.* 2000) and Myc-interacting zinc finger protein-1 (Miz-1) (Phan *et al.* 2005). Upon dimerisation, two symmetrical extended lateral grooves are produced, creating docking sites for the co-repressor proteins Silencing Mediator of Retinoic acid and Th thyroid hormone receptor (SMRT), Nuclear hormone receptor Co-Repressor 1 (NCoR1) (Dhordain *et al.* 1997; Dhordain *et al.* 1998; Huynh & Bardwell 1998; Ahmad *et al.* 2003) and BCL6-interacting Co-Repressor (BCoR) (Huynh *et al.* 2000; Ghetu *et al.* 2008) (Figure 1.3).

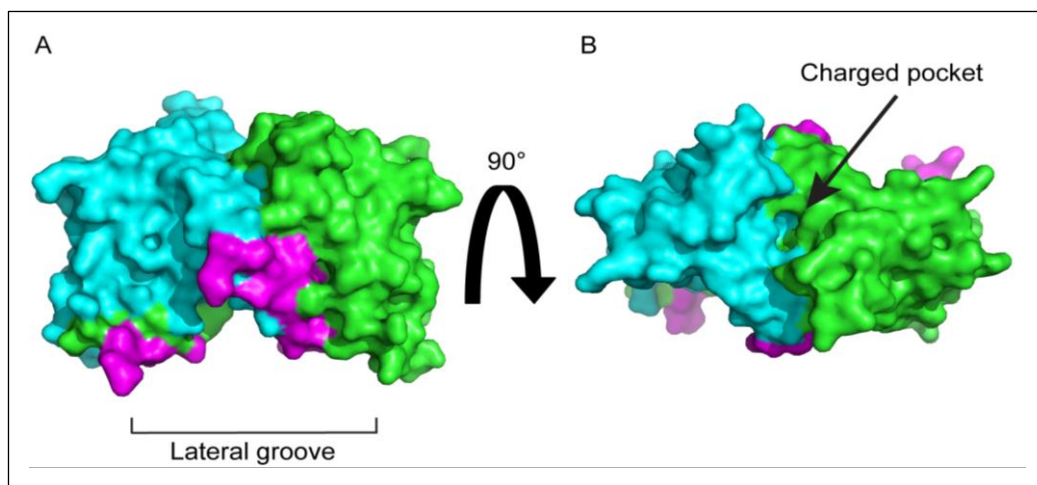


**Figure 1.3: Surface representation of the BCL6 BTB-POZ domain in complex with the co-repressor SMRT.**

BCL6 has the ability to homodimerise with itself and heterodimerise with other BTB-POZ domain containing proteins, such as PLZF, for transcriptional repression of its target genes via the BTB-POZ domain. Each dimer comprises of two monomers, coloured cyan and green. (A) An extensive hydrophobic groove is formed by two monomers upon dimerisation. Two SMRT peptides bind within the lateral groove as shown by the magenta surface representation (Ahmad *et al.* 2003). (B) Rotation by 90° from (A) exposes a charged pocket at the top of the dimer, formed by two  $\alpha 3/\beta 4$  loops. This has previously been the target of peptide aptamer interaction to antagonise BCL6 (Chattopadhyay *et al.* 2006).

SMRT and NCoR are large homologous proteins with an overall sequence identity of 40% (Chen *et al.* 1995; Hörlein *et al.* 1995). SMRT (also known as NCoR2), NCoR (also known as NCoR1) and BCoR bind to the BCL6 BTB-POZ domain in a mutually exclusive manner. All three co-repressor proteins bind to a common exposed surface, known as the lateral groove, by means of a 17 amino acid sequence termed the BCL6 binding domain (BBD) (Ahmad *et al.* 2003; Ghetu *et al.* 2008). The BBD of SMRT and NCoR share an almost identical sequence, whereas the BBD of BCoR possesses a completely different primary sequence (Figure 1.4), yet all three proteins bind to the lateral groove through both common interactions and different specific interactions with the BCL6 BTB-POZ domain (Ahmad *et al.* 2003; Ghetu *et al.* 2008). The residues that line the surface of the BCL6 lateral groove and mediate the interactions with the co-repressors are not conserved within the BTB family, and are therefore unique to BCL6 (Ahmad *et al.* 2003). In addition, SMRT and NCoR BBDs do not interact with other BTB-ZF repressors such as PLZF or leukemia/lymphoma-related factor (LRF) (Stogios *et al.* 2006).



**Figure 1.4: Sequence alignment of SMRT/NCoR2 and BCoR BCL6-binding domains (BBD).**

The BCL6-binding domains (BBD) of SMRT and NCoR2 each utilise an almost identical sequence for binding to the lateral groove of the BTB-POZ domain of BCL6. In comparison, BCoR lacks sequence similarity within its BBD motif. Grey shading indicates the five residues that form similar side chain contacts with the BCL6 BTB-POZ domain in relation to sequence similarity (I/V, W/H) or identity (P, S) between SMRT/NCoR2 and BCoR. (.) Indicates conservation between groups of weakly similar properties. Amino acid residues are coloured according to their physiochemical properties: Red (Small, hydrophobic), Blue (Acidic), Magenta (Basic), Green (Hydroxyl, Sulphydryl and amine). Sequence alignment was produced using Clustal Omega.

The central region of BCL6 is thought to be largely unstructured and contains a second repression domain, termed repression domain 2 (RD2), (residues 191-386). Recent work has suggested that the RD2 domain spans a 45 amino acid region (350-395) characteristic of the minimal region required to exhibit the same repressive effect as full length RD2 (Huang *et al.* 2014). It has been reported that the RD2 domain interacts with histone deacetylase II (HDAC II), metastasis associated 3/Nucleosome Remodelling Deacetylase (MTA3/NuRD) complex and C terminal binding protein 1 (CtBP) (Bereshchenko *et al.* 2002; Fujita *et al.* 2004; Mendez *et al.* 2008; Huang *et al.* 2014).

Within the RD2 domain lays a PEST domain, encompassing a functionally important KKYK motif susceptible to acetylation. The KKYK motif resembles a site on p53 which is acetylated by p300 (Gu & Roeder 1997), and p300 is also responsible for the acetylation of the KKYK motif of BCL6 (Bereshchenko *et al.* 2002). HDAC II and MTA3, which forms part of the Mi2/NuRD complex, (Mendez *et al.* 2008), binds to RD2 in an acetylation-dependent manner, and becomes dissociated from BCL6 when the KKYK motif becomes acetylated (Bereshchenko *et al.* 2002; Fujita *et al.* 2004). The recruitment of MTA3 to the RD2 domain is essential for the ability of BCL6 to inhibit plasma differentiation (Parekh *et al.* 2007). Both the RD2 and PEST domains are thought to play a role in BCL6 transcriptional repression and regulation of protein stability.

The C-terminal domain of BCL6 consists of six *Krüppel*-like C<sub>2</sub>H<sub>2</sub> zinc fingers (ZF) (residues 518-681) enabling BCL6 to target DNA in a sequence specific manner in addition to interacting with several proteins for nuclear targeting (Masclé *et al.* 2002). The site that seems to have the highest affinity for BCL6 binding is a 9 bp core sequence (TTCCTA/CGGA). Point mutation studies have shown that the roles of each of the six ZFs of BCL6 are not equal in function in regards to DNA-binding activity, for example; removal of the last two ZF domains abolished DNA binding and ZFs 3-6 are found to be required for the repressive activity of BCL6, whereas ZF1 and ZF2 do not participate in this activity (Masclé *et al.* 2002). The BCL6 DNA binding sequence has specific homology to a binding site at the promoter region of signal transduction and activators of transcription (STAT) transcription factors, which mediate cytokine signalling (Dent *et al.* 1997). STAT transcription factors recognise the gamma

activated sites (GAS) motif, (Schindler *et al.* 1995) which bears a resemblance to the BCL6 DNA binding site (Dent *et al.* 2002). BCL6 also interacts with the mid-region of the co-repressor eight-twenty-one (ETO), (residues 217-379) through its C-terminal ZFs and is believed to enhance HDAC activity during BCL6 transcriptional repression (Chevallier *et al.* 2004).

## **1.6 - An overview of transcriptional regulation**

The regulation of gene expression is a tightly controlled process orchestrated by many signalling processes and protein complexes. The nucleosome, a crucial component of chromatin, consists of two H2A/H2B dimers and a H3/H4 tetramer, surrounded by 146 bp of DNA, which tightly wraps around the histone octamer approximately 1.67 times (Beato & Eisefeld 1997). The packaging of the DNA around the nucleosomes represents an important factor in regulating gene expression. The regulation of gene activation and repression are mostly controlled by protein-protein interactions and post-translational modifications, leading to changes in chromatin structure induced by DNA methylation, chromatin remodelling and histone modifications of the amino-terminal tails, of which, lysine acetylation is the best characterised. In general, transcriptional repression is associated with low levels of histone acetylation, due to the removal of acetyl groups from lysine residues on histone tails by histone deacetylases (HDACs), therefore maintaining the DNA in a compact and inaccessible conformation, resulting in the prevention of transcription factors binding to their recognition sites (Wolffe 1994). In contrast, transcriptional activation is associated with high levels of acetylation, due to the transfer of acetyl groups onto the exposed lysine residues present on the histone tails by histone acetyl transferases (HATs), as a result, neutralising the positive charge of the lysine and reducing the interaction with DNA, leading to a relaxed chromatin conformation for the accessibility of transcription factors for gene transcription (Legube *et al.* 2003; De Ruijter *et al.* 2003; Villagra *et al.* 2010).

## 1.7 - BCL6 mechanisms of transcriptional repression and its target genes

HATs and HDACs exist within multi-subunit protein complexes to control transcriptional regulation. Many HDACs that aid BCL6 mediated transcriptional repression are either recruited directly to BCL6 (Lemercier *et al.* 2002) or indirectly through interactions with co-repressor complexes (Wong & Privalsky 1998; Huynh *et al.* 2000). Core components of the SMRT/NCOR repression complex consists of HDAC3, transducing  $\beta$ -like 1/ TBL related 1 (TBL1/TBLR1) and G-protein pathway suppressor 2 (GPS2) (Li *et al.* 2000; Jinsong Zhang *et al.* 2002; Oberoi *et al.* 2011; Watson *et al.* 2012). Transcriptional repression mediated by the interaction between SMRT and the BTB-POZ domain of BCL6 has been investigated in detail. The crystal structure of the BCL6 BTB-POZ domain in complex with SMRT has been solved (Ahmad *et al.* 2003). The main body of the BCL6 BTB-POZ domain dimer is made up of a cluster of  $\alpha$ -helices flanked by  $\beta$ -sheets at both the top and the bottom of the molecule (Figure 1.5). The N-terminus of one monomer makes an anti-parallel  $\beta$ -sheet with the  $\beta$ 5 strand of the other monomer. There are substantial contacts made between the two BCL6 BTB-POZ domain monomers upon dimerisation, these include  $\beta$ 1,  $\alpha$ 1,  $\alpha$ 2,  $\beta$ 5 and  $\alpha$ 6. There are two main obvious features of the BCL6 BTB-POZ domain, the first is a charged pocket at the top of the dimer formed by the two- $\alpha$ 3/ $\beta$ 4 loops, and secondly, an extensive hydrophobic groove formed at the dimer interface by  $\beta$ 1/ $\alpha$ 6'/ $\beta$ 1'/ $\alpha$ 6 ('denotes second monomer) at the "bottom" of the dimer. Two SMRT peptides (residues 1414-1430) bind to the BCL6 BTB-POZ domain in an extended conformation along a shallow groove, known as the lateral groove, formed at the dimer interface. Each SMRT peptide makes extensive contacts with both chains of the BTB-POZ domain. The N-terminal amino acids of the SMRT peptide introduce an additional parallel strand to the  $\beta$ 1/ $\beta$ 5 sheet (Ahmad *et al.* 2003; Ghetu *et al.* 2008; Watson *et al.* 2012).

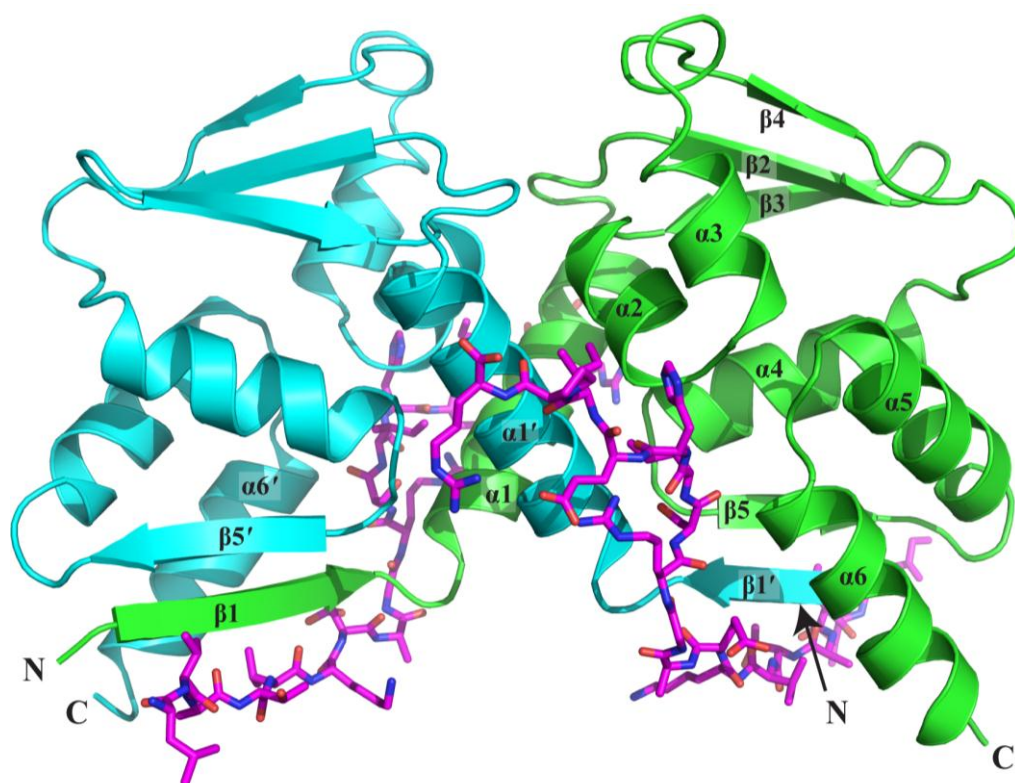


**Figure 1.5: Crystal structure of the BCL6 BTB-POZ domain in complex with the co-repressor SMRT.**

Cartoon representation of the BCL6 BTB-POZ domain dimer (cyan and green) co-crystallized with SMRT peptides (1414-1430) (magenta). Two SMRT peptides bind within the lateral groove, with the N-terminal amino acids of the SMRT peptide introducing an additional parallel strand to the  $\beta 1/\beta 5$  sheet (PDB ID: 1R2B) (Ahmad *et al.* 2003).

Repression through the BTB-POZ domain has been shown to regulate genes involved in survival and proliferation such as ATR (Ranuncolo *et al.* 2007), p53 (Phan *et al.* 2004), CDKN1A (Phan *et al.* 2005) and CHEK1 (Ranuncolo *et al.* 2008). Several groups have shown that perturbing the BTB-POZ/SMRT interaction with peptides or small molecule inhibitors leads to the re-expression of these genes and ultimately cell death. The first peptide inhibitor designed to perturb the BTB-POZ/SMRT interaction was based upon the SMRT BBD motif and termed BCL6 peptide inhibitor (BPI). The BPI also included an N-terminal pTAT sequence which enabled membrane permeability, a hemagglutinin tag for immunodetection and (HIS)<sub>6</sub> tag for use in purification. Although the BPI was specifically able to block BCL6-mediated recruitment of SMRT, and as a result, reactivate BCL6 target genes in addition to preventing the formation of GC *in vivo*, it

was highly unstable and required frequent re-administration (Polo *et al.* 2004; Privé *et al.* 2006). Following on from the BPI design, a 9 residue SMRT peptide (GRSIHEIPR) was synthesised in the retroinverso (RI) configuration. Retroinverso peptides are peptides whose amino acid sequence is reversed; in this case for example, the RI sequence is RPIEHISRG. In addition, they are generally composed of amino acids in the D-configuration to enable increased resistance to proteolytic degradation leading to a peptide with increased stability. It was reported that RI-BPI had greater potency when compared to the original BPI (Cerchietti *et al.* 2009).

A slightly different approach taken to inhibit BCL6 function came in the form of peptide aptamers. Peptide aptamers are proteins that have their amino and carboxy terminus anchored in a specific conformation, producing a protein scaffold. The advantage of a protein scaffold is that it can reduce the range of conformations of a particular sequence of amino acids, therefore increasing specificity of binding. Aptamer 48 (Apt-48) binds to the BCL6 BTB-POZ domain in a manner distinctly different to that used by SMRT. Apt-48 binds to a small charged pocket formed upon dimerisation and was shown to relieve BCL6 mediated repression (Figure 1.3) (Chattopadhyay *et al.* 2006).

The most recent attempt at designing a BCL6 inhibitor comes in the form of a small molecule, 79-6. Computer aided drug design (CADD) was used to search *in silico* chemical databases of commercially available drug-like compounds based upon the crystal structures of BCL6 in complex with the SMRT BBD and BCoR BBD (Cerchietti *et al.* 2010a). The crystal structures indicated specific regions of SMRT and BCoR, residues 1423–1428 and 506–511 respectively, that were involved in key molecular interactions with the residues that line the BCL6 lateral groove. Alanine scanning mutagenesis of this region revealed that these residues are required for the stability of the BCL6-SMRT complex (Ahmad *et al.* 2003; Ghetu *et al.* 2008), and therefore, this region was chosen for the use of CADD to identify compounds with the potential to bind to BCL6 (Cerchietti *et al.* 2010a). Like the peptides and the peptide aptamer preceding it, 79-6 was able to reactivate critical BCL6 target genes in BCL6 dependent DLBCL cell lines with almost no effect on BCL6 independent cell lines, and more importantly, it was specific to the BTB-POZ domain of BCL6 and so does not inhibit other BTB-POZ transcriptional repressors (Cerchietti *et al.* 2010a).

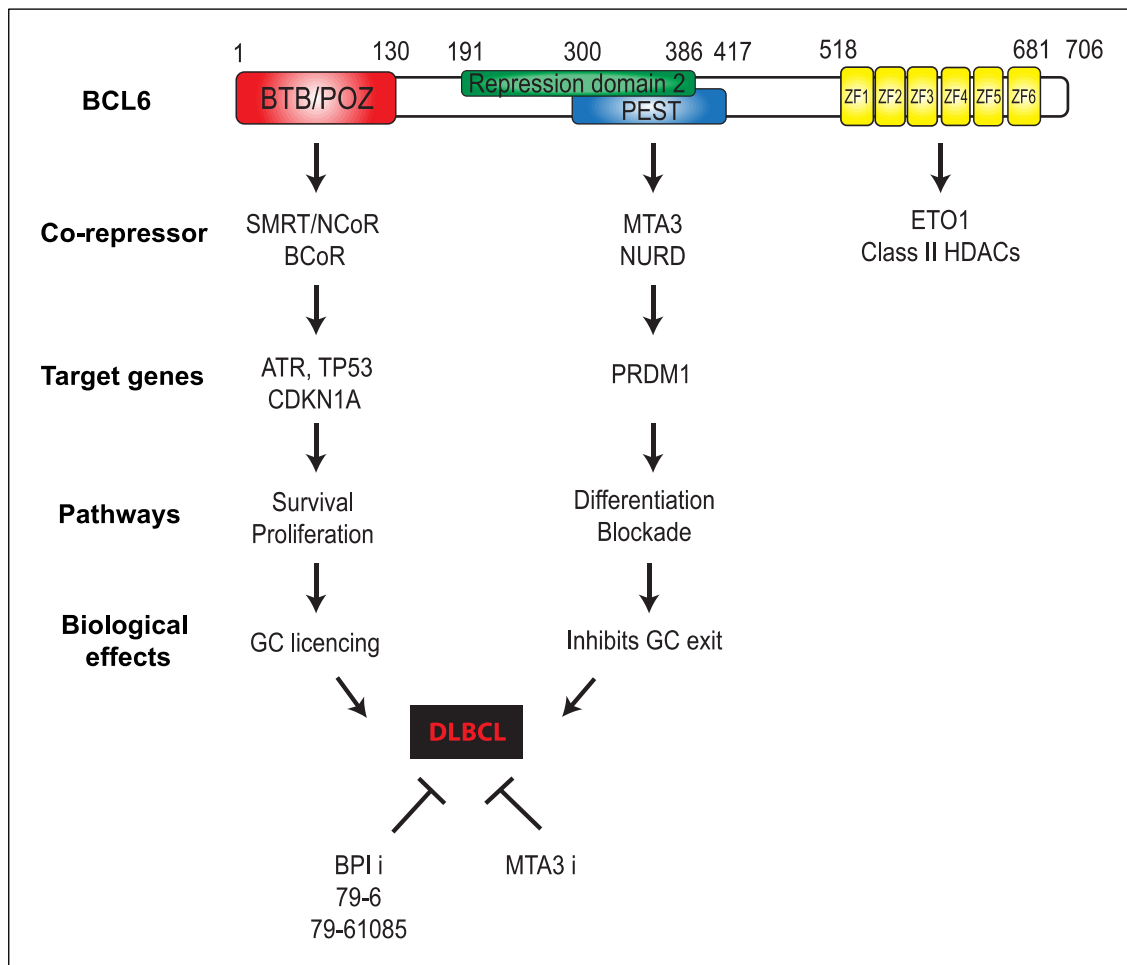


**Figure 1.6: BCL6 mediates transcriptional repression through distinct pathways.** BCL6 mediates its transcriptional repression through two repression domains, the BTB-POZ domain and the RD2 domain. Co-repressors SMRT, NCoR and BCoR are recruited to BCL6 through the BTB-POZ domain and mediate the repression of ATR, TP53 and CDKN1A, which are involved in cellular proliferation and survival. Recruitment of MTA3/NuRD complex to the RD2 domain mediates the repression of PRDM1 and blocks differentiation of B-cells to plasma cells or memory B-cells and exit from the GC, therefore contributing to lymphomagenesis. The ETO co-repressor and class II HDACs interact with the C-terminal ZFs. Inhibitors of each pathway are indicated by BPI-i, 79-6, 79-61085 and MTA3-i. Adapted from Parekh *et al.* 2007.

The BCL6 DNA binding sequence (TTCCTA/CGGA) resembles the motif recognised by the STAT-family of transcription factors (Seyfert *et al.* 1996; Dent *et al.* 1997; Shaffer *et al.* 2000), suggesting that some cytokine response genes may be targets of BCL6 repression (Dent *et al.* 1997; Gupta *et al.* 1999; Harris *et al.* 1999). Due to the similarity in DNA binding sequence between BCL6 and STATs, studies have shown that they can have opposing effects on gene regulation. The activity of STAT6 can be

repressed by BCL6 through binding to GAS within the promoter of CD23b and repress STAT mediated function (Dent *et al.* 1997; Gupta *et al.* 1999). In contrast, STAT5 has been shown to regulate the expression of BCL6 by binding to its first exon, which contains a negative auto-regulatory site, leading to the down-regulation of BCL6 expression, resulting in the re-expression of BCL6 target genes (Walker *et al.* 2007).

BCL6 has also been implicated in a range of other important processes and is estimated to regulate ~485 target genes (Polo *et al.* 2007) such as:

- *B-cell activation* (involving CD69 and CD44) (López-Cabrera *et al.* 1995; Camp *et al.* 1991)
- *B-cell differentiation* (Blimp-1) and *inflammation* (MIP-1 $\alpha$  and IP-10) (Krzysiek *et al.* 1999)
- *Cell cycle regulation* (involving p27kip1 and cyclin D2) (Solvason *et al.* 1996; Shaffer *et al.* 2000).

### **1.7.1 - Regulation of BCL6 expression in normal immunity**

As anticipated for a key regulatory gene there are both transcriptional and post-transcriptional mechanisms to tightly control the expression of BCL6 during GC development. The first exon of BCL6 contains a negative auto-regulatory BCL6 binding site (Pasqualucci *et al.* 2003; Wang *et al.* 2002). When BCL6 levels rise above a threshold occupancy for this binding site it represses transcription possibly through a mechanism involving CtBP (Mendez *et al.* 2008; Papadopoulou *et al.* 2010). BCL6 down-regulation is key for normal plasma cell differentiation and antibody responses. IRF4 is activated by CD40 signalling to down-regulate BCL6 in an NF- $\kappa$ B dependent manner (Saito *et al.* 2007) and this may be a critical step in allowing plasma cell differentiation at the end of the germinal centre response when a high affinity antibody has been produced.

At the protein level, interactions between antigen and the B-cell receptor (on completion of the germinal centre response) trigger the MAP kinase-mediated phosphorylation of BCL6, which in turn, leads to the degradation of BCL6 by the ubiquitin proteasome pathway (Niu *et al.* 1998; Saito *et al.* 2007). In addition, BCL6 is also targeted for ubiquitylation and degradation by FBXO11 (Duan *et al.* 2012).

Post-translational modifications such as acetylation, methylation and phosphorylation have been shown to regulate BCL6 expression. The KKYK motif located within the PEST/RD2 domains of BCL6 is the main site of acetylation by p300 (Bereshchenko *et al.* 2002). Acetylation of BCL6 abolishes BCL6-mediated transcriptional repression by interfering with the association of HDAC repression complexes

## **1.8 - Non-Hodgkin's lymphoma**

B-cell lymphomas are malignant cellular proliferations that can arise from various stages of normal B-cell development. Around 90% of lymphomas are of B-cell origin with the remaining 10% being T-cell malignancies. Around 15 types of B-cell lymphoma are defined in the WHO 2001 (Küppers 2005). NHL (all subtypes) is the sixth most common cancer in the UK, the fifth most common cancer in males and the seventh in females. Around 12,800 new cases of NHL were registered in the UK in 2011, with 4,646 deaths. Lymphomas can be grouped into those, which are clinically aggressive, and those that follow a more indolent course. The most common of the clinically aggressive NHL subtypes is diffuse large B-cell lymphoma (DLBCL), which accounts for around 48% of cases. Marginal zone lymphomas and follicular lymphomas make up 20% and 19% respectively of NHL but are indolent diseases (HMRN, 2014). The more clinically aggressive subtypes are treated with combination chemotherapy. With modern treatments, around 60% of patients are alive at 5 years following diagnosis, with the remainder dying either because disease resists treatment or because of the severe toxicities of chemotherapy i.e. neutropaenic sepsis.

### **1.8.1 - Risk factors for non-Hodgkin's lymphoma**

The incidence of NHL has risen steadily for several decades, and the reason behind this is unclear. Nevertheless, survival has improved over the last four decades due to the introduction of new combinations of chemotherapy and the addition of the anti-CD20 monoclonal antibody, rituximab, with 50.8% of patients expected to survive longer than 10 years, compared with only 27.8% of those diagnosed in the early 1970's (Shankland *et al.* 2012). One known risk factor for the development of NHL is suppression of the

immune system. It is known that patients with HIV have an increased risk of developing high-grade non-Hodgkin lymphoma. Other contributing factors are organ-transplant recipients and those with autoimmune disease especially if they are on long term immunosuppressive treatments (Shankland *et al.* 2012). An association between viral infections other than HIV and the development of NHL has been observed, primarily because of the involvement of the immune system. The Epstein-Barr virus is associated with Burkitt lymphoma and some types of T-cell lymphoma, and infections by bacteria such as *Helicobacter pylori* have been shown to be a risk factor for gastric mucosa-associated lymphoid tissue lymphoma (Craig *et al.* 2010).

### **1.8.2 - General overview of diffuse large B-cell lymphoma**

Although DLBCL is an aggressive form of lymphoma, remission can be achieved with the standard treatment of chemotherapy and immunotherapy, known as R-CHOP (Rituximab, Cyclophosphamide, Doxorubicin, Vincristine and Prednisolone), however, around 30% of patients are likely to die of their disease. One obstacle to successful treatment of DLBCL lies in the clinical heterogeneity, revealed by gene expression profiling (GEP). DLBCL comprises of at least three distinct subtypes, each having a different gene expression signature (Alizadeh *et al.* 2000). Germinal centre B-cell like (GCB) DLBCL is derived from GC B-cells, defined by the high expression levels of a number of GC markers including BCL6 and CD10. Activated B-cell (ABC) DLBCL is believed to derive from cells involved in the later stages of the GC reaction, such as plasma cell differentiation and is associated with the expression of MUM1 and IRF4. The third type, which is much less common, is primary mediastinal large B-cell lymphoma (PMBCL) (Alizadeh *et al.* 2000; Savage *et al.* 2003).

The t(3;14) chromosomal translocation involving BCL6 is the most common in DLBCL and involves a reciprocal exchange of genetic material between 3q27 (the region containing the BCL6 locus) and the immunoglobulin heavy chain locus on chromosome 14. This results in BCL6 being brought under the regulation of the immunoglobulin heavy chain enhancer to cause constitutive expression. A variety of other genetic mechanisms leading to BCL6 over-expression have subsequently been discovered e.g. mutations in the exon 1 auto-regulatory region of the BCL6 promoter (Pasqualucci *et al.*

2003; Wang *et al.* 2002), mutations in acetyl transferases (Cerchiotti *et al.* 2010b; Pasqualucci *et al.* 2011) and failure of BCL6 degradation (Duan *et al.* 2012). Collectively the numerous mechanisms resulting in BCL6 over-expression show that this critical regulator of normal immunity also has an essential role in lymphomagenesis.

## 1.9 - Why target the BCL6 BTB-POZ domain?

The regulation of many complex biological processes is essentially driven by DNA-protein and protein-protein interactions. Transcription factors are attractive therapeutic targets since their aberrant expression has been implicated in numerous malignancies. Nonetheless, it has been widely considered that targeting transcription factors can prove challenging as they mediate their functions through protein:protein/DNA interactions rather than enzymatic activities. This is thought to limit the effectiveness of current screening technologies in identifying small compounds suitable for targeting protein-protein interactions such as AML1-ETO (Darnell 2002; Majmudar *et al.* 2005; Koehler 2010). However, this obstacle can be overcome by use of techniques such as X-ray crystallography and NMR as they can provide information regarding the modes of binding and potential binding sites for small molecule inhibitors. STAT3 is an example of a transcription factor currently targeted by a small platinum containing compound, CPA7 (Turkson *et al.* 2004; Kortylewski *et al.* 2005; Redell *et al.* 2006).

Transcription factors such as BCL6 elicit their effects through the recruitment of HDAC containing repression complexes. HDACs can also be therapeutically targeted, and there are many HDAC inhibitors currently available within the clinic such as Trichostatin A (TSA) for the treatment of acute promyelocytic leukaemia (APL), characterised by the presence of fusion proteins PML-RAR $\alpha$  and PLZF-RAR $\alpha$  (Lin *et al.* 1998; Villa *et al.* 2006; Zhang *et al.* 2014). There is also particular interest in employing these compounds for the treatment of T-cell lymphomas. Suberoyl anilide hydroxamic acid (SAHA) is both a class I and class II HDAC inhibitor, and is used for the treatment of cutaneous T-cell lymphoma (CTCL) (Marks *et al.* 2007; Duvic *et al.* 2007). However, targeting HDAC's will produce off-target effects owing to their association with many transcription factors.

The structure of the BCL6 BTB-POZ domain has been analysed in great detail, especially when in complex with SMRT and BCoR. Early work first demonstrated the importance of this domain due to its association with HDACs via an interaction with co-repressors (Dhordain *et al.* 1997; Dhordain *et al.* 1998).

The lateral groove formed upon homodimerisation provides a unique docking site for the co-repressors SMRT and BCoR. Work leading to the solution of the X-ray co-crystal structure of the SMRT binding peptide and the BCL6 BTB-POZ domain (Ahmad *et al.* 2003) demonstrated that a relatively short peptide was responsible for binding. This suggested that the peptide could be utilised as a tool to study BCL6 function by competing for binding to the BCL6 BTB-POZ domain with SMRT. Such a peptide proved to be highly effective in causing apoptosis of BCL6 dependent B-cell lines, appeared not to interfere with function of other BTB-POZ domain containing proteins and also abrogated normal antibody responses to immunisation in mice (Polo *et al.* 2004). Targeting the co-repressor binding site appears to be a half-way house with more specific effects being observed than when targeting HDACs, in addition, this would be more manageable than targeting other portions of the protein such as the dimerisation interface (Figure 1.7).

Research by others has shown that BCL6 is able to mediate repression by utilising two distinct biological pathways through; 1) BTB-POZ and 2) the RD2 domain. The BTB-POZ domain is known to repress genes associated with proliferation and survival, whereas, the RD2 domain, via the recruitment of MTA3, a component of the Mi-2/NuRD repression complex, is known to control terminal differentiation within the GC. Blockade of RD2 induced targets of differentiation, such as BLIMP-1, but did not decrease viability of DLBCL cells (Parekh *et al.* 2007). Therefore, targeting the co-repressor binding site may be favourable if the indications for inhibiting BCL6 are malignancies characterised by a high proliferation rate.

BCL6 is required for the development of some subsets of T-helper cells (Nurieva *et al.* 2009) suggesting that complete disruption of BCL6 may abolish T-cell as well as B-cell function and would therefore cause major impairment of immunity and consequently induce risk of infection. Recent work (Huang *et al.* 2013) employing mice bearing

knock-in mutations of the BCL6 BTB-POZ domains to abrogate function, demonstrated that BTB-POZ domain function was not required for T-cells, but was for B-cells. This, therefore, increases the potential usefulness of inhibiting co-repressor binding to treat B-cell lymphomas.

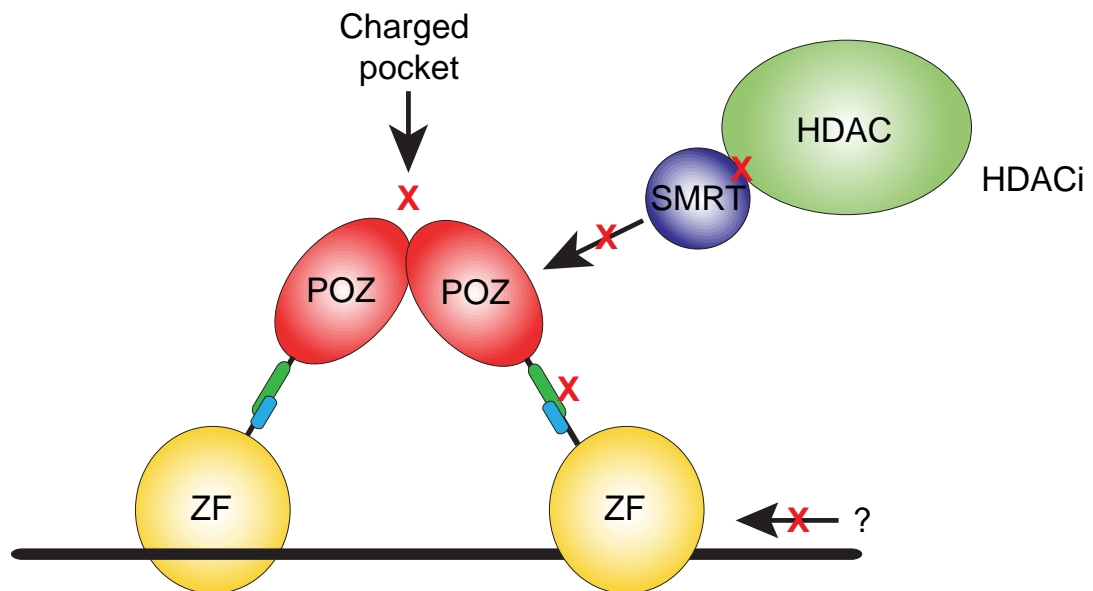


**Figure 1.7: Potential ways to target BCL6 and abolish its transcriptional repression activity.**

BCL6 has the ability to regulate two distinct biological pathways; therefore, inhibitors aimed at the two main repression domains (BTB-POZ and RD2) have been designed to down-regulate BCL6 transcriptional repression activity. Peptides based upon the SMRT BBD bind within the lateral groove of the BTB-POZ domain. Computer assisted drug design has been used to develop a small molecule inhibitor, 79-6 to perturb SMRT binding.

### 1.9.1 - BCL6 as a therapeutic target

There is a considerable amount of evidence showing that BCL6 plays a vital role in the development of lymphoma due in part to its constitutive expression observed in ~30-40% of DLBCL. BCL6 is not only involved in chromosomal translocations, but is also over expressed in DLBCL through mutation of a negative regulatory site in the promoter region, and by failure of mechanisms to degrade the protein i.e. mutations in acetyl transferases and a deubiquitinase.

Preventing the interaction between the co-repressors, SMRT and BCoR with the BTB-POZ domain of BCL6, has been the main focal point for the design of peptide inhibitors and small molecules, suggesting that this site may be suitable for drug discovery. Targeting this site would appear to have some advantages; firstly, T-cell function will not be affected as it seems that inhibiting the BTB-POZ domain only affects B-cells (Huang *et al.* 2013), and secondly, residues lining the lateral groove are unique to BCL6 suggesting the possibility of developing inhibitors that will be relatively specific for BCL6 whilst sparing other BTB-POZ domain proteins.

## **1.10 - Aims**

The aims of the work carried out in this thesis were to screen compounds for their potential as BCL6 BTB-POZ domain binders and to observe their effects as possible inhibitors of the BCL6 BTB-POZ domain biological function. Firstly, in order to accomplish this, the purification of recombinant BCL6 BTB-POZ domain will be optimised. NMR spectroscopy will be utilised to screen compounds for their ability to bind to the BCL6 BTB-POZ domain, and any interactions observed will then be further explored by X-ray crystallography. Compounds found to interact with the BCL6 BTB-POZ domain will subsequently be investigated for their potential to exert an effect on cell viability in BCL6 dependent cell lines.

## Chapter 2 - Materials and Methods

### 2.1 - Standard chemicals and reagents

Unless otherwise stated all chemicals and reagents were of analytical grade and were purchased from Sigma-Aldrich or Fisher Scientific.

### 2.2 - Buffers

#### 2.2.1 - Protein purification

<b>Lysis Buffer</b>	50mM	Tris, pH 8.5
	300mM	NaCl
	20mM	Imidazole
	5mM	Dithiothreitol (DTT)
	0.1% (v/v)	Triton X-100
	1	Roche complete protease inhibitor/50ml
<b>Wash Buffer</b>	50mM	Tris, pH 8.5
	300mM	NaCl
	20mM	Imidazole
	5mM	Dithiothreitol (DTT)
<b>Elution Buffer</b>	50mM	Tris, pH 8.5
	300mM	NaCl
	300mM	Imidazole
	10mM	EDTA
	5mM	Dithiothreitol (DTT)
<b>NMR Buffer pH6</b>	50mM	Sodium phosphate, pH6
	300mM	NaCl
	5mM	Dithiothreitol (DTT)

**Table 2.1: Buffers used for the purification of recombinant protein fused with a Ni-NTA affinity tag.**

## 2.2.2 - 2TY Growth media for bacterial cell culture

<b>2TY (1L)</b>	16g	Tryptone
	10g	Yeast extract
	5g	NaCl
<b>2TY agar (1L)</b>	15g	Agar
	8g	NaCl
	10g	Tryptone
	5g	Yeast extract

**Table 2.2: 2TY culture media and agar plate recipe.**

Make each up to 1L with dH<sub>2</sub>O. Once autoclaved, 2TY agar was allowed to cool prior to the addition of appropriate antibiotics swirled gently to mix and poured into culture plates.

## 2.2.3 - 2M9 Minimal media for use in NMR

<b>Solution A: (1L) (Made up with ddH<sub>2</sub>O)</b>	Na <sub>2</sub> HPO <sub>4</sub>	12.5g
	KH <sub>2</sub> PO <sub>4</sub>	7.5g
<b>Solution B (for 1L of solution A) (Made up with ddH<sub>2</sub>O)</b>	dH <sub>2</sub> O	10ml
	BME vitamins	10ml
	Glucose	4g
	1M CaCl <sub>2</sub>	0.1ml
	1M MgSO <sub>4</sub>	2ml
	Kanamycin	1ml of 50mg/ml
	<sup>15</sup> N NH <sub>4</sub> Cl	1g

**Table 2.3: 2M9 Minimal media for <sup>15</sup>N-labelled culture growth.**

Solution B was prepared in an autoclaved beaker. Glucose was added ‘bit by bit’ to the water/BME vitamin solution, stirring constantly to prevent the glucose solidifying. Solution B was then sterilised using a 0.2µm filter prior to addition to solution A.

## 2.2.4 - Fluorescence polarisation

<b>Peptide coupling</b>	25µl	1mM peptide
	0.625µl	0.05% v/v Triton X-100
	12.5µl	0.4M Sodium phosphate, pH6
	6µl	17.78mM Bodipy
	0.5µl	0.5M TCEP
	205.5µl	dH <sub>2</sub> O
<b>Reaction Buffer</b>	0.01% (v/v)	Triton X-100
	0.1mg/ml	BSA
	1x	PBS

**Table 2.4: Fluorescence polarisation peptide coupling and reaction buffer.**

## 2.2.5 - 2x SDS Sample buffer

<b>2x SDS Sample Buffer</b>	20% (v/v)	Glycerol
	70mM	Tris pH 6.8
	0.54mg/ml	Bromophenol Blue
	2%	SDS
	200mM	DTT

**Table 2.5: 2xSDS Sample Buffer.**

## 2.3 - Expression vectors

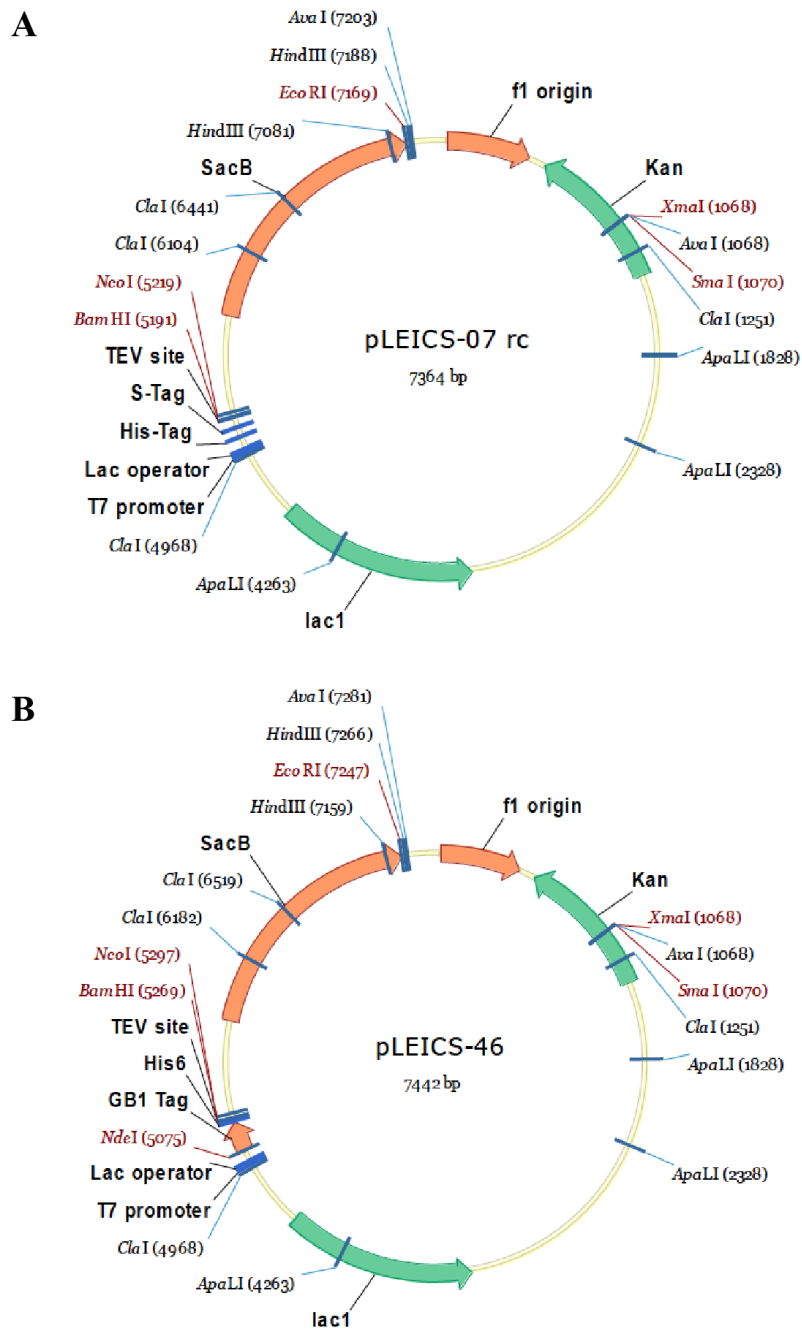


**Figure 2.1: Vector maps based on the pET 30a+ backbone for bacterial protein expression provided by PROTEX at the University of Leicester.**

pLEICS-7 encodes a cleavable 6xHistidine residue affinity tag followed by a Tobacco etch virus (TEV) protease cleavage site. pLEICS-46 encodes an immunoglobulin-binding domain of streptococcal protein G (GB1 solubility tag), followed by 6xHistidine residues, and a TEV cleavage site. Both provide kanamycin resistance.

### **2.3.1 - Oligonucleotides**

Primers/oligonucleotides were designed using EnzymeX software (Mekentosj) for mutagenesis and sub-cloning of the BCL6 BTB-POZ domain and peptide aptamers (Tables 2.6 and 2.7). Oligonucleotides were purchased from Eurofins MWG Operon with High Purity Salt Free (HPSF) purification and synthesised at the 0.01 $\mu$ M scale. Oligonucleotides were re-suspended in ddH<sub>2</sub>O.

### **2.4 - Molecular Biology**

The DNA template of the wild-type human BCL6 BTB-POZ domain (residues 7-128) and peptide aptamers L2-1 and L12-10 was provided by Dr Simon Wagner and Dr Paul Ko Ferrigno (Table 2.7). All cloning, including site directed mutagenesis was performed by the PROTEX (protein expression laboratory) facility at the University of Leicester. Vectors used within this project were also provided by PROTEX (Figure 2.1).

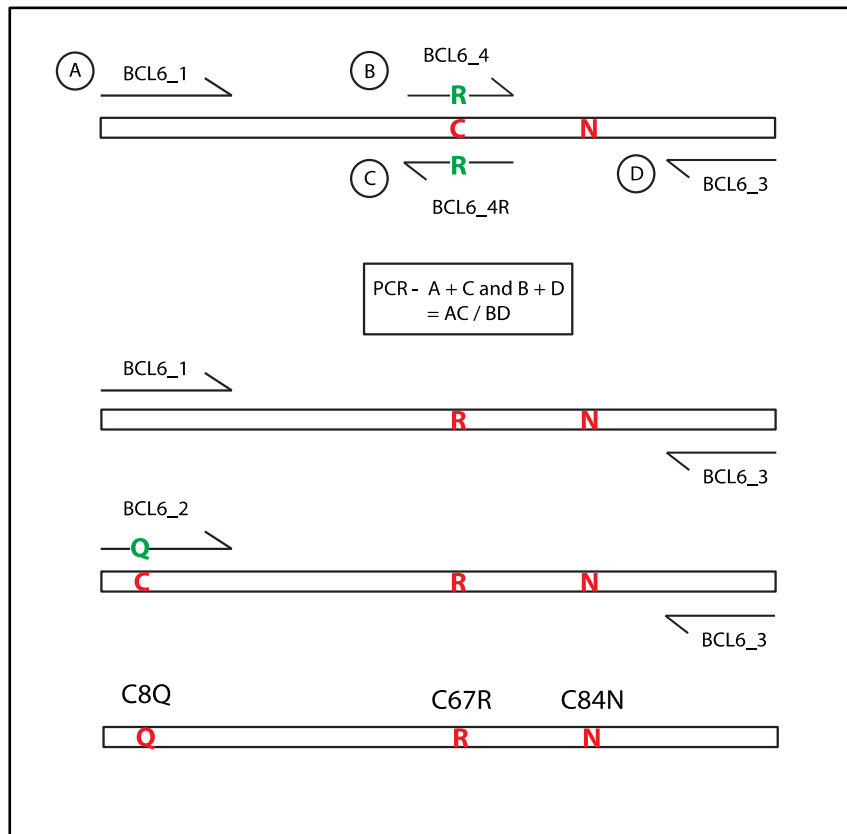


### Figure 2.2: Site directed mutagenesis

Site directed mutagenesis was performed by PROTEX to introduce surface cysteine mutations into the BCL6 BTB-POZ domain. Mutagenic primers were designed using to contain the required mutation. In the case of the BCL6 BTB-POZ domain, a construct containing C84N already existed. This was used as a template to incorporate both the C8Q and C67R mutation as shown above. All primers were designed using EnzymeX software.

	Primer Sequence	Function
BCL6_1	GTATTTTCAGGGCGCCAGCTGTATCCAGTTCACCCGC	Wild-type N-terminus beginning at residue Ser-7 (S)
BCL6_2	GTATTTTCAGGGCGCCAGCCAGATCCAGTTCACCCGCCATGCC	Mutant N-terminus beginning at residue Ser-7 incorporating C8Q mutation
BCL6_3	GACGGAGCTCGAATTCTAACTGGCCTTAATAAACTTCCG	Wild-type C-terminus ending at residue Ser-128
BCL6_4	TAGCATCTTTACAGACCAGTTGAAACGCAACCTTAGTGTG	Produces the C67R substitution
BCL6_4R	CACACTAAGGTTGCGTTTCAACTGGTCTGTAAAGATGCTA	Produces the C67R substitution
BCL6_5	GATCAACCCTGAGGGATTCAACATCCTCCTGGACTTCATG	Produces the C84N substitution
BCL6_5R	CATGAAGTCCAGGAGGATGTTGAATCCCTCAGGGTTGATC	Produces the C84N substitution

**Table 2.6: A list of primers designed to produce various BCL6 BTB-POZ domain constructs including the triple surface cysteine mutant (C8Q, C67R and C84N).**

Aptamer	Template	Forward Primer	Primer Sequence	Reverse Primer	Primer Sequence	Protein Sequence
L2-1 (1-106 aa)	L2-1	L12-3_SE_1	GTATTTTCAG GGCGCCATGA TACCTAGGGG CTTATCT	L12- 2_SE_2	GACGGAGCTCGAAT TCTAAAAGCCCGTC AGCTCGTCATC	MIPRGLSEAKPATPEIQEIVDKVK PQLEEKTNETYGKLEAVQYKTQV LASTNYYIKVRAGDNKYMHLKV FKSLT <b>WTIVLKTRSHD</b> ADRVLV GYQVDKNKDDDELTF
L12-10 (1-112 aa)	L12-10	L12-3_SE_1	GTATTTTCAG GGCGCCATGA TACCTAGGGG CTTATCT	L12- 2_SE_2	GACGGAGCTCGAAT TCTAAAAGCCCGTC AGCTCGTCATC	MIPRGLSEAKPATPEIQEIVDKVK PQLEEKTNETYGKLEAVQYKTQV LA <b>RNSQVL</b> STNYYIKVRAGDNK YMHLKVFKSLT <b>RCTLSNPFLH</b> ADRVLVGYQVDKNKDDDELTF

**Table 2.7: Primers designed to produce peptide aptamers**

Sequences in red indicate the peptide sequences inserted into the structural loops of the SQT backbone.

### **2.4.1 - Quantification of plasmid DNA**

DNA concentration was determined spectrophotometrically using a NanoPhotometer (IMPLEN) according to manufacturer's instructions.

### **2.4.2 - Plasmid DNA sequencing**

Plasmid DNA sequencing was performed by the Protein and Nucleic Acid Chemistry Laboratory (PNAACL) at the University of Leicester. Sequencing results were analysed using MacVector.

### **2.4.3 - Small scale purification of plasmid DNA**

2TY media (10ml) was supplemented with the appropriate antibiotic for the construct of interest and inoculated with a single colony from a transformation using DH5 $\alpha$ . The bacteria were cultured overnight in a shaking incubator at 37°C and then centrifuged at 3,202 x g for 10 minutes and the supernatant discarded. The cell pellet was either purified for DNA immediately or stored at -20°C until required. Plasmid DNA was extracted and purified from the bacterial pellet using a QIAprep spin mini-prep kit (Qiagen) according to manufacturer's instructions. The purified plasmid was stored at -20°C.

### **2.4.4 - Ethanol precipitation of DNA**

The volume of the DNA sample was measured and 1/10 volume of 5M NaCl was added and mixed. To the sample, 3 volumes of 100% ethanol was added and mixed well before placing on ice or in liquid nitrogen for 5-10 minutes. The sample was spun in a pre-cooled centrifuge at maximum speed (18,407 x g) for 10 minutes. The supernatant was carefully removed and the pellet was washed with 100 $\mu$ l of 100% ethanol, by mixing and spinning briefly. The supernatant was again carefully removed and the pellet air-dried. The pellet was resuspended in the appropriate volume of filter sterilised TE (10mM Tris pH8, 0.1mM EDTA).

## **2.5 - Plasmid constructs**

### **2.5.1 - BCL6 BTB-POZ domain**

The BTB-POZ domain of BCL6 (residues 7-128) was cloned into both pLEICS-7 and pLEICS-46 vectors based on the pET 30a+ backbone (PROTEX, University of Leicester) (Figure 2.1). Both pLEICS-7 and pLEICS-46 produced a fusion protein consisting of an N-terminal 6xHistidine tag and a Tobacco etch virus (TEV) protease cleavage site. pLEICS-46 also produces a fusion protein consisting of an N-terminal immunoglobulin-binding domain of streptococcal protein G (GB1 domain) solubility tag.

### **2.5.2 - Peptide aptamers**

Peptide aptamers were cloned into pLEICS-7, a vector based on the pET 30a+ backbone (Novagen) (PROTEX, University of Leicester) (Figure 2.1). Cloning into pLEICS-7 produced a fusion protein consisting of an N-terminal 6xHistidine affinity tag and a Tobacco etch virus (TEV) protease cleavage site (Table 2.7).

## **2.6 - Mammalian cell culture**

All mammalian cells were grown in a humidified incubator at 37°C with 5% CO<sub>2</sub>. Sterile handling of the cells was carried out in a Class II flow hood. DG75-AB7 cells were grown in RPMI 1640 (GIBCO, Invitrogen) supplemented with 10% FCS and 1x penicillin-streptomycin-glutamine. For tetracycline (tet)-regulated gene expression, 1µg/ml doxycycline (DOX) (Sigma) was added to the culture medium. Cells were cultured to ~80% confluence. Suspension cells were passaged by directly diluting into fresh culture media. Frozen cell stocks were made by re-suspending 10<sup>7</sup> cells in 1ml of freezing media (FCS containing 10% DMSO), transferred into cryovials, and then stored at -80°C. After 24 hours, frozen stocks of cells were transferred into liquid nitrogen. Cells were thawed in a 37°C water bath until a full cell suspension was achieved, then transferred into culture media pre-incubated at 37°C, collected by

centrifugation for 5 minutes at 200 x g, re-suspended in fresh culture media and seeded at a high density to aid recovery.

## **2.7 - Protein expression and purification of bacterial culture**

### **2.7.1 - Bacterial culture**

The two strains of *Escherichia coli* (*E.coli*) used within this project were DH5 $\alpha$  (Invitrogen) and Rosetta BL21 (DE3) (Novagen). To increase the quantity of DNA, DH5 $\alpha$  were utilised. For protein expression, BL21 (DE3) was utilised due to their ability to enhance the expression of eukaryotic proteins that contain codons rarely used in *E.coli*.

### **2.7.2 - Bacterial transformation**

BL21 (DE3) cells were transformed with the required protein expression vector. Briefly, 1 $\mu$ l of the expression vector was added to 100 $\mu$ l of BL21 (DE3) and incubated on ice for 30 minutes. Next, 500 $\mu$ l of 2TY media was added to the competent cells, mixed gently and incubated for 30 minutes in a shaking incubator at 37°C. The cells were then briefly pelleted, 500 $\mu$ l supernatant was discarded and the cell pellet was re-suspended in the remaining 100 $\mu$ l. Cells were then plated out onto 2TY agar containing the appropriate antibiotic for the vector of choice. Throughout this project 34 $\mu$ g/ml Chloramphenicol (Applichem) and 50 $\mu$ g/ml Kanamycin (Melford) was used. The plated cells were then incubated overnight at 37°C. The same procedure applies when transforming DH5 $\alpha$ , with the exception of the absence of chloramphenicol addition to the 2TY agar (Table 2.2).

### **2.7.3 - Starter cultures and growth**

Starter cultures containing the appropriate antibiotic for plasmid resistance (34 $\mu$ g/ml Chloramphenicol and 50 $\mu$ g/ml Kanamycin) were inoculated with a single colony from a transformation and incubated at 37°C in an orbital shaker for 4 hours or until the culture became cloudy in appearance. Cultures were then transferred aseptically into 750ml of

2TY containing the appropriate antibiotic (1x10ml starter/750ml flask). Culture flasks were incubated at 37°C in an orbital shaking incubator at 200rpm until the OD<sub>600</sub> had reached 0.6. Isopropyl-β-D-Thiogalactopyranoside (IPTG) (Melford), (40μM) was added to the culture for the induction of protein expression and the incubator temperature reduced to 20°C and the cells incubated for 16 hours. Bacterial cells were harvested by centrifugation at 4°C for 12 minutes at 3,501 x g (Sorvall SLC-6000). Cell pellets were either used for protein purification immediately or stored at -20°C. For the purpose of NMR experiments, the 2TY media was replaced with 2M9 minimal media, and the 10ml starter culture was added to 500ml (Table 2.3).

#### **2.7.4 - HIS-tagged protein purification**

Cell pellets were re-suspended in lysis buffer (Table 2.1), lysed by sonication using a 9.5mm probe (6x 30s ON, 30s OFF, with an amplitude of 10) (MSE, SoniPrep 150) and the insoluble fraction removed by ultracentrifugation at 4°C for 30 minutes at 128,794 x g (Beckman 50.1T). Cell lysate was added to Ni-NTA resin (Qiagen) (equilibrated in wash buffer (Table 2.1) at a ratio of 1ml resin/1L of original cell culture volume and incubated on a tube roller for 45 minutes at 4°C. The lysate and resin were separated by centrifugation at 3,202 x g for 10 minutes at 4°C. The subsequent steps of protein purification were carried out using an econo-column (Bio-Rad). The econo-column was equilibrated with 1x column volume of wash buffer. Cell lysate was decanted onto the column and allowed to drip by gravity flow and collected, followed by the addition of Ni-NTA resin.

The Ni-NTA resin was washed with 3x10ml wash buffer, each time agitating the resin to ensure sufficient washing before leaving the column by gravity flow and collected. Protein was eluted from the Ni-NTA resin via the addition of 15ml of elution buffer (Table 2.1). Ni-NTA resin and elution buffer were incubated together for 15 minutes, with 2x agitation of the Ni-NTA resin for efficient separation between protein and Ni-NTA resin. The Ni-NTA resin was allowed to settle before the supernatant containing the eluted protein left the column by gravity flow and was collected.

The eluted protein subsequently underwent buffer exchange on a desalting column (HiTrap 26/10, GE Healthcare) into 50mM sodium phosphate pH6, 300mM NaCl and 5mM DTT. Affinity tags were cleaved by the addition of TEV protease (0.1mg of TEV/10mg of tagged protein) to the protein solution and incubated overnight at 4°C

### **2.7.5 - Final stage of purification - separation of protein and affinity tag by gel filtration**

Following TEV cleavage overnight at 4°C, a further purification step was carried out to separate the affinity tag from the protein. Size exclusion chromatography on a Superdex S200 (26/60) column (GE Healthcare) was employed. The column was first equilibrated in the appropriate buffer; in this case NMR buffer (Table 2.1). Protein samples were filtered using a 0.2µM filter (Acrodisc, Life Sciences) prior to loading onto the column. Eluted fractions were collected in a volume of 2.5ml. Samples of the eluted fractions were analysed by SDS-PAGE and those containing only purified protein were pooled together and stored at 4°C until required. Proteins were concentrated by centrifugation at 4,000rpm at a temperature of 20°C, using an Amicon ultra-4 centrifugal unit with the appropriate molecular weight cut off. Protein solution was re-suspended in the centrifugal unit at 5-minute intervals until the desired concentration was achieved.

### **2.7.6 - Analysis of protein purification by SDS-PAGE gel electrophoresis**

The efficiency of the protein purification and TEV cleavage was analysed by SDS-Page electrophoresis. Protein samples were prepared with 2x SDS sample buffer (Table 2.5) and heated to 95°C for 5 minutes prior to loading on the gel. Samples were run on a 4-12% polyacrylamide gel (NuPage® 4-12% Bis-Tris Gel, Invitrogen) using the manufacturer recommended buffer at 230V for 40 minutes, or until the Bromophenol blue dye front reached the bottom of the gel. To approximate protein size, a SeeBlue2 protein marker (Invitrogen) was included on the gel. Gels were then stained using Instant Blue Coomassie stain (Expedeon) for 1 hour before de-staining with water.

## 2.7.7 - Protein Quantification

Protein concentration was determined by either the use of a Bio-Rad protein assay, which measures a shift in absorbance of the Coomassie dye from 465nm to 595nm when bound to arginine and hydrophobic residues present in protein, or by ultraviolet absorption, which is dependent on the presence of aromatic residues such as tyrosine and tryptophan, which absorb at approximately 280nm. The Bio-Rad assay was performed according to manufacturer's guidelines. A 1ml solution containing 20% Bio-Rad reagent diluted in ddH<sub>2</sub>O water was prepared. 2µl of protein was added, mixed, and the absorbance measured at 595nm, against a reagent blank. The protein concentration in mg/ml was then calculated using a factor which had been previously determined from a BSA standard curve. Protein concentration using absorbance at 280nm was calculated using the Beer-Lambert equation.

## 2.8 - NMR Spectroscopy

### 2.8.1 - Sample preparation

Protein samples were prepared in a final volume of 280µl, in 3mm glass tubes (GPE Scientific Limited). Each sample included 5% v/v D<sub>2</sub>O. Nuclear magnetic resonance (NMR) titration experiments were performed on a Bruker AVANCE DRX 600 or AVANCE AVII 800 spectrometer, both equipped with cryoprobes. Titrations were carried out in 3mm NMR tubes using 280µM BCL6 BTB-POZ in 50mM sodium phosphate pH6, 300mM NaCl, 5mM DTT, 5% v/v D<sub>2</sub>O. Rifabutin, rifamycin SV, rifapentine, Rifaximin, 3-formyl rifamycin and rifampicin were re-suspended in deuterated DMSO (DMSO-d<sub>6</sub>). 2D <sup>1</sup>H<sup>15</sup>N heteronuclear single-quantum correlation (HSQC) spectra were acquired with transverse relaxation optimisation (TROSY) (Pervushin *et al.* 1997) using 32 scans and 92 increments. (<sup>1</sup>H-<sup>15</sup>N) TROSY spectra were collected on BCL6 BTB-POZ alone then with increasing amount of compound. Data were analysed using The Collaborative Computing Project for NMR (CCPN) Analysis (Vranken *et al.* 2005).

## **2.9 - X-ray crystallography**

### **2.9.1 - Protein and compound preparation**

Following size exclusion chromatography, purified BCL6 BTB-POZ domain protein was concentrated to ~3.8mg/ml. For co-crystallisation trials, BCL6 BTB-POZ protein was mixed with compound (rifamycin SV or rifabutin) at a molar ratio 1:8 and maintained at room temperature.

### **2.9.2 - Non-divalent ion crystallisation plate**

Commercially available JCSG+ and PACT crystallisation screens (Molecular Dimensions) were specifically modified from their original conditions within Professor John Schwabe's laboratory to ensure that they were absent of divalent metal ions, such as calcium and magnesium. The JCSG screen is based on a combination of classic and modern conditions previously used in successful crystallisation trials, and PACT is a comprehensive screen containing conditions which can test the effects of pH, anions and cations using PEG as a precipitant. The modifications of these screens were important due to the presence of phosphate in the protein buffer as many divalent ions are particularly insoluble and as a result can lead to the presence of phosphate rather than protein crystals. The BCL6 BTB-POZ domain protein was concentrated to ~3.8mg/ml, and mixed with rifamycin SV or rifabutin at a molar ratio of 1:8. Crystallisation experiments were set up by hand into a 96-well plate sitting drop format (MRC, Molecular Dimensions), using 1µl protein complex (BCL6 + rifamycin SV/rifabutin) plus 1µl precipitant at room temperature. Crystals grew within five days.

### **2.9.3 - Harvesting and cryo-cooling of crystals**

For data collection, crystals are harvested and routinely cooled to 100K by immersion into liquid nitrogen. This requires specifically designed cryo-protectants based upon the initial buffer condition in which the crystal grew. Preliminary screening of each cryo-protectant analysed on an 'in-house' X-ray set displayed a clear covering around the crystal, absent of ice formation and ice rings in the diffraction images.

## **2.9.4 - Data collection**

Crystallographic data were collected at the Diamond Light Source Synchrotron on the I24 microfocus beamline, Didcot, Oxford.

## **2.10 - Cell Titre Glo assay**

On day 0, the tet-inducible cell line, DG75-AB7 was seeded at a density of  $1 \times 10^5$  cells/ml in a 96-well plate, in a final volume of 100 $\mu$ l/well. DG75-AB7 cells were treated  $\pm$  DOX (1 $\mu$ g/ml) for four days, followed by treatment with rifabutin or rifamycin SV at a range of concentrations (0, 1, 5, 10, 25 and 50 $\mu$ M) for 24 hours. Cell viability was measured using the Cell Titre-Glo (CTG) (Promega) luminescence assay. 100 $\mu$ l of CTG reagent was added to each well, the plate contents were mixed for 10 minutes at room temperature and the luminescence immediately measured using an X5 plate reader (Perkin Elmer).

## **2.11 - Fluorescence polarisation**

### **2.11.1 - Peptide synthesis**

Peptides within this project for use in fluorescence polarisation (FP) were purchased from Biomatik at the 95% purity scale or synthesised within the Chemistry department at the University of Leicester by Dr Andrew Jamieson.

### **2.11.2 - Peptide coupling**

Peptides for use in FP were coupled to BODIPY-TMR C<sub>5</sub>-maleimide (Invitrogen) via a cysteine residue fused at the N-terminal of the peptide during synthesis. 25 $\mu$ l of 1mM peptide was incubated with 6 $\mu$ l BODIPY-TMR at a concentration of 17.78mM in a final reaction volume of 250 $\mu$ l, with constant stirring for 2 hours in darkness at room temperature (Table 2.4).

### **2.11.3 - BODIPY labelled peptide purification**

A PD-10 column (GE Healthcare) was equilibrated with 25ml reaction buffer, and allowed to drip by gravity flow. Labelled peptide was purified away from free dye and the eluted fractions containing labelled peptide were collected (Table 2.4).

### **2.11.4 - Fluorescence polarisation reaction**

Fluorescence polarisation assays were performed using a black 96-well plate (Corning) and a reaction volume of 100 $\mu$ l. The BCL6 BTB-POZ domain protein was serially diluted across the plate, and BODIPY-labelled peptides were added at a fixed concentration of 1 $\mu$ M and a binding curve produced. From the binding curve, BCL6 concentration with 50% occupancy was determined. For competition experiments, 1 $\mu$ M Bodipy labelled peptide and 3 $\mu$ M BCL6 BTB-POZ domain protein were kept constant, and competing compounds were titrated. Plates were immediately read using an X5 plate reader (Perkin Elmer). All samples were mixed on the in-built shaker before measurements were taken with excitation wavelength of 531nm and the emission wavelength of 595nm.

## **Chapter 3 - Screening potential small molecule inhibitors of the BCL6 BTB-POZ domain by NMR**

### **3.1 - Introduction**

A peptide aptamer is a protein that has its amino and carboxy-terminus anchored in a specific conformation, producing a protein scaffold. The advantage of a protein scaffold is that it can reduce the range of conformations of a particular sequence of amino acids, therefore increasing the specificity of binding (Chattopadhyay *et al.* 2006). Several aptamers were designed within Dr Paul Ko Ferrigno's group at the University of Leeds to target the BTB-POZ domain of BCL6, and from their initial screening, two were chosen for further investigation by NMR.

Prior to the work described in this chapter, a commercial natural product library consisting of 480 compounds (TIMTEC) was screened by Dr Paul Ko Ferrigno's laboratory for their ability to reduce BCL6 mediated transcriptional repression in DG75, a BCL6 expressing Burkitt's lymphoma cell line. Nine compounds were found that altered transcriptional activity in the initial screen. However, due to the similarities shared between BCL6 and STAT DNA binding sequences, the results may have been due to the repression of transcription factors other than BCL6. To elucidate whether it was indeed BCL6 transcription that was inhibited, HEK293T cells, which do not express endogenous BCL6, were co-transfected with a luciferase reporter and a BCL6 expression construct. BCL6 was able to successfully repress luciferase expression, and this was relieved by the addition of rifamycin SV (Robert J. Ford, MSc Thesis 2008).

This chapter describes the steps taken to purify the BCL6 BTB-POZ domain for use in NMR, and the approaches taken to improve the sample further based upon initial NMR experiments. Then NMR experiments were used to (1) screen peptide aptamers as potential binders of the BCL6 BTB-POZ domain, (2) further validate the interaction observed between BCL6 and rifamycin SV in the luciferase assay, and (3) screen derivatives of rifamycin SV for binding to the BCL6 BTB-POZ domain.

## **3.2 - Results**

### **3.2.1 - Initial purification of the wild-type human BCL6 BTB-POZ domain.**

The wild-type BTB-POZ domain of BCL6 (residues 7-128) was sub-cloned into the pLEICS-7 vector supplied by PROTEX at the University of Leicester, producing a fusion protein encoding an N-terminal 6xhistidine affinity tag and a Tobacco Etch Virus (TEV) protease cleavage site (Figure 2.1A). Preliminary attempts to purify the wild-type human BCL6 BTB-POZ domain protein were based upon previously published buffer conditions (20mM TRIS-HCl, 75mM NaCl, 5mM DTT at pH7.5), which were used for the crystallisation and structure determination of the wild-type BTB-POZ domain (Stead *et al.* 2008a). These conditions were then used as a base of manipulation for the NMR conditions of wild type BCL6 POZ.

Following purification using Ni-NTA, cleavage of the histidine affinity tag by TEV proteases occurred during buffer exchange by dialysis at 4°C. At this stage, the elution buffer (50mM Tris-HCl, pH8.5, 300mM NaCl, 300mM imidazole, 5mM DTT and 10mM EDTA) was exchanged for a buffer more suited for NMR experiments (50mM sodium phosphate, pH6, 300mM NaCl and 5mM DTT) (Kelly *et al.* 2002). This method proved unsuccessful as the protein had a tendency to precipitate somewhat throughout the purification, but at a much greater extent during dialysis/TEV cleavage stage.

### **3.2.2 - Investigating the effects of different affinity tags to improve protein purification.**

#### **3.2.2.1 - Non-cleavable HIS tag**

In order to elucidate if indeed TEV cleavage of the affinity tag was the cause of protein precipitation, an N-terminal non-cleavable histidine tag was employed (based on pLEICS7) (Figure 2.1). This short sequence of 6xHis residues remains fused to the wild-type BCL6 BTB-POZ domain, eliminating precipitation potentially caused by

TEV cleavage, and has the added advantage of being small enough to prevent interference during NMR experiments. However, in spite of this, protein precipitation still occurred as shown by the lack of protein present in the elution when compared to the larger sized band representing the BCL6 BTB-POZ domain bound to Ni-NTA resin (Figure 3.1).

#### 3.2.2.2 - GB1 solubility tag

To improve the solubility of the wild-type BCL6 BTB-POZ domain throughout purification, residues 7-128 were sub-cloned into the pLEICS-46 vector supplied by PROTEX at the University of Leicester. The pLEICS-46 vector generates a fusion protein encoding an N-terminal immunoglobulin-binding domain of streptococcal protein G (GB1 domain) solubility tag (Gronenborn *et al.* 1991; Huth *et al.* 1997), 6xHistidine residues and a TEV protease cleavage site (Figure 2.1B).

The expression of the GB1-BCL6 BTB-POZ domain fusion protein greatly improved the solubility and stability of the BCL6 BTB-POZ domain throughout purification (Figure 3.2). In addition, the HSQC spectrum of the GB1 solubility tag has been previously assigned by NMR (Huth *et al.* 1997; Sommer *et al.* 2012), and for these reasons it seem logical for the GB1 tag to remain fused to the BCL6 BTB-POZ domain protein in NMR experiments to improve solubility, as these assignments would make it possible to distinguish the signals produced by both GB1 and the BCL6 BTB-POZ domain. However, despite GB1 improving protein solubility, it became evident that the presence of the GB1 tag caused great interference with the HSQC signal of the BCL6 BTB-POZ domain during NMR experiments. A series of intense peaks were observed in the 2D ( $^1\text{H}$ - $^{15}\text{N}$ ) heteronuclear single-quantum correlation (HSQC) spectrum of the GB1-BCL6 fusion protein. A 2D ( $^1\text{H}$ - $^{15}\text{N}$ ) HSQC of GB1 alone (provided by Ben Goult) was overlaid with the spectrum of GB1 fused to BCL6. It became clear that the intense peaks observed were in fact due to GB1 (Figure 3.3A). Due to the interference caused by the GB1 tag it was necessary to cleave it from the BCL6 BTB-POZ domain. Once cleaved, a sample containing a mixed population of cleaved BCL6 and the GB1 tag revealed many more peaks within the spectrum, which could clearly be associated to BCL6 only (Figure 3.3B). However, soon after cleavage, the BCL6 protein began to precipitate.

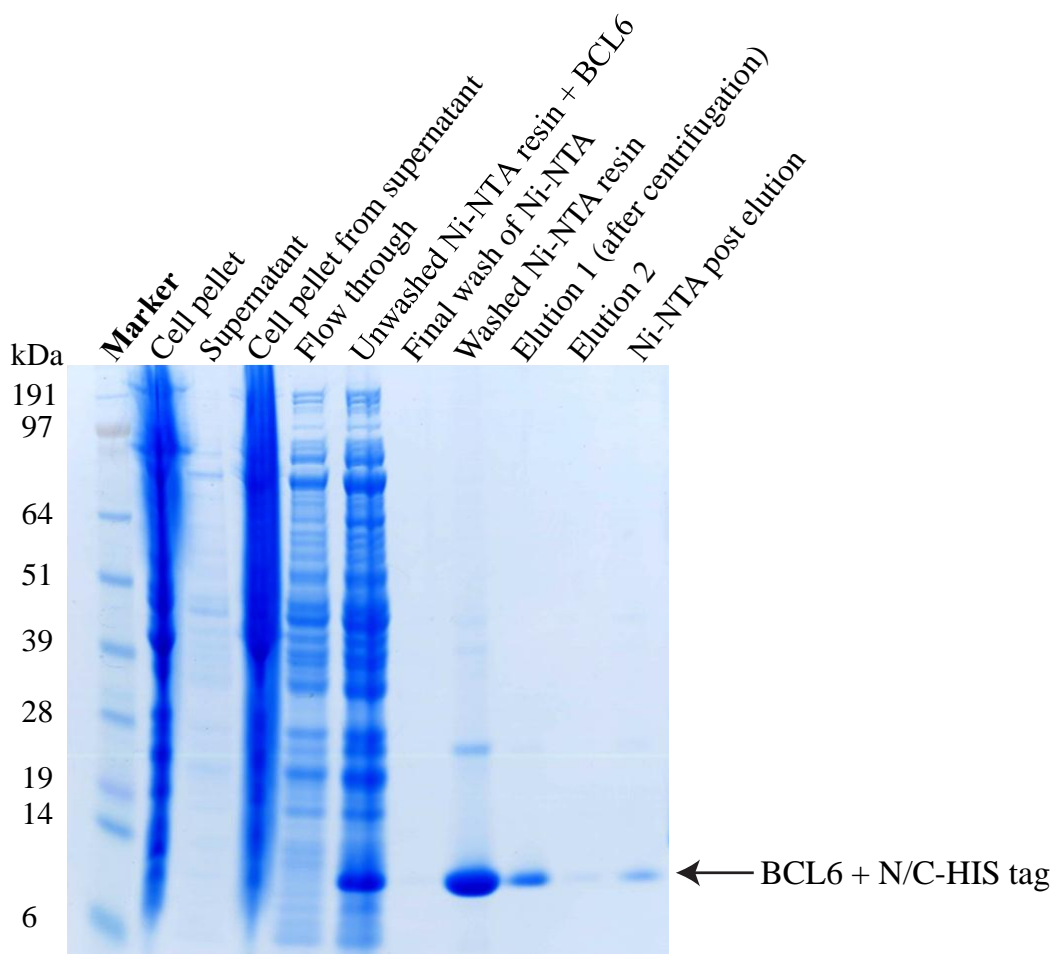


**Figure 3.1: Purification of the wild-type BCL6 BTB-POZ domain expressed with a non-cleavable 6xHis affinity tag.**

Samples were taken at each stage of the purification (2 $\mu$ l of sample and 13 $\mu$ l 2xSDS sample buffer) and ran on a 4-12% polyacrylamide gel. SeeBlue2 (Life Technologies) protein marker was loaded for size comparison. Eluted samples were centrifuged prior to loading for the removal of protein precipitation (Elution 1 and 2).

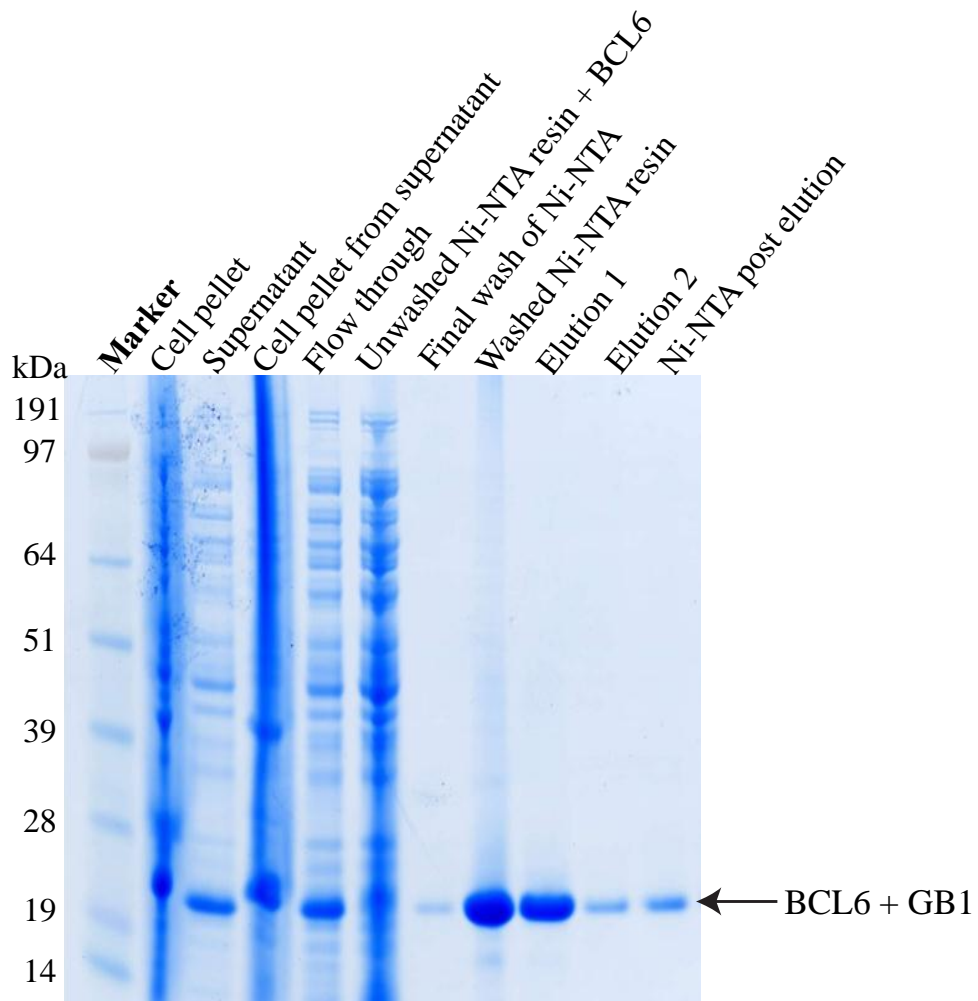


**Figure 3.2: Purification of the wild-type BCL6 BTB-POZ domain expressed with the GB1 solubility tag.**

Samples were taken at each stage of the purification (2 $\mu$ l of sample and 13 $\mu$ l 2xSDS sample buffer) and ran on a 4-12% polyacrylamide gel. SeeBlue2 protein marker was loaded for size comparison. BCL6-GB1 protein was purified using Ni-NTA resin and eluted (Elution 1 and 2).

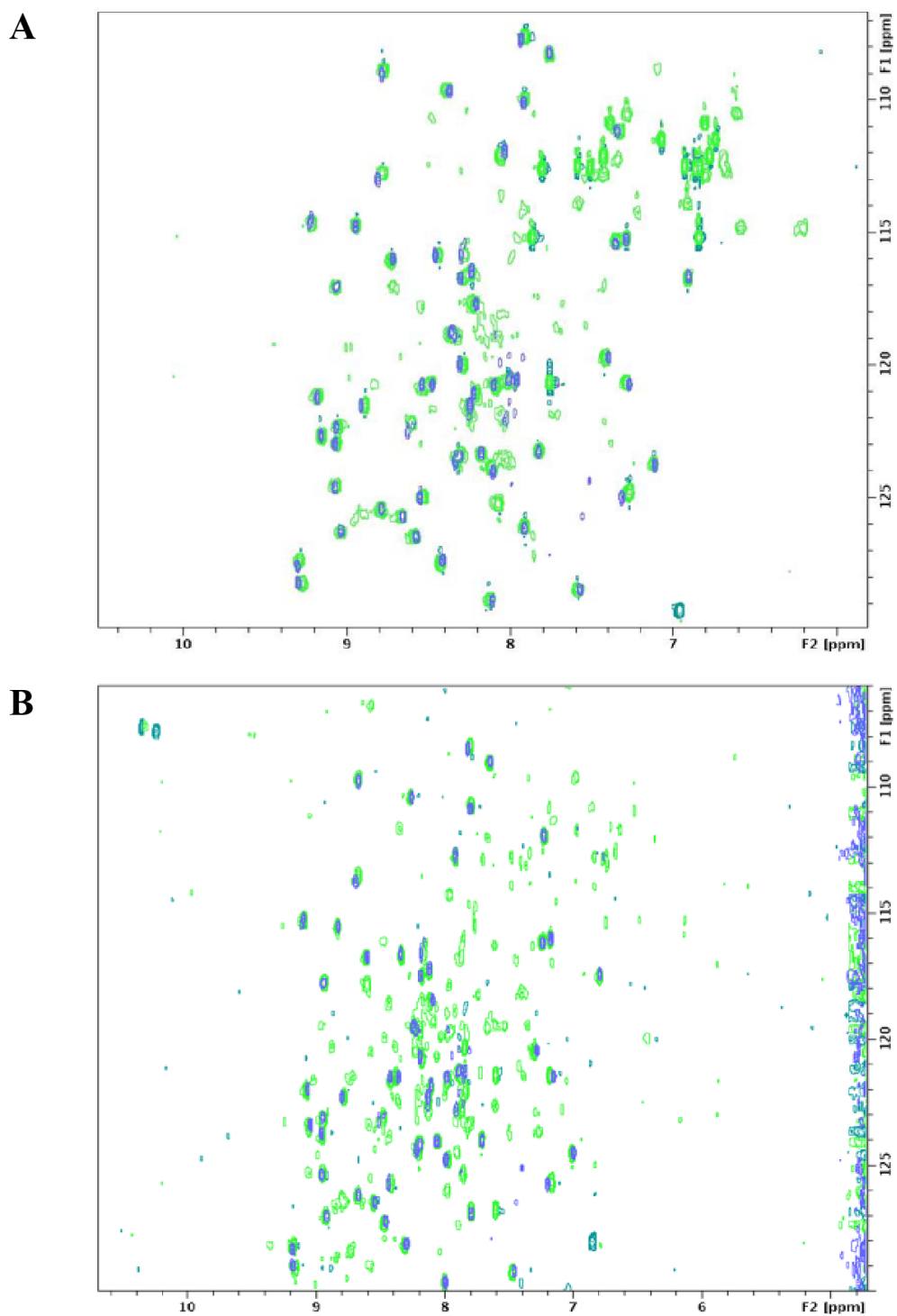


**Figure 3.3: 2D ( $^1\text{H}$ - $^{15}\text{N}$ ) HSQC of the BCL6 BTB-POZ domain plus GB1.**  
 (A) 2D ( $^1\text{H}$ - $^{15}\text{N}$ ) HSQC of the GB1 solubility tag fused to the N-terminus of the BCL6 BTB-POZ domain (green), overlaid with a 2D ( $^1\text{H}$ - $^{15}\text{N}$ ) HSQC of GB1 only (blue) (provided by Ben Goult). (B) The GB1 tag has been cleaved from the BTB-POZ domain. The NMR sample contains a mixed population of cleaved BCL6 and GB1 (green). A 2D ( $^1\text{H}$ - $^{15}\text{N}$ ) HSQC of GB1 only is overlaid (blue).

The original idea was to work with the wild-type BCL6 BTB-POZ domain protein, however other groups found it necessary to mutate three non-conserved surface cysteines (C8Q, C67R and C84N) to prevent protein aggregation and obtain soluble protein (Ahmad *et al.* 2003). These mutations did not affect the function of the BCL6 BTB-POZ domain when compared to wild-type (Ahmad *et al.* 2003). Another group, also mutated the same non-conserved surface cysteines for structural studies (Cerchietti *et al.* 2010a), two years after the wild-type crystal structure had been determined (Stead *et al.* 2008b), suggesting that the 3xCys mutant provides more stability for biochemical studies than the wild-type. Based on this information, a triple mutant construct was designed comprising the C8Q, C67R and C84N mutations with the addition of the N-terminal GB1 solubility tag. The construct was produced by site-directed mutagenesis within the PROTEX facility at the University of Leicester. From this point the 3xCys mutant construct will be used throughout this work, and is termed the BCL6 BTB-POZ domain.

Together with the surface cysteine mutations, further modifications to the purification protocol were made. It was suggested that the presence of imidazole in a protein sample could encourage protein precipitation. Imidazole is present in the elution buffer and acts by competing with the tagged protein for binding to the Ni-NTA resin, leading to displacement of protein from the resin. It was also noted that irrespective of TEV cleavage, precipitation still occurred during dialysis. It was speculated that the slow rates of (1) buffer exchange during dialysis, (2) pH change (from pH8.5 to pH6), (3) imidazole removal and (4) constant agitation of the protein solution during dialysis, all contributed to protein precipitation.

To address all potential contributing factors, the purification protocol was modified. This included the immediate removal of imidazole post-elution with the use of a desalting column (Sephadex G-25 Fine). This technique enables the rapid removal of imidazole from the eluted protein, whilst simultaneously carrying out buffer exchange, placing the BCL6 BTB-POZ protein in a buffer suitable for use in the NMR experiments (50mM sodium phosphate, pH6, 300mM NaCl and 5mM DTT) (Figure 3.4).

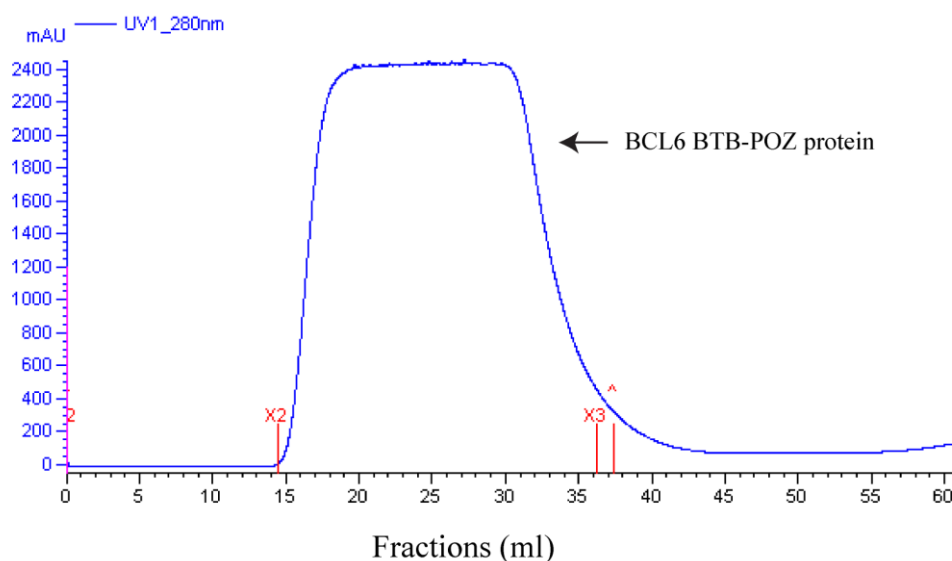


**Figure 3.4: A chromatogram showing the A280nm protein trace of the BCL6 BTB-POZ domain produced by the de-salting column (Sephadex G-25 Fine).**

Eluted BCL6 BTB-POZ domain protein was loaded onto a desalting column. Collection of the protein sample begins once protein absorbance at A280nm is detected (X2). Collection ends when the absorbance value (mAU) returns to just above zero (X3).

Cleavage of the GB1 solubility tag was carried out immediately following the desalting column. Protein concentration was estimated using the Bio-Rad assay at A595nm and by the absorbance at A280nm. Concentration of BCL6-GB1 protein was needed in order to calculate the amount of TEV protease required for cleavage of the GB1 solubility tag. Post-desalting, a yield of 15mg/ml in a volume of 15ml, was routinely achieved from 3L of cell culture. TEV protease was added to the sample and incubated overnight at 4°C. Desalting, followed by TEV cleavage resulted in an absence of visible protein precipitation using this method. The final step of protein purification involved separation of the GB1 solubility tag and BCL6 by gel filtration. The eluted protein sample containing a mixed population of cleaved BCL6 and GB1 was separated on an S200 gel filtration column, producing two distinct peaks. BCL6 forms a dimer in solution with a total molecular weight of ~ 26kDa. The GB1 solubility tag has a molecular weight of ~ 8kDa. The S200 separates by size, with the largest products eluting first. Therefore the BCL6 BTB-POZ domain eluted first, followed by the GB1 solubility tag. Finally, the purity of the protein sample was analysed by SDS PAGE gel electrophoresis (Figure 3.5).

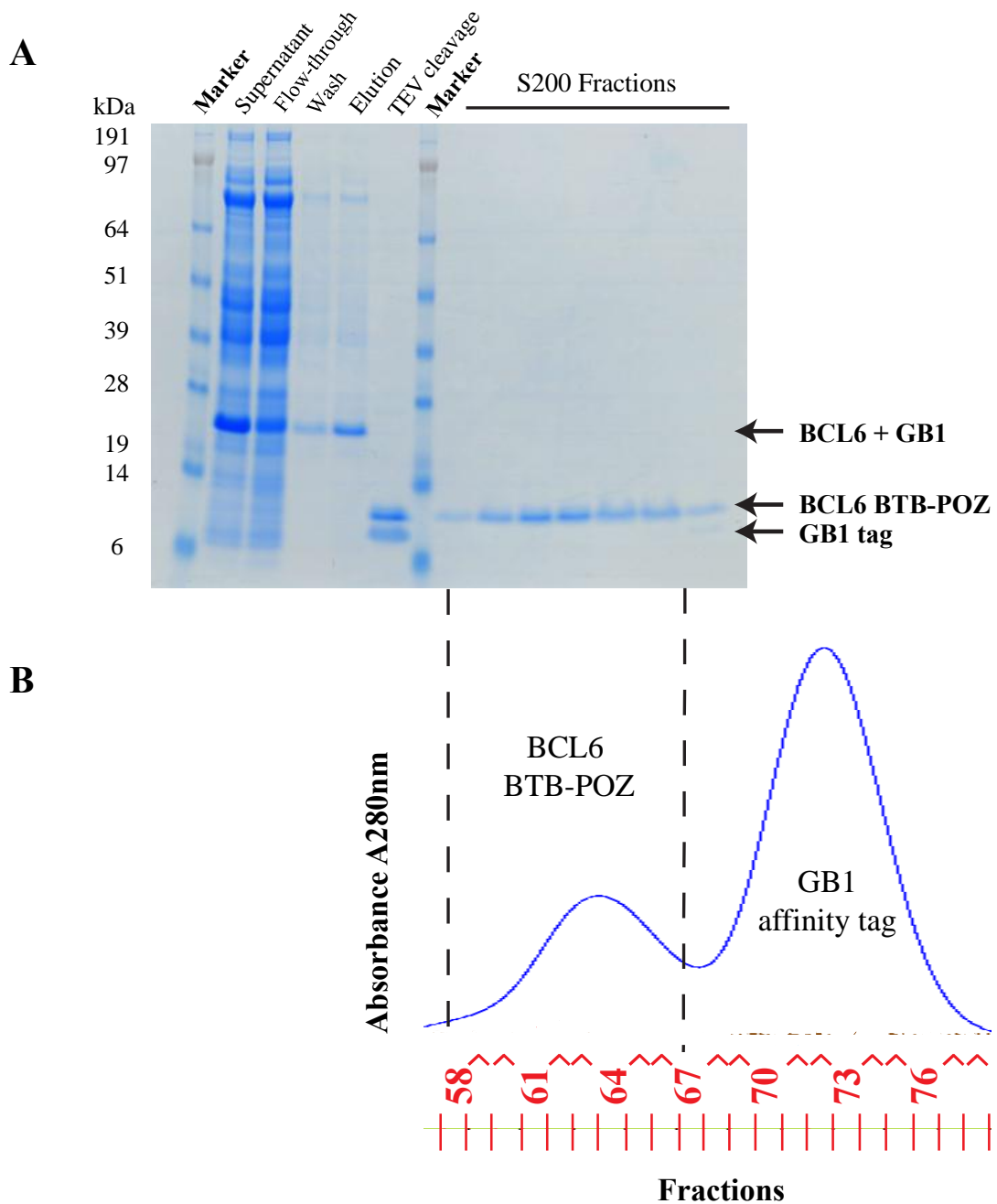


**Figure 3.5: Protein purification and gel filtration of the BCL6 BTB-POZ domain.** Samples of the purification and gel filtration were analysed by SDS PAGE gel electrophoresis. (A) Coomassie stained SDS PAGE gel showing the progress of the purification at each stage. (B) A chromatogram was obtained based on the absorbance of protein at A280nm. The fractions were analysed by SDS PAGE electrophoresis.

### 3.2.3 - 2D ( $^1\text{H}$ - $^{15}\text{N}$ ) TROSY of the BCL6 BTB-POZ domain.

The BCL6 BTB-POZ domain (residues 7-128) was expressed and purified as described in detail in materials and methods. NMR titrations were carried out using 280 $\mu\text{M}$  BCL6 BTB-POZ protein in 50mM sodium phosphate pH6, 300mM NaCl, 5mM DTT and 5% v/v  $\text{D}_2\text{O}$ .

BCL6 forms a dimer at the BTB-POZ domain resulting in a total molecular mass of ~26kDa. Initial 2D ( $^1\text{H}$ - $^{15}\text{N}$ ) HSQC experiments of the BCL6 BTB-POZ domain produced broad peaks and poor signal. Proteins and protein complexes with a molecular mass above 25kDa generally produce poor quality spectra due to a high transverse relaxation rate of the NMR signal, known as  $T_2$  (Wider 2005). The width of resonance lines in the spectrum is inversely proportional to  $T_2$ , which is dependent on the size of the molecule. The NMR signal for small molecules in solution relaxes slowly and therefore has a long ( $T_2$ ), producing narrow line widths. In contrast, NMR signals for large molecules relax faster, ( $T_2$  is smaller), resulting in a weak signal due to line broadening (Pervushin *et al.* 1997; Wider 2005). Employing the transverse relaxation-optimised spectroscopy (TROSY) experimental technique can reduce the transverse relaxation rate,  $T_2$ , resulting in increased spectral resolution and sensitivity for large molecules with molecular weights up to 1000kDa (Pervushin *et al.* 1997; Fernández & Wider 2003).

The 2D ( $^1\text{H}$ - $^{15}\text{N}$ ) TROSY NMR spectrum of the BCL6 BTB-POZ homodimer showed good dispersion and uniform line widths indicative of a stable well-folded protein (Figure 3.6). It was clear that optimisation of the BCL6 BTB-POZ domain protein purification had been successful in yielding a sample of sufficient concentration, for use in NMR studies to explore potential binding partners to the BTB-POZ domain.

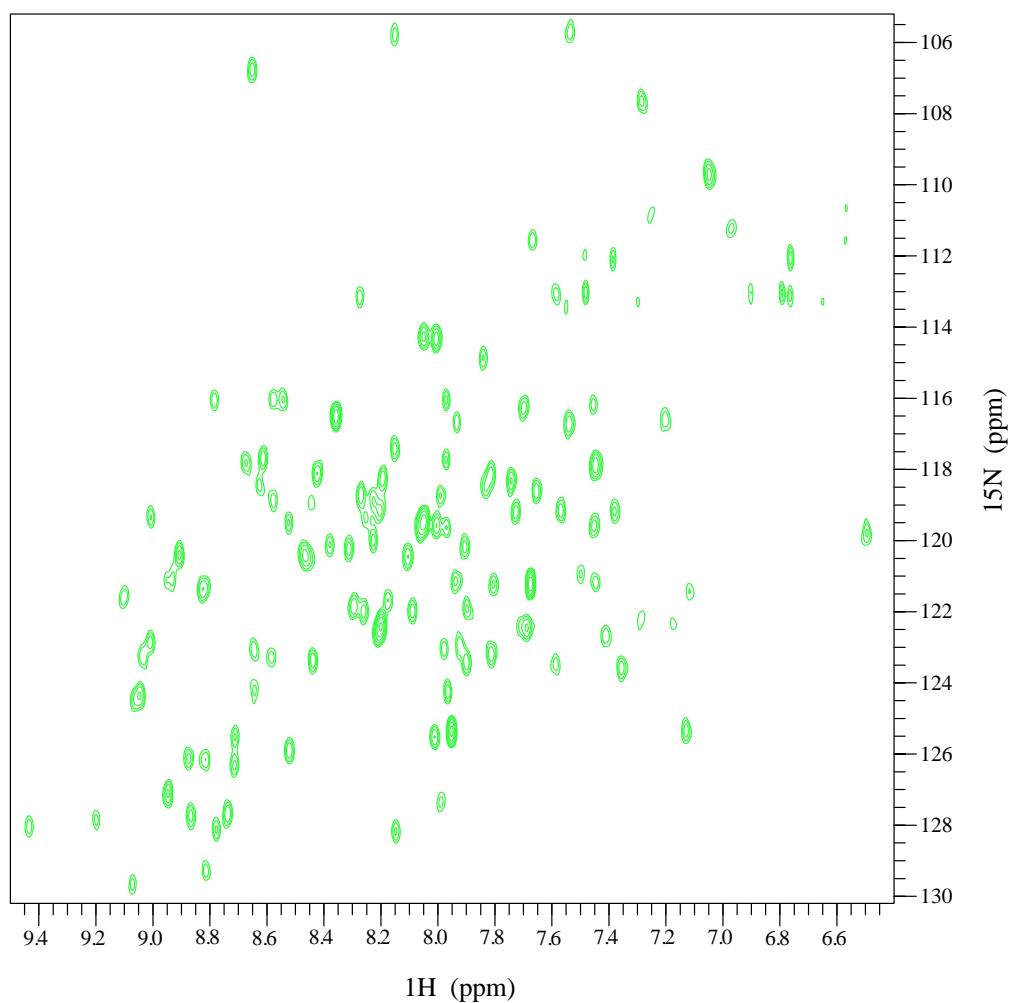


**Figure 3.6: 2D ( $^1\text{H}$ - $^{15}\text{N}$ ) TROSY of the BCL6 BTB-POZ domain (residues 7-128).** NMR experiments were carried out using 280 $\mu\text{M}$  BCL6 BTB-POZ protein in 50mM sodium phosphate pH6, 300mM NaCl, 5mM DTT and 5% v/v  $\text{D}_2\text{O}$ . Spectrum was acquired using Bruker AVANCE DRX 800 spectrometer equipped with a CryoProbe.

### 3.3 - NMR studies of the interaction between BCL6 and peptide aptamers.

NMR spectroscopy is a valuable tool for screening protein-protein and protein-ligand interactions, especially weak affinity interactions. A shift in peak position within the 2D ( $^1\text{H}$ - $^{15}\text{N}$ ) TROSY of protein alone compared to protein in the presence of ligand, is an indication of binding, as the position is dependent on the chemical environment of the atom, which will undergo change in the presence of a ligand, this is known as a chemical shift perturbation.

Peptide aptamers, L2-1 and L12-10, are based on the Stefin-A Quadruple Mutant-Tracey (SQT) backbone. The Stefin-A scaffold can interact with its target using three distinct features; the amino terminus and two loop structures termed loop 1 and loop 2. The SQT is able to tolerate insertions of peptide sequences within these loops to increase specificity and stability of binding to its target (Stadler *et al.* 2011; Stadler *et al.* 2014). L2-1 and L12-10 were expressed and purified by the same method used for the BCL6-GB1 fusion protein. The BCL6 BTB-POZ domain was used throughout NMR titration experiments at a concentration of 280 $\mu\text{M}$ , in the presence of L2-1 or L12-10 at a molar ratio of 1:2.

Despite the validation of binding observed between the peptide aptamers and the BTB-POZ domain of BCL6 by various assays such as Yeast Two-Hybrid carried out within Dr Paul Ko Ferrigno's laboratory, no changes were observed in the 2D ( $^1\text{H}$ - $^{15}\text{N}$ ) TROSY spectra of BCL6 BTB-POZ domain upon the addition of either aptamer, L2-1 or L12-10 (Figure 3.7). This observation suggests that these aptamers do not interact with the BTB-POZ domain of BCL6. The peptide aptamers were not investigated further.

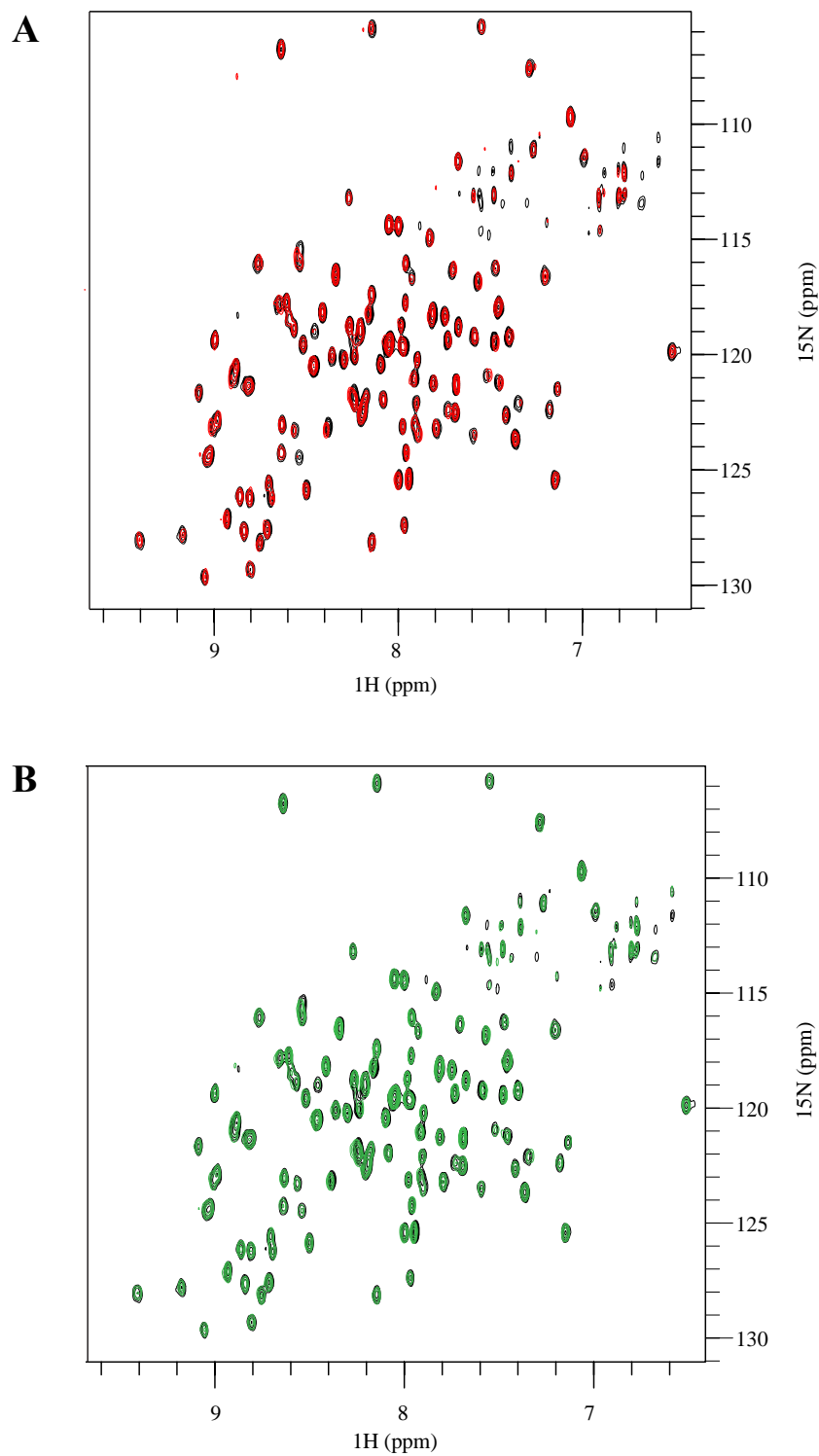


**Figure 3.7: 2D ( $^1\text{H}$ - $^{15}\text{N}$ ) TROSY spectra of BCL6 in the presence of peptide aptamers L2-1 and L12-10.**

BCL6 BTB-POZ domain protein alone at a concentration of 280  $\mu\text{M}$  (black) overlaid with the addition of peptide aptamers (A) L2-1 (red) and (B) L12-10 (green) at a final concentration of 560  $\mu\text{M}$ .

### 3.4 - Rifamycin SV interacts with the BCL6 BTB-POZ domain.

The ansamycin antibiotic rifamycin SV, previously shown to relieve BCL6 mediated transcriptional repression, was investigated by NMR spectroscopy. Rifamycin B, the natural fermentation product of *Streptomyces mediterranei* was the first member of the rifamycin family identified in 1957. Although rifamycin B lacks intrinsic antibacterial properties, when degraded, it produces highly active derivatives, such as rifamycin S. Low concentrations of the derivative rifamycin S have been shown to inhibit growth of gram-positive bacteria. The rifamycin family of antibiotics have demonstrated clinical relevance especially in the treatment of tuberculosis. The major disadvantage of this agent is its lack of oral bioavailability/activity. Determination of the chemical structure in the early 60's, enabled the synthesis of both orally active and semi-synthetic derivatives of this family, such as rifampin and rifabutin (Wehrli *et al.* 1971; Spanogiannopoulos *et al.* 2014).

2D ( $^1\text{H}$ - $^{15}\text{N}$ ) TROSY NMR titration experiments were carried out using the BCL6 BTB-POZ domain protein in the presence of increasing concentrations of rifamycin SV at molar ratios of 1:0, 1:4, 1:8 and 1:16. Rifamycin SV was dissolved in DMSO, a solvent known to cause chemical shift perturbations of spectral peaks (Jones *et al.* 2005). To ensure that any effects observed were due to an interaction with BCL6 only, the same amount of DMSO was included in each sample. Small shifts were observed upon the addition of rifamycin SV, with a subset of peaks shifting in a concentration dependent manner. This data supports the results generated from the initial luciferase assay, that rifamycin SV does indeed interact directly with BCL6 (Figure 3.8).

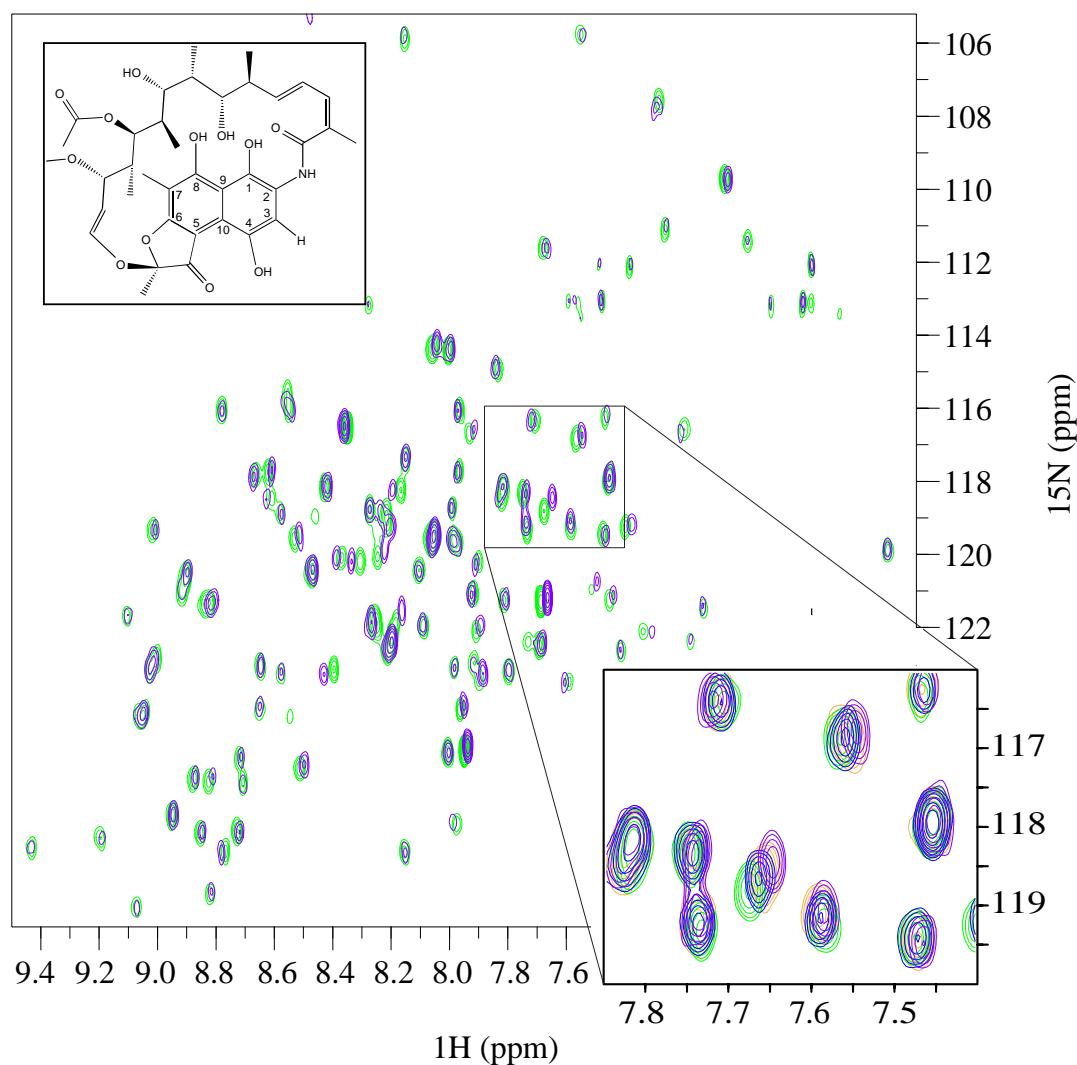


**Figure 3.8: Rifamycin SV binds to the BCL6 BTB-POZ domain.**

A 2D ( $^1\text{H}$ - $^{15}\text{N}$ ) TROSY spectrum of the BCL6 BTB-POZ domain in complex with rifamycin SV. The BTB-POZ domain at a concentration of  $280\mu\text{M}$  is shown in the absence (green) and presence (purple) of rifamycin SV at a molar ratio of 1:16. Small shifts are observed across the spectrum, with a subset shifted in a concentration dependent manner with molar ratios of 1:4 (blue), 1:8 (orange) and 1:16 (purple) (inset image). A schematic showing the chemical structure of rifamycin SV is shown (top left).

### 3.5 - Screening of rifamycin SV derivatives by NMR

Rifamycin SV belongs to a family of ansamycin antibiotics, comprising of a chromophoric naphthoquinone ring bridged by a long aliphatic chain (Figure 3.8 inset) (Wehrli & Staehelin 1971). The observation of rifamycin SV binding to the BCL6 BTB-POZ domain by NMR, led to speculation over whether other members of the rifamycin SV family could also bind to the BTB-POZ domain, due to the structural similarity conserved throughout the derivatives.

The commercially available derivatives, 3-formyl rifamycin, rifampicin, rifapentine, rifaximin and rifabutin were analysed by 2D ( $^1\text{H}$ - $^{15}\text{N}$ ) TROSY NMR titration experiments. Each derivative caused spectral changes of varying magnitudes (Figures 3.9 and 3.10), with the greatest chemical shift perturbations caused by rifabutin (Figure 3.11).

The estimated order of binding from weakest to strongest based on the subset of peaks which had shifted in the presence of rifamycin SV, were rifaximin, rifapentine, 3-formyl rifamycin, rifampicin, rifamycin VS and rifabutin.

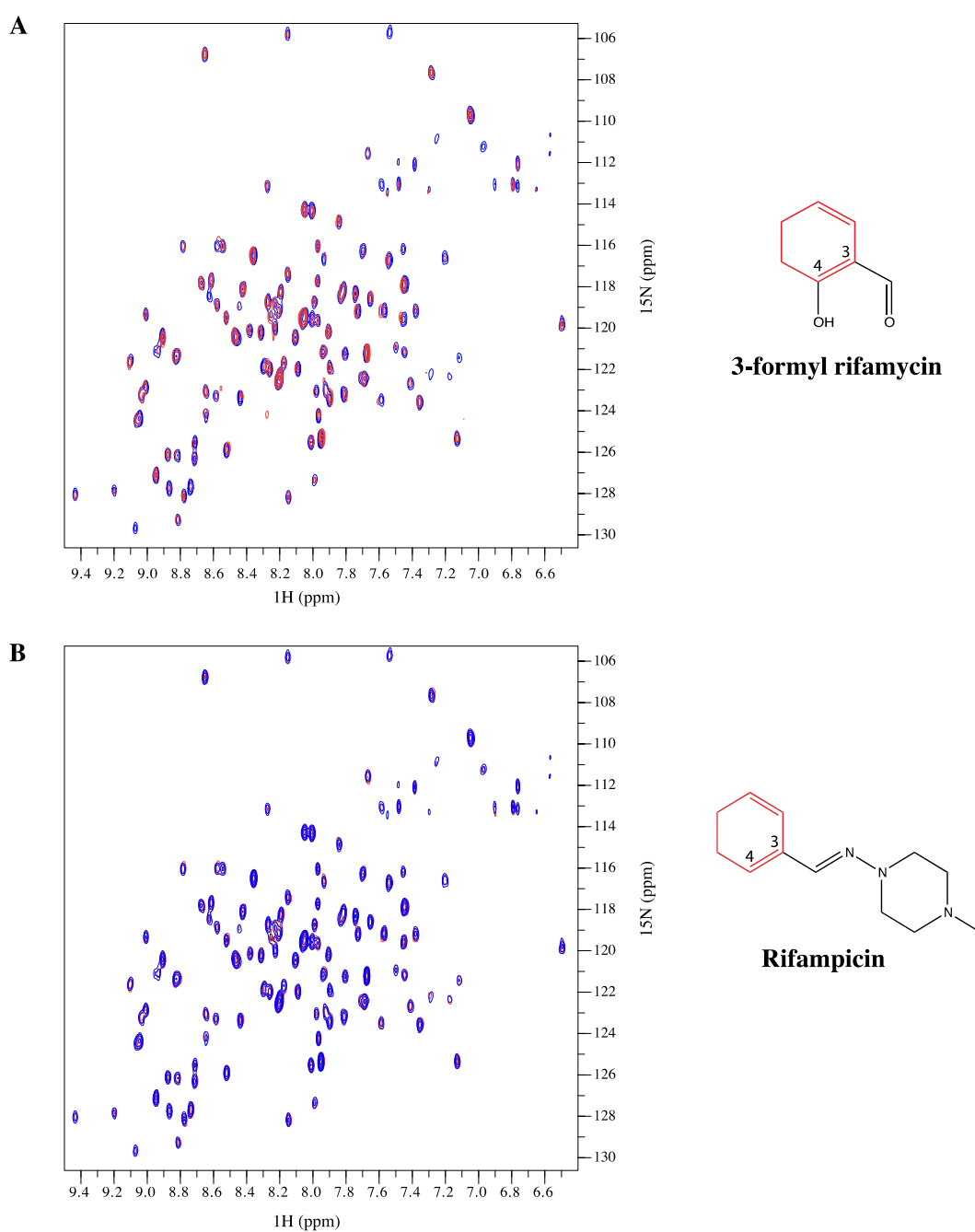


**Figure 3.9: 2D ( $^1\text{H}$ - $^{15}\text{N}$ ) TROSY spectra for rifamycin SV derivatives (1).**

2D TROSY spectra of the BCL6 BTB-POZ domain at a concentration of  $280\mu\text{M}$  is shown in the absence (blue) and presence of (A) 3-formyl rifamycin or (B) rifampicin (red) at a molar ratio of 1:16. The family of rifamycins differ primarily in their tails, found at position C-3 and C-4. A schematic of each tail corresponding to the derivative is also shown.

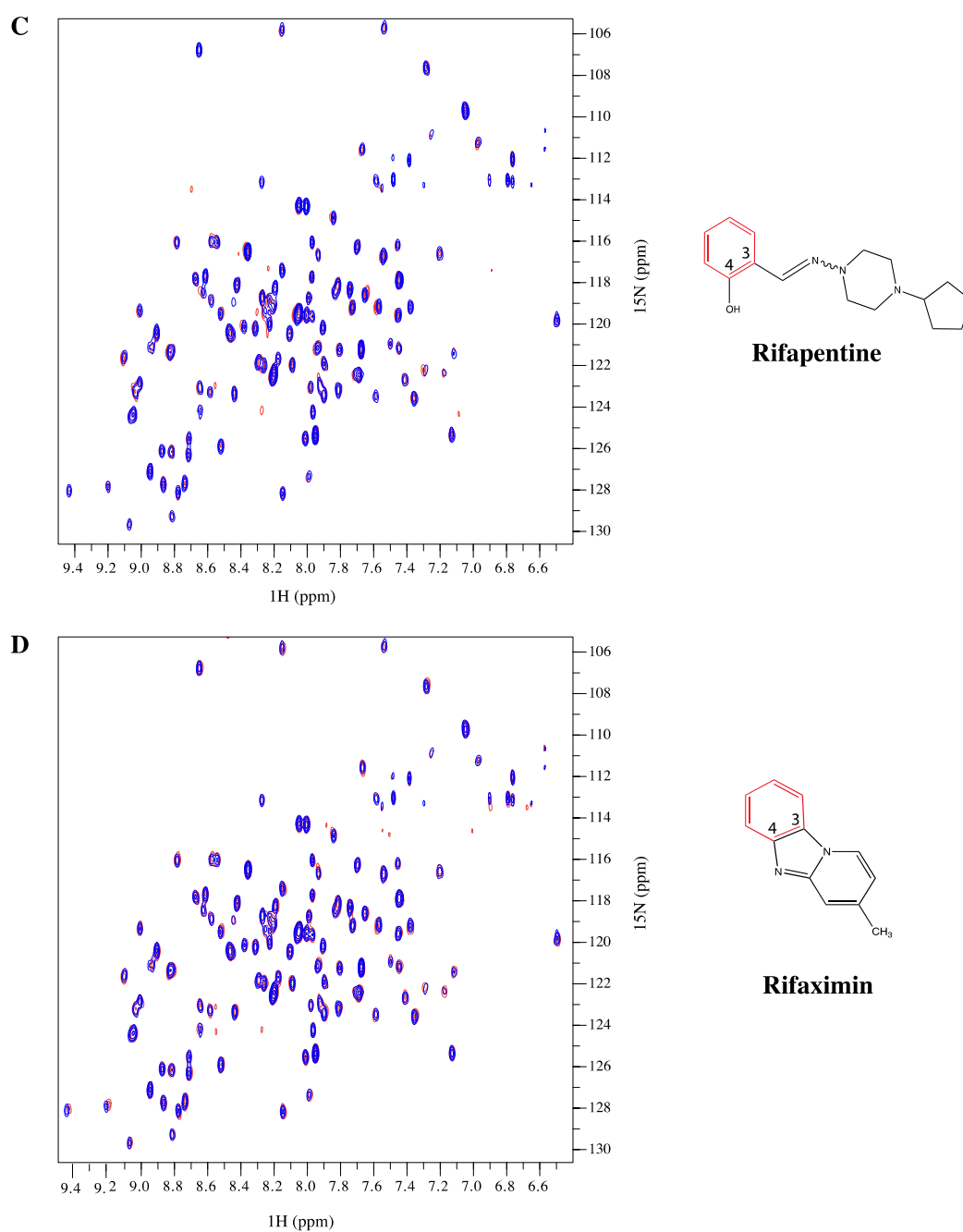


**Figure 3.10: 2D ( $^1\text{H}$ - $^{15}\text{N}$ ) TROSY-HSQC spectra for rifamycin SV derivatives (2).** 2D TROSY spectra of the BCL6 BTB-POZ domain at a concentration of  $280\mu\text{M}$  is shown in the absence (blue) and presence of (C) rifapentine or (D) rifaximin (red) at a molar ratio of 1:16. The family of rifamycins differ primarily in their tails, found at position C-3 and C-4. A schematic of each tail corresponding to the derivative is also shown.

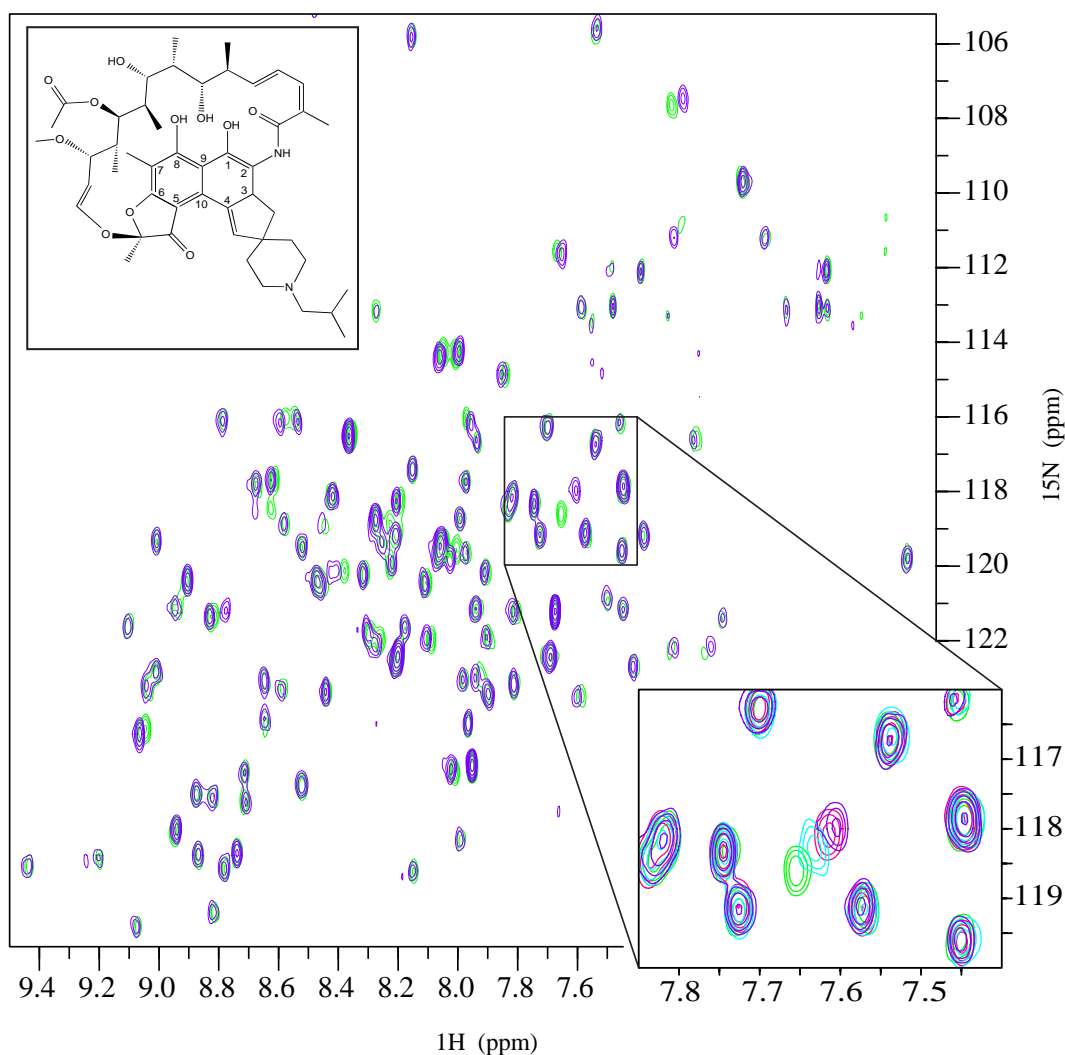


**Figure 3.11: Rifabutin binds directly to the BCL6 BTB-POZ domain.**

A 2D ( $^1\text{H}$ - $^{15}\text{N}$ ) TROSY spectrum of rifabutin in complex with the BCL6 BTB-POZ domain. The BTB-POZ domain at a concentration of  $280\mu\text{M}$  is shown in the absence (green) and presence (purple) of rifabutin at a molar ratio of 1:16. As seen with rifamycin SV, small shifts are also observed across the spectrum, but with a subset of peaks shifting a slightly greater distance and in a concentration dependent manner with molar ratios of 1:4 (blue), 1:8 (pink) and 1:16 (purple) (inset image). A schematic showing the chemical structure of rifabutin is shown (top left).

### **3.6 - Investigating which residues of the BCL6 BTB-POZ domain are involved with rifamycin and rifabutin binding.**

To elucidate the residues involved in the interaction between rifamycin SV or rifabutin and the BCL6 BTB-POZ domain by NMR, backbone assignments of the protein needed to be determined. Within the 2D ( $^1\text{H}$ - $^{15}\text{N}$ ) TROSY spectrum, each peak represents an amide proton bound to a nitrogen atom (NH), and a signal is then observed for each residue within the protein, with the exception of proline and the N-terminal amino acid. In order to assign a spectral peak to a residue in the protein sequence, triple resonance experiments are required.

Partial NMR assignment of the BTB-POZ domain has previously been published. Cerchietti *et al*, 2010a were able to assign 82 out of 121 observed peaks. These assignments were supplied by Cerchietti *et al*, and immediately overlaid with the TROSY spectrum of the BCL6 BTB-POZ domain, to identify which amino acids were affected by the presence of rifamycin SV or rifabutin. However, the assignments did not directly overlap with our spectrum, therefore it was not possible to definitively determine the residues involved in the interaction by this method (Figure 3.12A).

It was however, possible to estimate a binding affinity for rifabutin. By plotting the chemical shift change ( $\delta\Delta$ ) of the most shifted peak, as a function of rifabutin concentration, it was possible to estimate the  $K_d$  of the interaction as being in the order of  $\sim 1\text{mM}$  (Figure 3.12B). In order to acquire a very rough estimation of which peaks shifted in the presence of rifabutin or rifamycin SV, chemical shift perturbations that were in close proximity to an assignment were tentatively mapped onto the surface of the BCL6 BTB-POZ domain structure in complex with SMRT. It appeared that the potential binding site of rifabutin or rifamycin SV could overlay with the binding site of SMRT (Figure 3.12C).

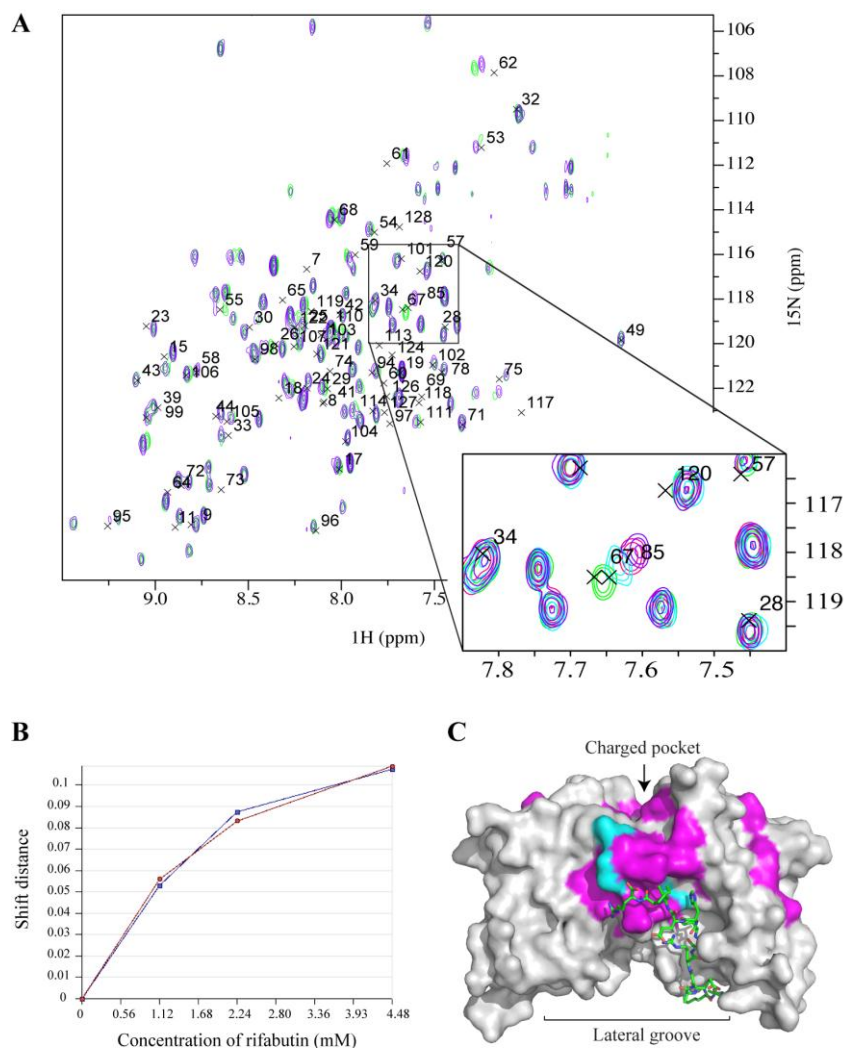


### Figure 3.12: Analyzing the interaction between rifabutin and the BCL6 BTB-POZ domain

Partial NMR assignments of the BTB-POZ domain are overlaid with the 2D ( $^1\text{H}$ - $^{15}\text{N}$ ) TROSY spectrum of the BTB-POZ domain of BCL6. An estimation of binding affinity of rifabutin for BCL6, and the potential residues involved in the interaction are shown. (A) BTB-POZ domain in the absence (green) and presence (purple) of rifabutin at a ratio of 1:16. Numbers represent amino acid residue within the BTB-POZ domain protein sequence. The peak with the greatest chemical shift perturbed in a concentration dependent manner (molar ratios of 1:4 (blue), 1:8 (pink) and 1:16 (purple)) is shown inset. (B) Chemical shift changes are plotted against rifabutin concentration for both residues residing at the position of the shifted peak. (C) Chemical shift perturbations that are in close proximity to an assignment (magenta) are tentatively mapped onto the surface of the co-crystal structure of BCL6 BTB-POZ in complex with SMRT (shown in green, in stick representation) to estimate the binding region. Residues highlighted in cyan also represent a peak shift, with slightly less confidence in which assignment it correlates to. (PDB ID 1R2B) (Ahmad *et al.* 2003).

### 3.7 - Discussion

This chapter describes the steps taken to optimise the purification of the BCL6 BTB-POZ domain protein for use in NMR studies. NMR spectroscopy was employed as a tool to explore potential BCL6 binding partners in the form of peptide aptamers, and to further investigate the interaction observed from the natural compound screen between rifamycin SV and BCL6.

In order to produce a stable, soluble protein it was necessary to mutate three non-conserved surface cysteines, C8Q, C67R and C84N to prevent aggregation of the recombinant protein (Ahmad *et al.* 2003). The addition of the GB1 tag greatly enhanced solubility throughout purification (Figure 3.2), however it became evident that the presence of GB1 would cause interference of the BCL6 signal during NMR experiments. As mentioned previously, BCL6 forms a dimer at the BTB-POZ domain, and therefore, each dimer will possess 2x GB1 solubility tags, one fused to each monomer at the amino terminus. Furthermore, there is a long linker region between the BCL6 BTB-POZ domain and the GB1 tag. This allows free rotation of GB1 resulting in greater movement and the production of a much stronger signal within NMR experiments than BCL6. Therefore, the signals arising from GB1 masked the spectral peaks of BCL6. However, once GB1 was cleaved, many more peaks were observed which could be identified as BCL6 (Figure 3.3). Together, the surface cysteine mutations, GB1 and the optimisation of the purification, led to the production of a stable, soluble protein suitable for NMR studies.

Peptide aptamers were designed within Dr Paul Ko Ferrigno's laboratory and screened by yeast two-hybrid for potential binding ability to the BCL6 BTB-POZ domain. Within their laboratory, each aptamer was validated as a potential BCL6 binding partner, and from those, two were chosen for further investigation by NMR spectroscopy. No chemical shift perturbations were observed in the TROSY spectrum upon addition of the aptamer, suggesting that L2-1 and L12-10 do not bind to the BTB-POZ domain. However, L2-1 and L12-10 were titrated at a maximum concentration of  $\sim 560\mu\text{M}$ , whereas, rifamycin SV and rifabutin were titrated at 1.12 (1:4), 2.24 (1:8) and 4.48mM (1:16). The concentrations of both BCL6 and aptamers were the limiting

factors during these titration experiments. Both rifamycin SV and rifabutin were prepared at a stock concentration of 100mM, therefore, only a very small volume of compound was needed to titrate with BCL6 to achieve the concentration required, in addition to minimally affecting the concentration of BCL6 at 280µM. In contrast, the aptamers were at a much lower stock concentration, therefore requiring a much larger volume for the same concentrations achieved for rifamycin SV and rifabutin. Increasing the volume of aptamers to BCL6 would lead to the dilution of BCL6 and poor quality spectrum.

Rifamycin SV has been shown to relieve transcriptional repression induced by BCL6, and as a result has been further investigated by NMR. Rifamycin SV belongs to a family of ansamycin antibiotics (Latin *ansa* = handle) (Floss & Yu 2005), so called because of their basket like structure, consisting of chromophoric naphthoquinone rings bridged by a long aliphatic chain. Structural similarity is demonstrated throughout the derivatives, with the main differences observed in the side chain tails at position C-3 and C-4 (Sensi *et al.* 1974). The difference in binding affinity observed between rifamycin SV, rifabutin, rifaximin, rifapentine, rifampicin and 3-formyl rifamycin, might be due in part to this structural difference.

In the NMR titration, rifabutin induced the largest chemical shift perturbation, and interestingly, perturbed the same peaks as rifamycin SV. In order to determine the residues involved in the interactions between rifamycin SV/rifabutin and BCL6, partial NMR assignments of the BCL6 BTB-POZ domain, supplied by Cerchietti *et al.*, were overlaid with our 2D (<sup>1</sup>H-<sup>15</sup>N) TROSY spectrum. The assignments did not directly overlay, but nevertheless, it was still possible to tentatively estimate the residues involved in the interaction. Chemical shift perturbations that were in close proximity to an assignment were tentatively mapped onto the surface of the BCL6 BTB-POZ domain structure in complex with SMRT (PDB ID 1R2B) (Ahmad *et al.* 2003)(Figure 3.12C).

Interestingly, it seemed that the residues of BCL6 involved in the interaction were located within the lateral groove of the BTB-POZ domain. The lateral groove is an important feature of the BCL6 BTB-POZ domain, due to the binding of co-repressors SMRT, NCoR and BCoR to this region, enabling BCL6 to induce transcriptional repression of its target genes (Ahmad *et al.* 2003; Huynh *et al.* 2000; Ghetu *et al.* 2008).

The chemical shift perturbations observed, in addition to mapping of potential residues involved in the interaction onto the crystal structure of the BTB-POZ domain, has supported the initial observation from the natural compound screen that the ansamycin antibiotic, rifamycin SV, and its derivative, rifabutin do indeed bind to the BTB-POZ domain of BCL6. Co-crystallisation experiments for BCL6 in the presence of rifamycin SV or rifabutin were carried out simultaneously to NMR titrations. Small crystals were obtained for both compounds. To precisely determine which residues of the BTB-POZ domain are involved in the interaction with both rifamycin SV and rifabutin, X-ray crystallography was employed, therefore further NMR experiments were not pursued.

## **Chapter 4 - Structure of BCL6 BTB-POZ domain in complex with rifabutin.**

### **4.1 - Introduction**

As described in Chapter 3, the BCL6 BTB-POZ domain construct (residues 7-128) bearing an N-terminal GB1 solubility tag and three non-conserved surface cysteine (C8Q, C67R and C84N) mutations yielded a stable protein sample suitable for structural studies. NMR experiments showed that both rifamycin SV and rifabutin bind to the N-terminal BTB-POZ domain of BCL6. However, due to the incomplete assignment of the BTB-POZ domain spectra, it was not possible to determine the residues involved with ligand binding. Since the BCL6 BTB-POZ domain protein was stable throughout the NMR experiments, it seemed likely that it would also be suitable for crystallisation trials. This chapter describes the use of X-ray crystallography to determine the binding location of rifamycin SV and rifabutin on the BCL6 BTB-POZ domain.

### **4.2 - Results**

#### **4.2.1 - Initial crystallisation experiments**

The buffer conditions of the initial crystallisation experiments carried out to investigate the binding location of rifamycin SV and rifabutin on the BCL6 BTB-POZ domain, were based upon the buffer conditions previously published that yielded the crystal structure of the wild-type BCL6 BTB-POZ domain. To replicate these conditions, it was necessary to carry out a buffer exchange of the BCL6 BTB-POZ domain after the final stage of protein purification using a disposable PD-10 desalting column to exchange the purification buffer: 50mM sodium phosphate pH 6, 300mM NaCl, 5mM DTT (buffer A), for the buffer conditions that were used to crystallise the structure of the wild-type BCL6 BTB-POZ domain: 20mM Tris-HCl, 250mM NaCl, 5mM DTT, 5% glycerol pH 8.5 (buffer B) (Stead *et al.* 2008b).

However, when concentrating the BCL6 BTB-POZ domain protein using these conditions it became evident that the protein had a tendency to precipitate when

concentrated beyond 1mg/ml using 'buffer B', and as a result, crystallisation experiments failed to yield any crystals.

Nevertheless, since the BCL6 BTB-POZ domain protein was stable in a buffer consisting of 50mM sodium phosphate pH6, 300mM NaCl and 5mM DTT as demonstrated throughout the NMR experiments in Chapter 3, it seemed logical to revert back to the phosphate buffer. This required tailoring the crystallisation screens to accommodate the presence of phosphate. Most commercially available screens contain divalent ions, many of which are salts such as calcium, magnesium and zinc and are all particularly insoluble, it is therefore, a common occurrence to find salt crystals during crystallisation trials when using screens containing divalent ions in combination with phosphate buffers (Raghunathan *et al.* 2010)

#### **4.2.2 - Optimisation of crystallisation experiments**

Crystallisation screens were derived from the commercially available JCSG+ and PACT (Molecular Dimensions) screens by Jacquie Greenwood in Professor John Schwabe's group. These screens did not contain divalent ions in order to accommodate the presence of phosphate within the protein buffer.

The BCL6 BTB-POZ domain protein was concentrated to 3.8mg/ml. Rifamycin SV and rifabutin were added to the BCL6 BTB-POZ domain protein at a molar ratio of 1:8. Crystallisation experiments were set up by hand into a 96-well sitting drop crystallisation plate (MRC, Molecular Dimensions), using 1µl protein complex + 1µl precipitant at room temperature. Crystals grew within five days.

Examples of crystal forms for both rifamycin SV and rifabutin are shown (Figure 4.1). Due to the colour of each compound, crystals exhibited a yellow colour and a slight purple colour (for rifamycin SV and rifabutin respectively). More conditions yielded crystals of rifamycin SV in complex with the BCL6 BTB-POZ domain than crystals of rifabutin in complex with the BCL6 BTB-POZ domain. A list of crystallisation conditions yielding crystal formation can be found (Table 4.1).

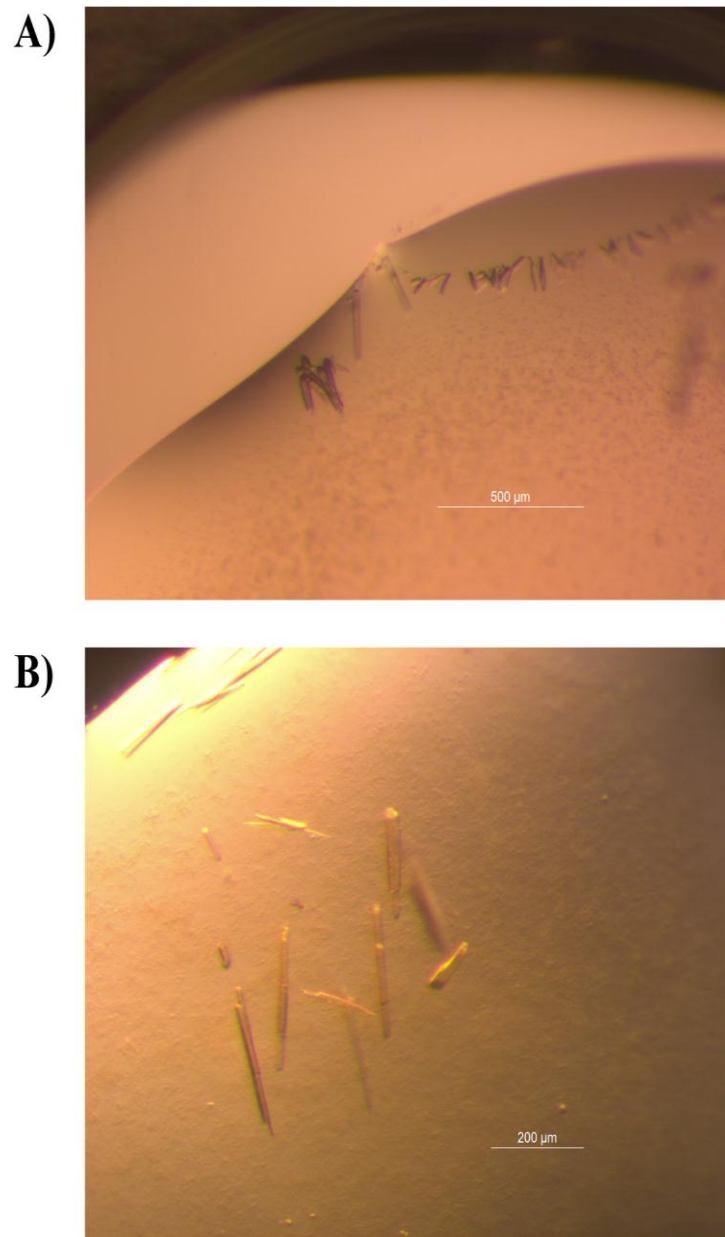


**Figure 4.1: Examples of crystal forms for the BCL6 BTB-POZ domain grown in the presence of (A) rifabutin and (B) rifamycin SV.**

<u>Compound</u>	<u>Well</u>	<u>Precipitant</u>	<u>Buffer (100mM)</u>	<u>pH</u>	<u>Salt (200mM)</u>	<u>Crystal form</u>
<b>Rifamycin SV</b>	A5	20% PEG 8000	CHES/ NaOH	9.5	-	Sheets
	A6	20% PEG 3350	-	-	Ammonium Formate	Sheets
	F6	2M Di-ammonium sulphate	Bis/TRIS-HCl	5.5	-	Needles
	F9	25% PEG 3350	Bis/TRIS-HCl	5.5	-	Sheets
	G12	20% PEG 2000 MME	MES/ NaOH	6.5	Sodium Chloride	Swords/ Plates
	H5	10% PEG 4000	Sodium citrate/ Citric acid	5.5	Sodium Acetate	Swords/ Plates
<b>Rifabutin</b>	A12	20% PEG 3350	-	-	Sodium Isothiocyanate	Sheets
	B6	20% PEG 6000	Sodium citrate/ Citric acid	5	-	Needles/ 3D rods

**Table 4.1: Crystallisation hit conditions.**

Crystallisation hits from the screens based upon JCSG+ for the BCL6 BTB-POZ domain in complex with rifamycin SV and rifabutin.

## **4.3 - Structure determination**

### **4.3.1 - Harvesting crystals**

To shield the crystals from radiation damage received from the X-ray beam during data collection, crystals were routinely cooled to 100K. This requires specifically designed cryo-protectants (based upon the initial hit condition in which each crystal grew) to be prepared. Preliminary screening of each cryo-protectant analysed on an 'in house' X-ray set displayed a clear 'glass appearance' covering around the crystal, absent of visual ice formation and ice rings in the diffraction images. In all cases, the inclusion of 20% 2-Methyl-2, 4-pentanediol (MPD) was found to be a sufficient addition to the precipitant in order to cryo-protect the crystal. Crystals were then harvested using appropriately sized cryo loops in the appropriate cryo-protectant and immediately cooled to 100K by immersion into liquid nitrogen (Figures 4.2A and 4.3A).

### **4.3.2 - Data collection**

Crystallographic data was collected at the Diamond Synchrotron I24 microfocus beamline, Didcot, Oxford. Crystals containing rifamycin SV in complex with the BCL6 BTB-POZ domain produced a 1.5Å diffraction data set in the space group C 1 2 1 (Figure 4.2B). A single crystal was sufficient to produce a complete data set. Crystals containing rifabutin in complex with the BCL6 BTB-POZ domain produced a 2.3Å diffraction data set in the space group P1 21 1 (Figure 4.3B). Data from three crystals were merged into one file to produce a complete data set. Crystallographic statistics are described in Table 4.2 and Table 4.3 for the rifamycin SV and rifabutin crystals respectively.

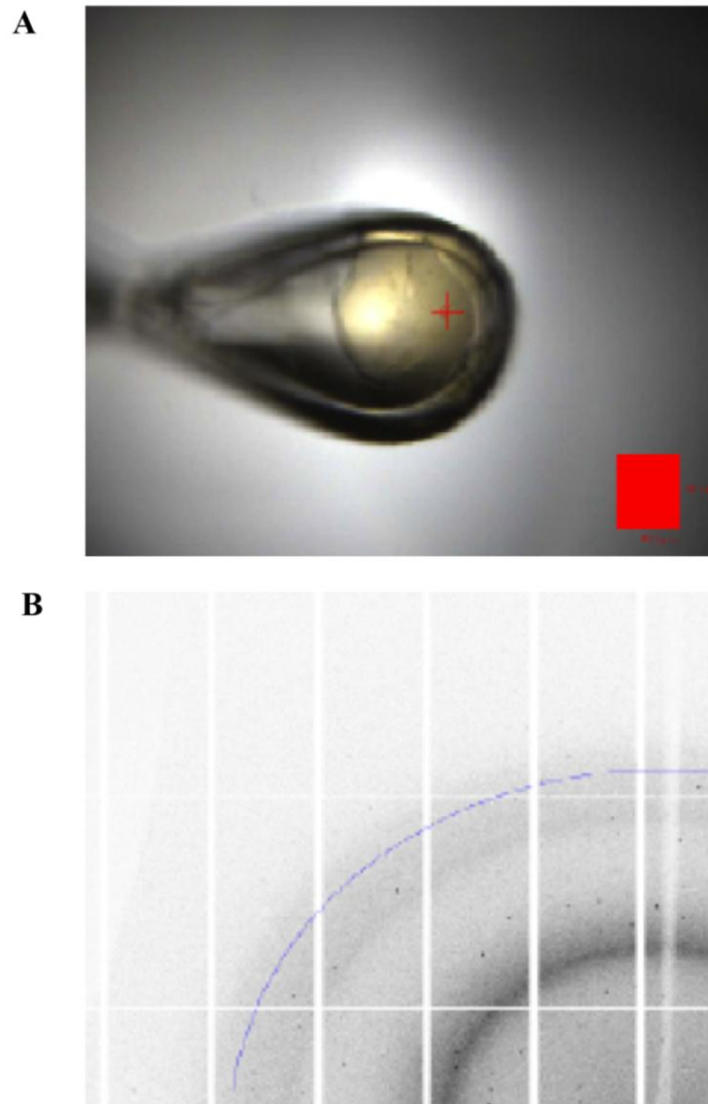


**Figure 4.2: Image of a BCL6 BTB-POZ domain crystal grown in the presence of rifamycin SV and the diffraction pattern produced.**

(A) An image of the BCL6 BTB-POZ domain crystal mounted in a loop at the Diamond Synchrotron, beamline I24. (Red box represents  $25.9 \times 25.9 \mu\text{m}$ ). (B) Diffraction image of the crystal diffracting to a resolution of  $1.5\text{\AA}$  as indicated a by the outer blue line.

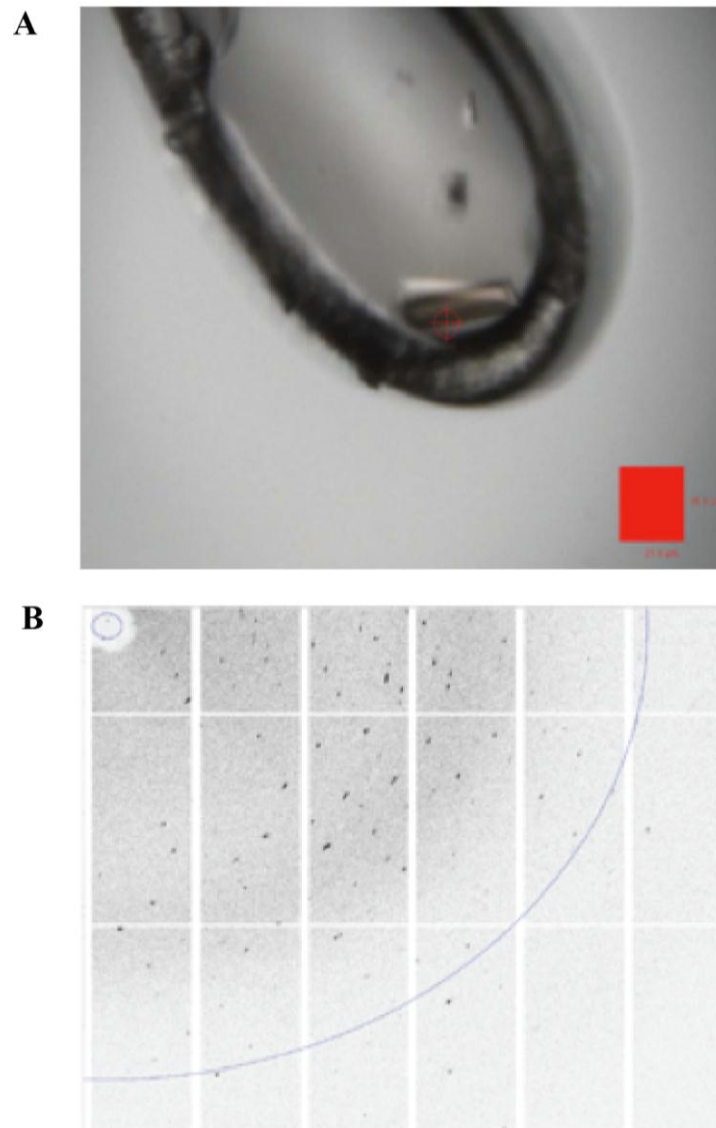


**Figure 4.3: Image of a BCL6 BTB-POZ domain crystal grown in the presence of rifabutin and the diffraction pattern produced.**

(A) An image of the BCL6 BTB-POZ domain crystal mounted in a loop at the Diamond Synchrotron, beamline I24. (Red box represents 25.9 \* 25.9  $\mu\text{m}$ ). (B) Diffraction image of the crystal diffracting to a resolution of 2.3Å as indicated a by the outer blue line.

### 4.3.3 - Data processing

The diffraction data were indexed, integrated and scaled using XDS (X-ray Detector Software) automatically at the Synchrotron. The data were also processed in house using iMosflm, Pointless and Aimless (Leslie 2006; Evans et al. 2013). Pointless and Aimless are part of the CCP4 (Collaborative Computational Project, Number 4 1994) Software Suite. The CCP4 Software Suite is comprised of numerous crystallographic software programs which can be used to determine macromolecular structures by X-ray crystallography.

Data processing can essentially be divided into distinct stages known as indexing, integration and data reduction. Both the indexing and integration steps were performed using iMosflm. Indexing is primarily based upon spot (reflection) positioning. Initially, two diffraction images are chosen, this is generally the first image, with the second image rotated away from the first image by approximately 90°. A spot search is then carried out on both images. The spots found are highlighted based on their intensity when compared to the default intensity setting within iMosflm, which is usually 20, but this can be reduced for weak images (using iMosflm: red indicates the intensity is above the threshold and yellow indicates an intensity below the threshold).

Spots found above the minimum threshold are then used for indexing. Indexing provides an approximation of unit cell dimensions (which gives an indication to the likely Laue group of the crystal), the orientation of the crystal within the x-ray beam (in addition to parameters such as the wavelength of radiation and the distance between the crystal and the detector), and an initial estimate of the Bravais lattice. These components enable the prediction of the position of each spot on the image. Based on this information, a list of solutions is made, arranged in order of increasing penalty score. The preferred solution is generally the one with the highest symmetry and the lowest penalty score. Following indexing, cell parameters are further refined before integration using the method known as post-refinement.

Following post-refinement, the next stage of data processing is known as

integration. Integration involves determining the intensity of each reflection ( $I$ ) and their uncertainties ( $\sigma I$ ), as well as deducting background noise. This step is extremely important because any background noise integrated at this stage can negatively affect the data. Other corrections are also applied at this stage. At the end of integration, an MTZ file is generated, which contains the information produced from the steps above.

Following the integration of the observed diffraction spots (reflections), the process of data reduction initially aims to determine the true Laue symmetry and to determine the likely space group. The space group provides information about the symmetry of a crystal and the complete group of crystal symmetry operations that generate the three-dimensional lattice and defines its symmetry. This step is performed by Pointless.

The data is then scaled using the program Aimless. During scaling, the average intensity for equivalent reflections in addition to merging partially recorded reflections across a number of adjacent images is determined. This places all reflections and allows estimates of the structure amplitudes to be derived from the intensities on a common scale, this produces a data set that is internally consistent (Evans 2006; Evans et al. 2013). This produces statistics that provide the first important measures of data quality.

#### **4.3.4 - Model building and refinement**

In order to determine a structure from the diffraction data, both the amplitudes and the phases of the reflections are required. However, only the intensity of the waves can be detected during data collection. A method used to overcome this problem is Molecular Replacement (MR). Molecular Replacement is a computational technique used to calculate the phases of an unknown structure based on the phases calculated from a homologous molecule (which should possess >30% sequence identity to the target protein). By combining these calculated phases with the amplitudes experimentally determined an electron density map is created into which a model can be built. The process involves computationally rotating on translating the model structure and comparing the calculated amplitudes and with those observed. .

Crystal structures of the BCL6 BTB-POZ domain in complex with co-repressors, small molecules and in its apo form have previously been solved (PDB ID 1R2B (Ahmad *et al.* 2003), PDB ID 3BIM (Ghetu *et al.* 2008), PDB ID 3LBZ (Cerchietti, Ghetu, *et al.* 2010a), PDB ID 3E4U (Stead *et al.* 2008b)). This enabled the structures of rifamycin SV and rifabutin in complex with the BCL6 BTB-POZ domain to be solved by Molecular Replacement. Molecular Replacement was carried out using Phaser (McCoy *et al.* 2007) and the BCL6 BTB-POZ domain in complex with SMRT (1R2B). A clear electron density map was produced for each complex.

Model building into the electron density map and structural refinement performed using the programs Coot (Emsley *et al.* 2010) and Refmac5 (Murshudov *et al.* 2011) respectively. Rifabutin was built into the extra density observed after the initial round of refinement. Iterative rounds of model building and refinement followed, and with each round the map improved. Water molecules were added at the later stages. There was no extra density visible for rifamycin SV within its complex.

Statistics of the refinement for rifamycin SV and rifabutin in complex with the BCL6 BTB-POZ domain are shown in tables 4.2 and 4.3 respectively.

#### **4.4 - Structure of rifamycin SV in complex with the BCL6 BTB-POZ domain**

Analysis of the diffraction data for rifamycin SV co-crystallised with the BCL6 BTB-POZ domain produced a clear electron density map at a resolution of 1.5Å (Data statistics in Table 4.2). However, there did not appear to be any density within the 2Fo-Fc map readily identifiable for rifamycin SV (Figure 4.4). The absence of rifamycin SV in the complex seems to be due to crystal packing. The location on the BTB-POZ domain where rifamycin SV would be expected to bind, due to the data observed for rifabutin, suggests the binding region is in close proximity to Tyr-58. However, this pocket was involved in crystal packing with a symmetry related molecule (Figure 4.5).

<b>BCL6/Rifamycin SV</b>	
<b>Data Collection</b>	
Space Group	C 1 2 1
Cell dimensions	
<i>a, b, c</i> (Å)	140.96, 32.75, 48.90
$\alpha, \beta, \gamma$ (°)	90, 94.64, 90
Resolution (Å)	41.69-1.5 (1.53-1.5)
<i>R</i> <sub>merge</sub> (%)	8.4 (59.1)
<i>I</i> / $\sigma$ <i>I</i>	16.8 (5.8)
Completeness (%)	96.83 (97)
Redundancy	6.9 (6.0)
<b>Refinement</b>	
Resolution (Å)	1.5
No. reflections	33211
<i>R</i> <sub>work</sub> / <i>R</i> <sub>free</sub>	18.7/22.4
No. Atoms	2046
Protein	1927
Water	119
B-factors	
Protein	14.9
Water	20.9
R.M.S. deviations	
Bond lengths (Å)	0.022
Bond angles (°)	2.032

\*Highest resolution shell is shown in parenthesis.

**Table 4.2: Data collection and refinement statistics of the BCL6 BTB-POZ domain crystallised in the presence of rifamycin SV.**

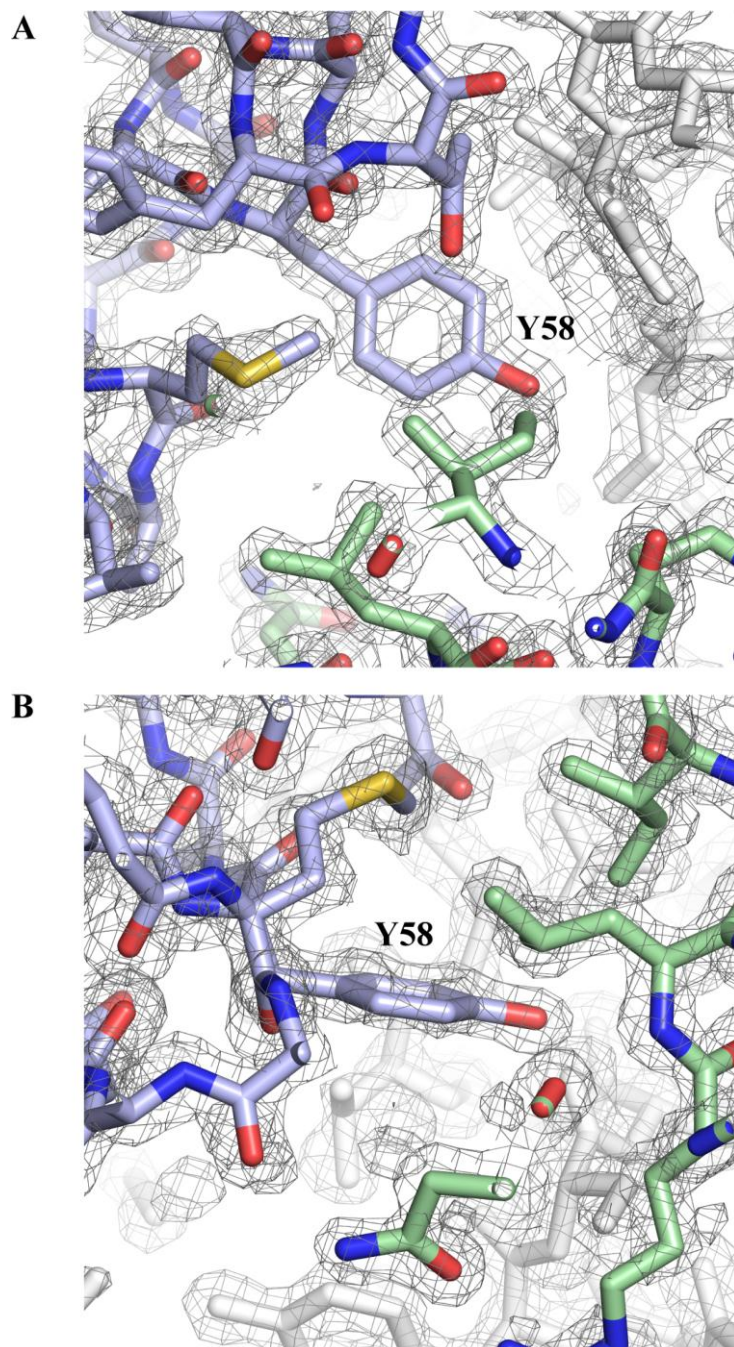


**Figure 4.4: Electron density of the BCL6 BTB-POZ domain crystallised in the presence of rifamycin SV.** Crystal diffracted to 1.5Å. A section of the 2Fo-Fc density map for the BCL6 BTB-POZ contoured at 1σ. The monomers within the dimer of BCL6 are shown in purple and green. The symmetry related molecule is shown in white. Figures (A) and (B) are shown in different orientations around Tyr-58 of BCL6. Tyr-58 is labelled due to its involvement of binding with rifabutin (see below). (A) and (B) clearly show that there is no available density identifiable for rifamycin SV.

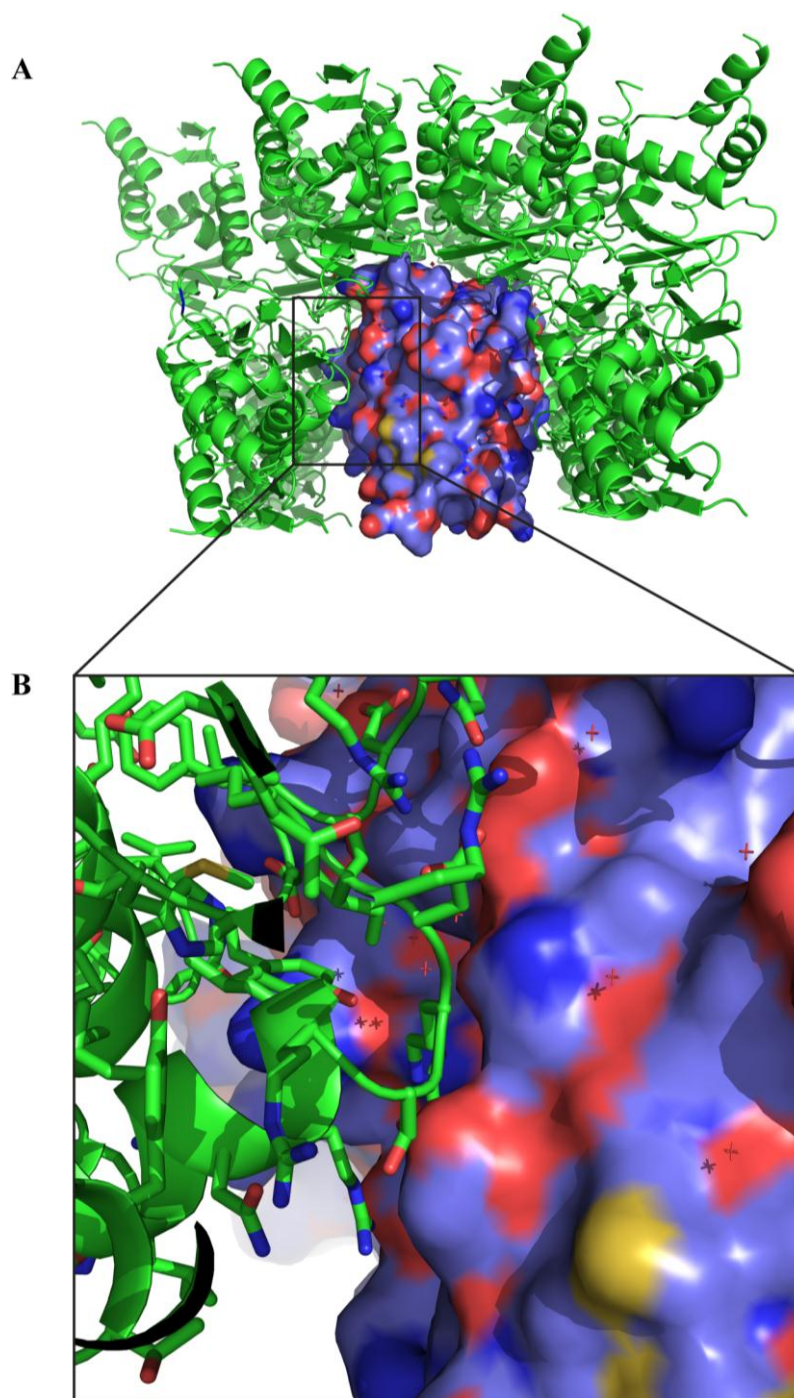


**Figure 4.5: BCL6 BTB-POZ domain crystallised in the presence of rifamycin SV.** (A) A side on view of the BCL6 BTB-POZ domain dimer is shown and represented in surface view (purple), surrounded by symmetry related molecules, which are shown in cartoon representation (green). (B) A close up of the potential binding site of rifamycin SV based upon the rifabutin binding pocket. The side chains of the symmetry molecule are shown to be protruding into a shallow pocket within the lateral groove, filling the space that could potentially accommodate rifamycin SV.

## 4.5 - Structure of rifabutin in complex with the BCL6 BTB-POZ domain

Analysis of the electron density map contoured at  $1\sigma$  for rifabutin in complex with the BCL6 BTB-POZ domain showed clear density for the BCL6 BTB-POZ domain to be modelled into. The map also provided an area of extra density that was not accounted for in the model. The extra unoccupied electron density was clearly identifiable as rifabutin (Figure 4.6).

The naphthoquinone rings of rifabutin are parallel to the aromatic ring of Tyr-58 from one monomer (purple), and appear to form a  $\pi$ -stacking interaction (Figure 4.6A). The ansamycin “handle” of rifabutin makes electrostatic interactions with Asn-21 and Arg-24 from the other monomer (pink) (Figure 4.6B). Surface representation of the BCL6 BTB-POZ dimer shows the binding location of rifabutin residing in a shallow pocket formed within the lateral groove upon dimerisation of BCL6 comprising of basic residues (including Asn-21 and Arg-24) in blue, and acidic residues in red. Despite the BCL6 BTB-POZ domain forming a symmetrical dimer, only one molecule of rifabutin was present and bound across the dimer interface within the asymmetric unit (Figure 4.7A and B). The rifabutin handle is also interacting with a symmetry related dimer of BCL6 (Figure 4.7B).

<b>BCL6/Rifabutin</b>	
<b>Data Collection</b>	
Space Group	P 1 21 1
Cell dimensions	
<i>a, b, c</i> (Å)	35.17, 54.83, 58.16
$\alpha, \beta, \gamma$ (°)	90, 95.21, 90
Resolution (Å)	39.82-2.3 (2.38-2.3)
<i>R</i> <sub>merge</sub> (%)	10.8 (51.8)
<i>I</i> / $\sigma$ <i>I</i>	9.8 (4.1)
Completeness (%)	97.13 (97)
Redundancy	3.0 (2.9)
<b>Refinement</b>	
Resolution (Å)	2.3
No. reflections	9168
<i>R</i> <sub>work</sub> / <i>R</i> <sub>free</sub>	20.2/26.9
No. Atoms	2053
Protein	1969
Rifabutin	61
Water	23
B-factors	
Protein	27.9
Rifabutin	48
Water	24.6
R.M.S. deviations	
Bond lengths (Å)	0.013
Bond angles (°)	1.885

\*Highest resolution shell is shown in parenthesis.

**Table 4.3: Data collection and refinement statistics of the BCL6 BTB-POZ domain crystallised in the presence of rifabutin.**

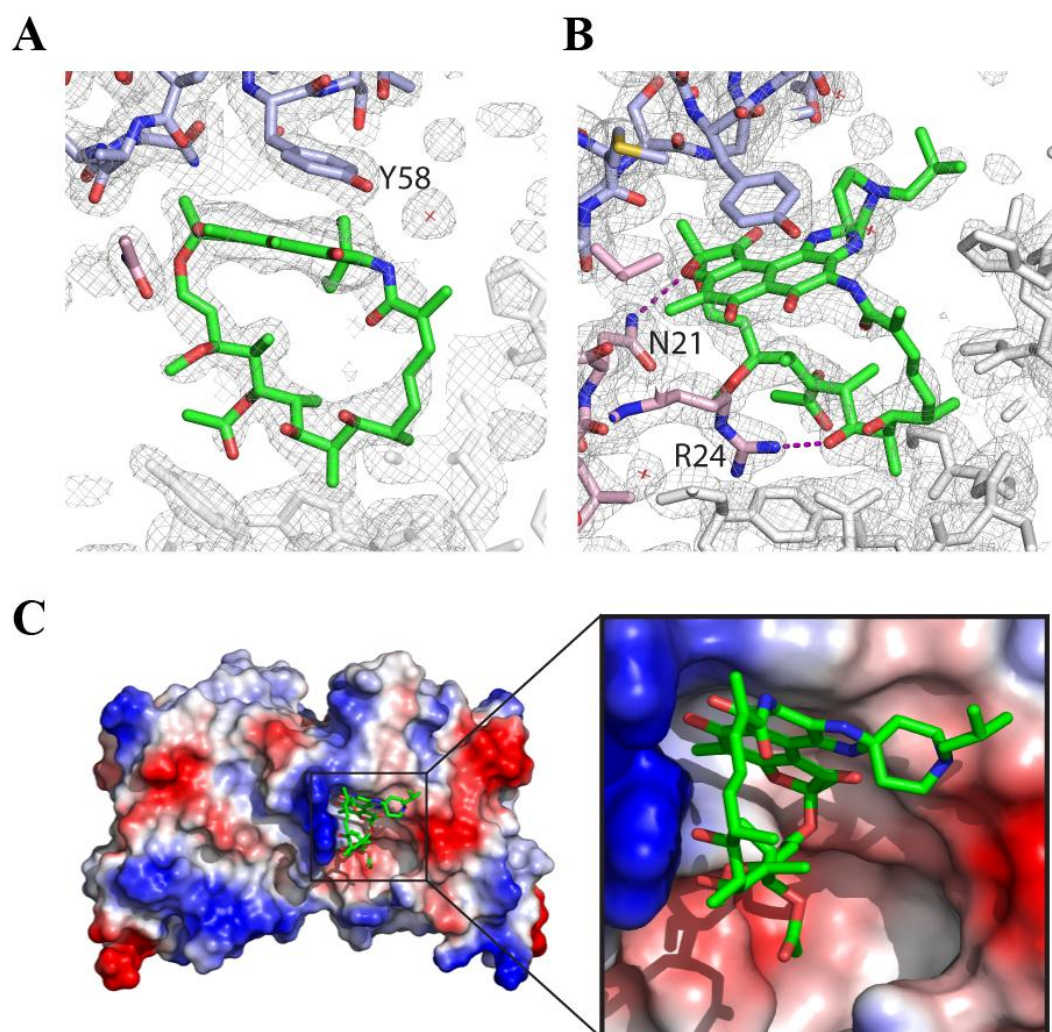


**Figure 4.6: Interaction of BCL6 with rifabutin.**

The 2Fo-Fc density map contoured at 1σ shows clearly that there is density readily interpretable for rifabutin. The interaction of rifabutin can be seen with (A) Tyr-58 from one monomer of the BTB-POZ dimer (purple) and (B) Asn-21 and Arg-24 from the other monomer (pink). The symmetry molecule is shown in white. (C) surface representation of BCL6 BTB-POZ with basic residues (including Asn-21 and Arg-24) in blue, and acidic residues in red.

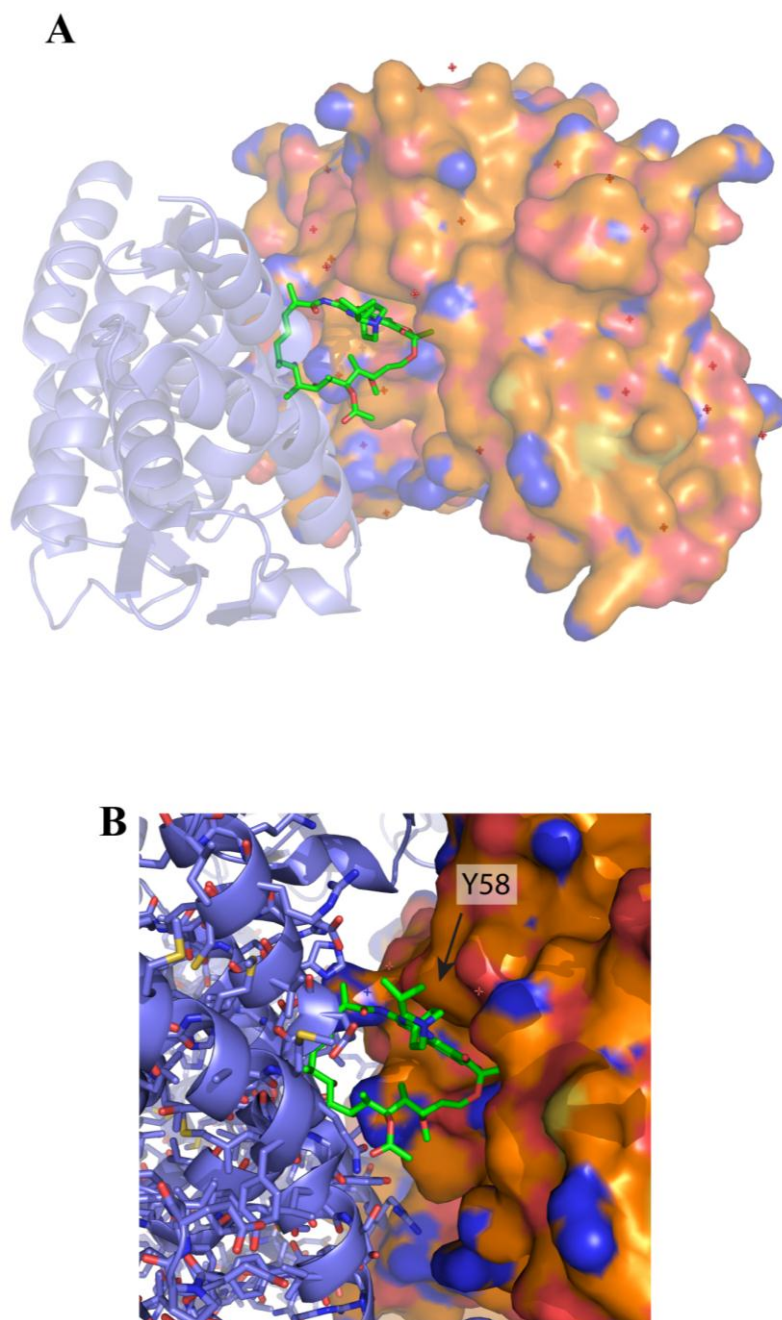


**Figure 4.7: Crystal packing of rifabutin in complex with the BCL6 BTB-POZ domain.**

(A) A side on view of the BTB-POZ domain shown in surface view (orange) with a symmetry related molecule (shown in cartoon, coloured light purple) within 4 Å of the main molecule, with 60% transparency. Rifabutin is shown in stick representation (green). Rifabutin binds to the BCL6 BTB-POZ domain within the lateral groove. The symmetry molecule is rotated 180° and packed against the surface view BTB-POZ (B) Shows the naphthoquinone rings of rifabutin lay parallel with Tyr-58 lining the top of the pocket.

#### **4.6 - Rifabutin binds to the BTB-POZ domain in the same location as the co-repressor SMRT and the small molecule inhibitor, 79-6.**

A comparison between the co-repressors SMRT and BCoR, the small molecule 79-6 and rifabutin shows that all three bind within the same location of the BCL6 BTB-POZ domain (Figures 4.8 and 4.10). SMRT and NCOR possess similar binding sequences for interacting with the BTB-POZ domain, in comparison, BCoR binds through an entirely different amino acid sequence (Ghetu *et al.* 2008).

A small molecule, 79-6, has previously been documented to bind within the shallow pocket formed at the lateral groove upon dimerisation (Cerchietti *et al.* 2010a). Rifabutin binds in a similar location to 79-6 on the BTB-POZ domain (Figure 4.8). The published small molecule inhibitor, 79-6, possesses the ability to kill DLBCL cells in vitro and in vivo, due to the perturbation of SMRT binding (Cerchietti *et al.* 2010a). An alignment of rifabutin and 79-6 reveals the naphthoquinone ring of rifabutin overlaps with the indolazine ring of 79-6, and both molecules are observed protruding into the same pocket, which is empty in the apo structure, and occupied by residues H1426 of SMRT and W509 of BCoR of the co-repressor structures (Figure 4.8). The co-repressors SMRT and BCoR (shown in stick representation, coloured pink and green, respectively) (Figure 4.8) indicate the location of the lateral groove, overlaid with the positions of where rifabutin and 79-6 bind in relation to the co-repressors.

A detailed comparison of the binding of rifabutin and 79-6 was obtained using LIGPLOT (Figure 4.9). LIGPLOT is a bioinformatics computer program that generates schematic 2D representations of protein-ligand complexes from 3D co-ordinates found within Protein Data Bank (PDB) files (Wallace *et al.* 1995). The LIGPLOT diagrams represent intermolecular interactions including hydrogen bonds (indicated by dashed lines between the atoms involved) and hydrophobic interactions (represented by an arc with spokes radiating towards the ligand atoms they contact). The LIGPLOT analysis of rifabutin and 79-6 reveal strikingly similar interactions with the BCL6 BTB-POZ domain. Comparison of the LIGPLOT schematic of rifabutin in complex with BCL6 (Figure 4.9A) (PDB ID 4CP3), and the small molecule inhibitor 79-6 in complex with BCL6, (Figure 4.9B) (PDB ID 3LBZ), indicates common hydrophobic interactions with

the BTB-POZ domain such as Tyr-58, and electrostatic interactions with Asn-21 and Arg-24 (Figure 4.9C). In addition, the comparison also shows that 79-6 forms hydrogen bonds with Met-51 and Arg-28, whereas rifabutin forms a hydrophobic interaction with Met-51. The binding affinity of 79-6 with the BCL6 BTB-POZ domain is 140 $\mu$ M (Cerchietti *et al.* 2010a), this is approximately 10x higher than the 1.4mM affinity of rifabutin for BCL6 as estimated by NMR titrations (Figure 3.12b).

Hence the X-ray crystal structure of rifabutin demonstrates that it binds in a very similar manner to 79-6 and makes contact with the same residues of the BCL6 BTB-POZ domain (Figure 4.9). This observation is of significant interest because it is also the same binding site for the co-repressor SMRT. The fact that both rifabutin and 79-6 bind in the same place as SMRT highlights an area of the BCL6 BTB-POZ domain that is functionally important with a potential of being a druggable site for the inhibition of co-repressor binding.

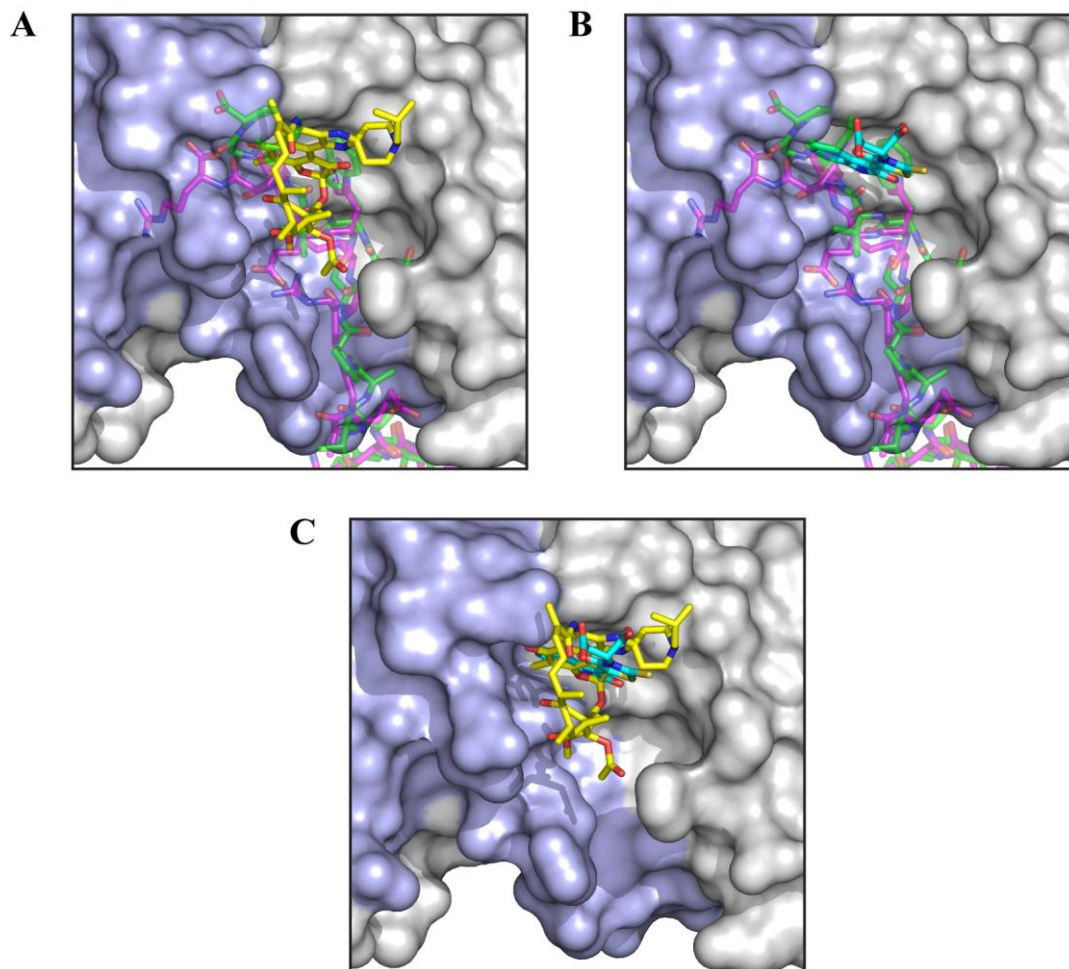


**Figure 4.8: A comparison between SMRT, BCoR, 79-6 and rifabutin to the BCL6 BTB-POZ domain.**

(A) and (B) are a comparison of binding location between (A) rifabutin (shown in yellow) and (B) 79-6 (shown in cyan). In addition (A) and (B) show the binding location of the co-repressors SMRT and BCoR (pink and green respectively) shown in stick representation with transparency effect. Figure (C) is an overlay of rifabutin and 79-6. Each monomer (grey and purple) is shown in surface view.

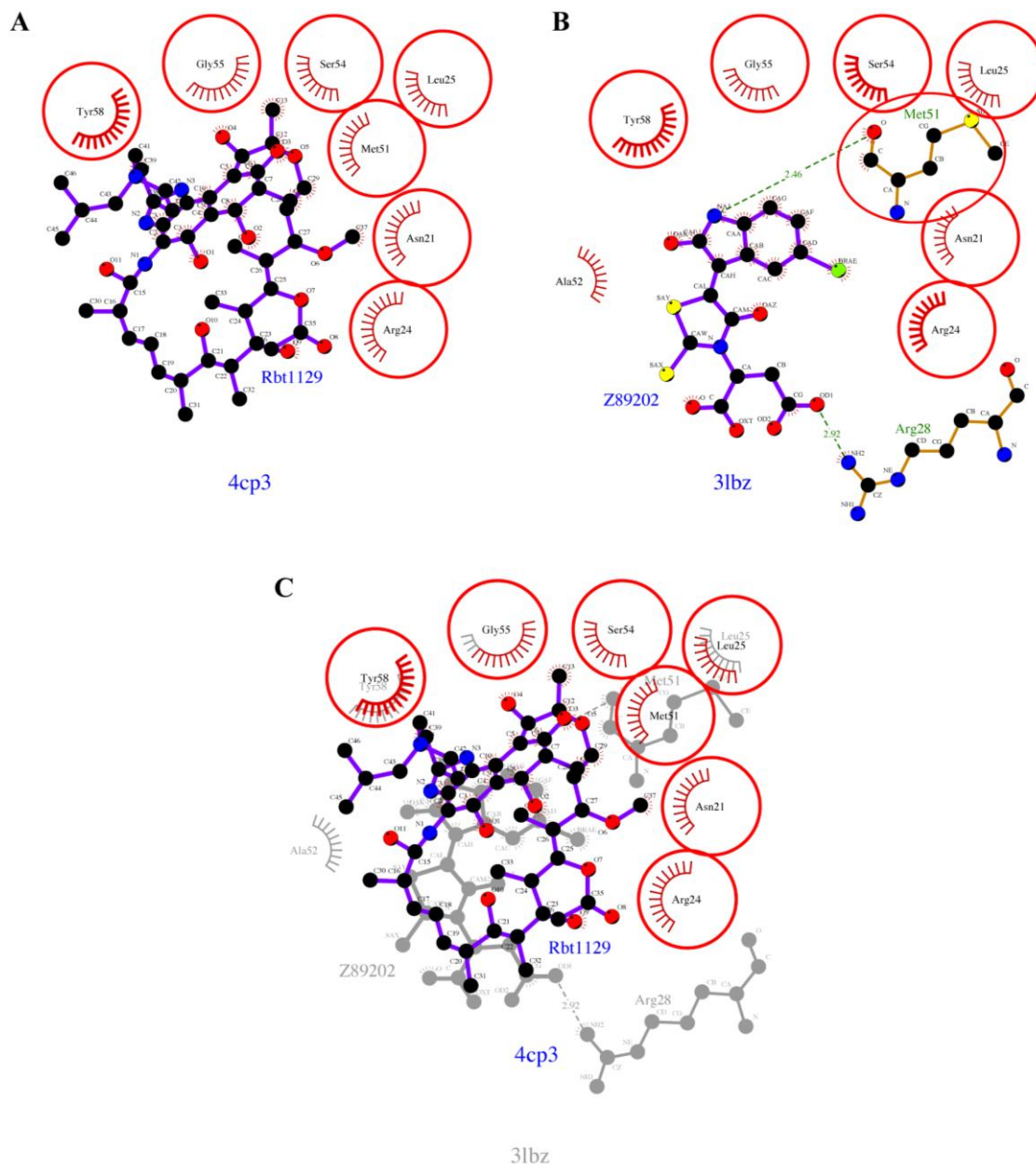


**Figure 4.9: Schematic diagrams of protein-ligand interactions generated from the 3D co-ordinates located within their respective PDB files.**

LIGPLOT diagrams represent intermolecular interactions including hydrogen bonds (indicated by dashed lines between the atoms involved) and hydrophobic interactions (represented by an arc with spokes radiating towards the ligand atoms they contact). (A) BCL6 in complex with rifabutin (PDB ID 4CP3). (B) BCL6 in complex with the small molecule inhibitor, 79-6 (PDB ID 3LBZ). (C) A superimposition of common interactions shared between rifabutin and 79-6. Images produced by the bioinformatics program LIGPLOT.

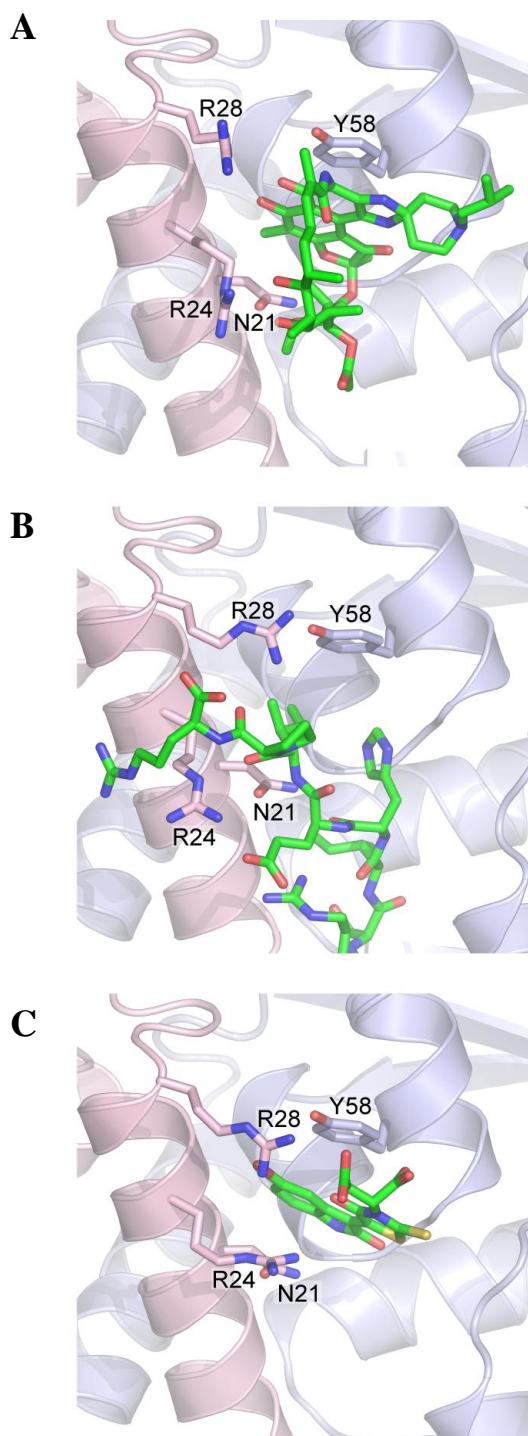


**Figure 4.10: A comparison between the binding locations of rifabutin, SMRT and 79-6 on the BCL6 BTB-POZ domain.**

Each view within the panel shows identical orientations of the BCL6 BTB-POZ domain in complex with (A) rifabutin, (B) SMRT and (C) 79-6.

## 4.7 - Discussion

This chapter describes co-crystallisation experiments for the ansamycin antibiotics rifamycin SV and rifabutin in complex with the BCL6 BTB-POZ domain.

Crystals of the BCL6 BTB-POZ domain in the presence of rifamycin SV and in complex with rifabutin were obtained. The 2Fo-Fc electron density map provided an area of extra density that was clearly identifiable as rifabutin (Figure 4.6). However, despite the structural similarity of these molecules (Chapter 3), the rifamycin SV-BCL6 complex did not produce crystals with rifamycin SV bound. As estimated by NMR titration experiments, the affinity of rifamycin SV to the BTB-POZ domain is weaker compared to the affinity of rifabutin. In addition, each complex was solved in a different space group (rifamycin SV, C1 2 1 and rifabutin, P1 21 1), therefore two different packing environments. Crystal packing of the rifamycin SV-BCL6 complex clearly shows a loop belonging to a symmetry molecule protruding into the groove that would be expected to accommodate rifamycin SV, based upon the location where rifabutin binds to the BTB-POZ domain, therefore preventing rifamycin SV binding within the crystal complex (Figure 4.5).

The crystal structure of the rifabutin-BCL6 complex shows that one molecule of rifabutin is bound within a shallow pocket on the dimer interface in the asymmetric unit (Figure 4.7). Interestingly, this is also the site occupied by the SMRT, NCoR and BCoR peptides, in addition to the small molecule inhibitor, 79-6 (Ahmad *et al.* 2003; Ghetu *et al.* 200; Cerchietti *et al.* 2010a) (PDB ID 1R2B, 3BIM and 3LBZ respectively). The comparison of all four crystal structures, (SMRT, BCoR, 79-6 and rifabutin) reveals a common binding site on the BTB-POZ domain located within the lateral groove formed upon dimerisation (Figures 4.8 and 4.10).

Peptides based upon the minimum sequence required for SMRT binding to BCL6, termed the BCL6 BTB Binding Domain (BBD), are able to specifically inhibit the transcriptional repressor activity of BCL6 by blocking the lateral groove and in addition, kill DLBCL cells *in vitro* and *in vivo* (Polo *et al.* 2004; Cerchietti *et al.* 2009). A small molecule, 79-6, derived from an in-silico screen, was able to disrupt the ability

of BCL6 to recruit SMRT and NCoR to the lateral groove of the BTB-POZ domain, leading to reactivation of BCL6 target genes in BCL6 dependent DLBCL cells, a function that has previously been shown to be required to kill lymphoma cells (Cerchietti *et al.* 2009). This common feature in binding between SMRT, BCoR and 79-6 suggests that the BCL6 BTB-POZ domain is indeed the druggable target site for BCL6.

As shown in Figure 4.8, rifabutin and 79-6 bind to the BTB-POZ domain within the same shallow groove. The indolazine ring of 79-6 forms a hydrophobic interaction with Tyr-58 located on one monomer of the BTB-POZ domain, in comparison, the naphthoquinone ring of rifabutin occupies this same space, and also forms a hydrophobic interaction with Tyr-58 (Figures 4.9 and 4.10). The binding of SMRT perturbed by the presence of 79-6 within this specific site, and as a result, leading to the reactivation of target genes provides information on the importance of this region. Due to the similarity in structure and binding position of 79-6 and rifabutin, it was speculated whether rifabutin could also prevent SMRT binding to the BCL6 BTB-POZ domain.

Residues of SMRT and BCoR involved in binding to the shallow pocket, in addition to the structural similarity of rifabutin and 79-6 will be explored further in Chapter 5

## **Chapter 5 - Are there specific effects of rifabutin on cellular function or co-repressor binding?**

### **5.1 - Introduction**

It has been shown using NMR and X-ray crystallography that rifabutin binds to the BCL6 BTB-POZ domain in a shallow pocket formed within the lateral groove (Chapters 3 and 4). Interestingly, it is the same region that is occupied by SMRT, NCoR and BCoR (Figures 4.8 and 4.10) and by the previously described BCL6 small molecule inhibitor, 79-6 (Cerchiatti *et al.* 2010). The residues that line the surface of the BCL6 lateral groove and mediate the interactions with the co-repressors are not conserved within the BTB family, making this an attractive site to target the BCL6 co-repressor interaction with small molecules and peptides (Ahmad *et al.* 2003; Stogios *et al.* 2006; Ghetu *et al.* 2008). Indeed, peptides and 79-6, which target this site, have already demonstrated the ability to interfere with co-repressor binding and produce functionally important effects on survival of DLBCL cell lines thus demonstrating potential clinical utility.

The BCL6-rifabutin structure (Chapter 4) revealed that rifabutin binds to BCL6 in the same location as 79-6 (Figure 4.8); leading to speculation that rifabutin might also be able to perturb the BCL6/co-repressor interaction. The aims of the work presented in this chapter are to investigate the effects of rifamycin SV and rifabutin on a BCL6 expressing cell line, DG75-AB7, to explore whether rifamycin SV or rifabutin can compete with SMRT for binding to the BTB-POZ domain and to produce a peptide with higher affinity for BCL6 than the native SMRT-BBD. To achieve this, modified SMRT-BBD peptides were designed which incorporated different artificial amino acids in place of H1426.

## 5.2 - Results

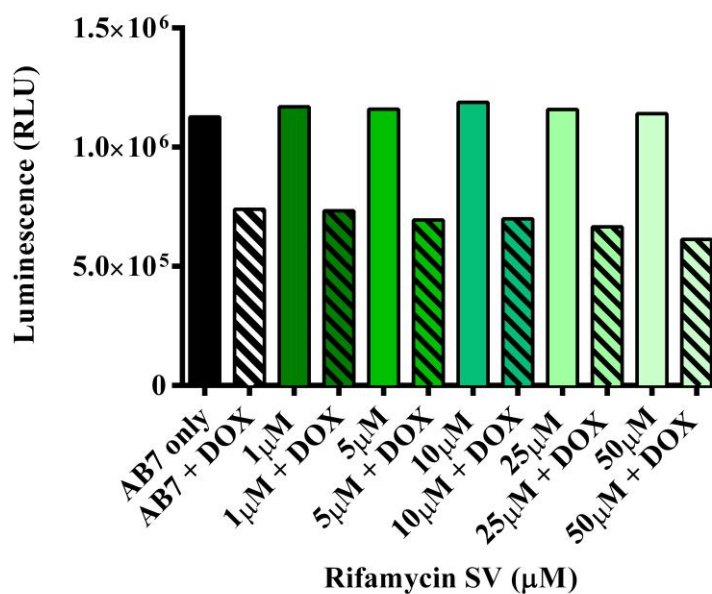
### 5.2.1 - Investigating the effects of rifabutin and rifamycin SV on cell viability.

To test the effects of rifabutin and rifamycin SV on cell viability, the DG75-AB7 cell line (produced by Dr. Simon Wagner, University of Leicester and Dr Andy Porter, Imperial College London) was used. DG75-AB7 bears homozygous disruption of its BCL6 alleles and harbours a tet-off system for the controlled expression of BCL6. When cultured in doxycycline (DOX), BCL6 expression is switched off, making this an ideal platform to investigate the effects of compounds on BCL6. DG75-AB7 cells were initially treated  $\pm$  DOX for 4 days followed by treatment with rifabutin or rifamycin SV at a range of concentrations (0, 1, 5, 10, 25 and 50 $\mu$ M) for 24 hours. Cell viability was measured using the Cell Titre Glo assay (CTG) (Section 2.10); the levels of luminescence represent cell viability with lower values indicating reduced viability (Figure 5.1).

DG75-AB7 has advantages as a cell line to test BCL6 inhibitors because the effects of BCL6 deficiency on growth can be precisely determined allowing the effects of potential inhibitors to be assessed. In addition, a targeted BCL6 inhibitor is anticipated to have no effect on DG75-AB7 that is rendered BCL6 deficient by culture in DOX.

DG75-AB7 cells treated with rifamycin SV alone showed no change in cell viability with increasing concentration of rifamycin SV when compared to untreated cells (Figure 5.1A). The combined treatment of DOX and rifamycin SV again showed no additional effect of the drug (Figure 5.1A). In comparison, cells treated with rifabutin alone showed a decrease in cell viability, in a concentration dependent manner (Figure 5.1B) but, DOX plus rifabutin also showed a decrease in viability similar to that observed for DOX, and also in a concentration dependent manner suggesting that the observed effects were not mediated through inhibition of BCL6 alone.

A)



B)

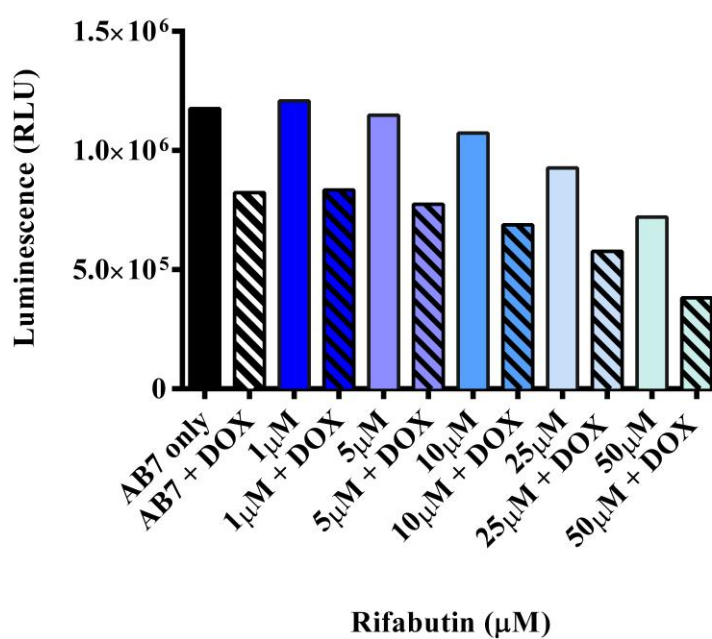


**Figure 5.1: Investigating the effects of rifamycin SV and rifabutin on cell viability.** DG75-AB7 cells were treated with or without DOX for 4 days, followed by the addition of (A) rifamycin SV or (B) rifabutin at a range of concentrations (0-50 $\mu\text{M}$ ) for 24 hrs. Cell viability was measured using the CTG assay and luminescence measured. n=1.

### **5.2.2 - Development of a fluorescence polarisation assays to explore the ability of rifamycin SV and rifabutin to compete with SMRT for binding to BCL6.**

To explore the abilities of rifamycin SV and rifabutin to bind to the BCL6 BTB-POZ domain and compete with SMRT for binding, a fluorescence polarisation (FP) competition assay was developed. Peptides based on the SMRT-BBD and BCoR-BBD sequences, were synthesised with a N- or C-terminal cysteine to allow coupling of a fluorophore for use in FP assays (Table 5.1) (Section 2.11).

In order to carry out an FP competition assay, the affinity of the fluorescently labelled peptide for the protein needs to be determined. Binding curves of Bodipy labelled SMRT and BCoR peptides binding to the BTB-POZ domain of BCL6 were obtained. The BCL6 BTB-POZ domain protein was titrated with a fixed concentration of fluorescently labelled ligand (1 $\mu$ M), resulting in similar K<sub>d</sub> values for both SMRT and BCoR (2.8 and 3.1 $\mu$ M) respectively, (Figure 5.2A) which are in line with published figures (Ghetu *et al.*, 2008). The binding curve was then used to determine the concentration of the BCL6 BTB-POZ domain when 50% is occupied by ligand, which in this case was 3 $\mu$ M (Figure 5.2A).

For the competition assays, the competing compound or peptide was titrated with a fixed concentration of BCL6 BTB-POZ domain protein (3 $\mu$ M), and a fluorescently labelled peptide (1 $\mu$ M). The small molecule inhibitor 79-6 was used as a positive control for competition. By measurement of the chemical shifts induced by increasing concentrations of 79-6 observed in NMR experiments, Cerchiatti *et al* shown that 79-6 has a K<sub>d</sub> 138 $\pm$ 31 $\mu$ M (Cerchiatti, Ghetu, *et al.* 2010a). A competitive binding curve showing the displacement of the labelled peptide from the BCL6 BTB-POZ domain in the presence of 79-6 was produced, showing an IC<sub>50</sub> value of  $\sim$ 140 $\mu$ M. (Figure 5.2B). 79-6 was found to successfully compete with SMRT for binding to the BTB-POZ domain. Rifabutin and rifamycin were tested for their ability to compete with SMRT for binding to the BCL6 BTB-POZ. However, it was not possible to show that rifabutin or rifamycin SV could displace the SMRT-BBD and therefore an IC<sub>50</sub> could not be determined for either compound (Figure 5.2C). The inability of Rifabutin and

rifamycin to displace the SMRT-BBD could be due to the large difference in  $K_d$  between the SMRT-BBD and rifabutin for BCL6.

To try to determine an accurate  $IC_{50}$  for rifabutin by FP, peptides based upon the SMRT-BBD was designed to bind to BCL6, but with weaker affinity than the wild-type SMRT-BBD, potentially enabling rifabutin an opportunity to compete with SMRT. All peptides tested included an N- or C-terminal cysteine residue for coupling of the Bodipy-TMR (Table 5.1).

Mutations and/or deletions based upon the data published by Ahmad *et al*, 2003, within the SMRT-BBD (residues 1414-1430) produced various effects on BCL6 binding affinity. Full length/wild-type SMRT-BBD and various peptides corresponding to different lengths of the SMRT-BBD were tested for their abilities to bind to BCL6 using an FP assay. Out of the six peptides designed with mutations and/or deletions, only two showed binding to the BCL6 BTB-POZ domain, and both retained the same binding affinity as the wild-type SMRT-BBD (Figure 5.2D and Table 5.1). In this assay, the SMRT-BBD sequences investigated displayed ‘all or nothing’ binding to the BCL6 BTB-POZ domain. A peptide with lower binding affinity, which might have been useful in determining  $IC_{50}$  of rifamycin SV or rifabutin, could not be obtained.

Protein	Peptide sequence	Domain boundaries	Aa	Kd ( $\mu$ M)	Bound
SMRT	LVATVKEAGRSIHEIPR	1414 – 1430 (BBD)	17	-	-
SMRT	<b>C</b> LVATVKEAGRSIHEIPR	1414 – 1430 (BBD)	18	1.8	✓
SMRT	<b>C</b> LVATVKEAGRS <u>V</u> HEIPR	1414 – 1430	18	2	✓
SMRT	<b>C</b> ATVKEAGRSIHEIP	1416 – 1429	15	1.8	✓
SMRT	<b>C</b> ATVKEAGRSIHE <u>A</u> P	1416 – 1429	15	-	✗
SMRT	<b>C</b> KEAGRSIHEIPR	1419 – 1430	13	-	✗
SMRT	KEAGRSIHEIPR <b>C</b>	1419 – 1430	13	-	✗
SMRT	<b>C</b> GRSIHEIPR	1422 – 1430	10	-	✗
BCoR	RSEIISTAPSSWVVP GP	498 – 514 (WT)	17	-	-
BCoR	<b>C</b> RSEIISTAPSSWVVP GP	498 – 514 (WT)	18	3.1	✓

**Table 5.1: Comparisons between the bindings of different lengths of the BBD peptides to BCL6.**

Peptides based upon the SMRT-BBD sequence were synthesised with an N- or C-terminal cysteine to allow coupling of a fluorophore (denoted by the magenta C within the peptide sequence). Peptides were designed based upon the data published by Ahmad *et al*, 2003, substitutions of amino acids are shown underlined in blue. Specific residues of the SMRT-BBD were deleted and/or substituted to produce a version of SMRT-BBD that could bind to the BTB-POZ domain with weaker affinity to allow rifabutin the opportunity to displace the SMRT-BBD. Peptides that bound and their respective binding affinities (Kd) are shown in the table.

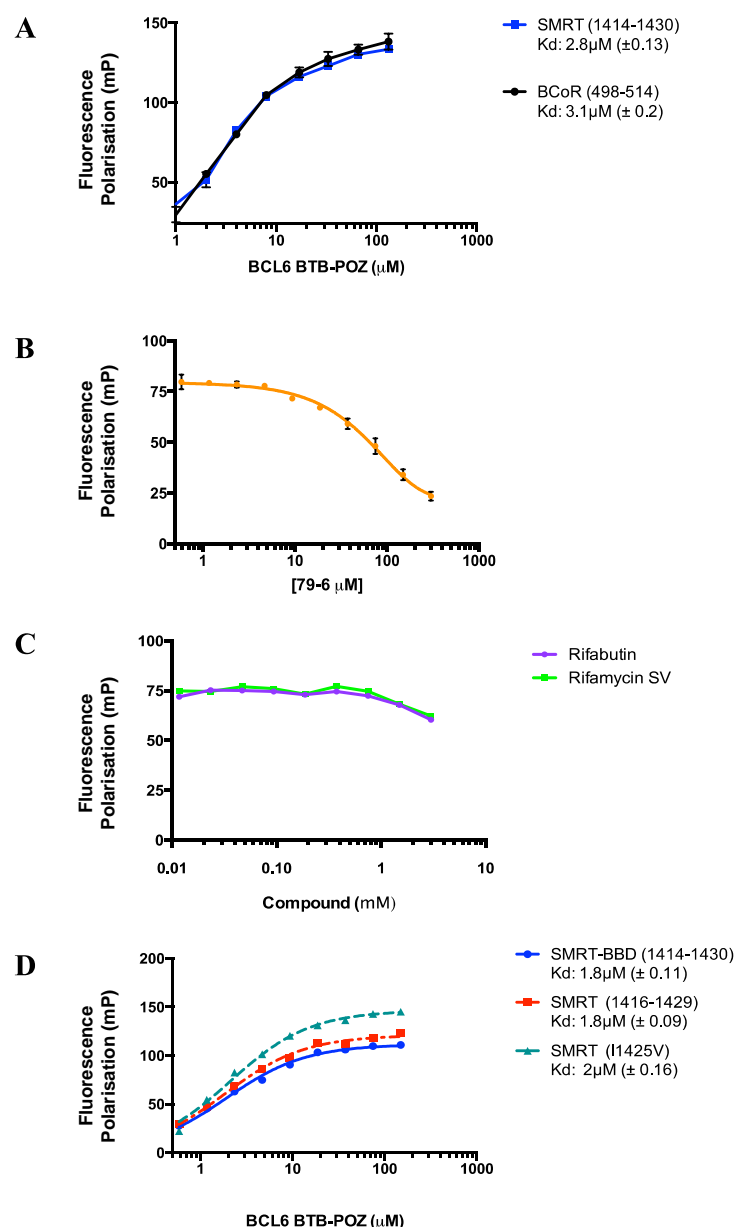


**Figure 5.2: Fluorescence polarisation assays used to investigate the ability of rifabutin and rifamycin SV to displace SMRT from the BCL6 BTB-POZ domain.**

(A) Binding of SMRT and BCoR peptides to BCL6. Competition assays (B) and (C) were performed using  $3\mu\text{M}$  BCL6 BTB-POZ and  $1\mu\text{M}$  SMRT. (B) Competitive binding curve of 79-6 displacing SMRT from the BCL6 BTB-POZ domain, (C) Rifabutin and rifamycin SV tested for the ability to displace SMRT and (D) binding curves of peptides based on the SMRT-BBD comprising of mutations and/or deletions to produce a weaker binding peptide for the BCL6 BTB-POZ domain. Binding curves were fitted using one site binding based on the equation  $Y=B_{\text{max}}*x/(K_d+x)$ . Error bars on (A) and (B) represent SEM calculated from 3 independent experiments. Peptides synthesised by Biomatik.

### 5.2.3 - Development of a substituted SMRT-BBD peptide

The naphthoquinone ring of rifabutin occupies a small pocket formed upon dimerisation within the lateral groove of the BCL6 BTB-POZ domain, near Tyr-58, which is empty in the apo structure (Chapter 4). This region is also occupied by residue H1426 of SMRT, or W509 of BCoR in the co-repressor structures (Figure 5.3) (Ahmad *et al.* 2003; Ghetu *et al.* 2008). The naphthoquinone ring of rifabutin makes  $\pi$ -stacking interactions with Tyr-58 from one BCL6 chain and the aliphatic handle of rifabutin has electrostatic interactions with Asn-21 and Arg-24 from the other chain (Figure 4.6). The perturbation of co-repressor binding by 79-6, which binds in this same region has been shown by gene expression profiling to reactivate critical target genes of BCL6 and cause apoptosis of BCL6-dependent lymphoma cell lines (Cerchietti, Ghetu, *et al.* 2010a).

Therefore, in order to explore the importance of H1426 of SMRT in the binding pocket of the BTB-POZ domain, peptides were designed with various artificial amino acids replacing H1426 to mimic the structural similarities to those of SMRT, 79-6, BCoR and rifabutin, for the production a peptide with potentially higher affinity for BCL6 than the native SMRT-BBD for the perturbation of native SMRT from the lateral groove (Figure 5.4). Substituted SMRT-BBD peptides were synthesised by Dr Andrew Jamieson, University of Leicester.

An FP assay was used to compare the binding affinities between the artificial amino acid SMRT-BBD peptides and the native SMRT-BBD (1414-1430) to the BCL6 BTB-POZ domain. The  $K_d$  of the native SMRT-BBD was measured as  $5\mu\text{M}$  (Figure 5.5A). All of the artificial amino acids used to replace H1426 of SMRT showed a reduced binding affinity to the BTB-POZ domain compared to native SMRT-BBD (Figure 5.5A). Whilst the peptide bearing a 1-naphthyl residue had a binding affinity of  $11\mu\text{M}$ , the 2-naphthyl peptide had a much lower binding affinity of  $154\mu\text{M}$ . Homophenylalanine and styryl side chains were employed to place aromatic rings, potentially capable of interacting with Tyr-58, within closer proximity to the BTB-POZ domain than H1426 found in the native SMRT-BCL6 structure, and both exhibited intermediate affinities. In silico modelling of these artificial amino acids, in the same

orientation as H1426 shows that (Figure 5.5B-F), whilst 1-naphthyl is orientated well within the pocket, 2-naphthyl clashes with the BCL6 BTB-POZ domain, which is likely to prevent specific binding.

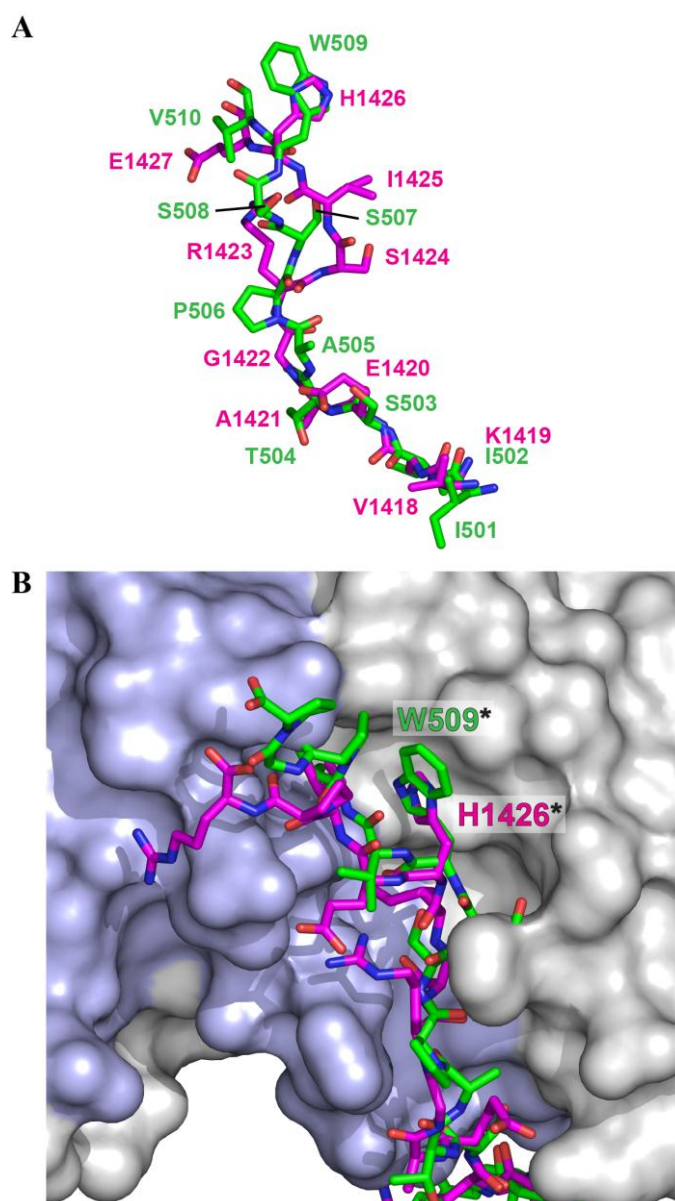


**Figure 5.3: Overlay of H1426 of SMRT and W509 of BCoR binding to the BTB-POZ domain of BCL6.**

(A) Superimposed structures of SMRT-BBD (magenta) and BCoR-BBD (green) and (B) a view of the BCL6 BTB-POZ domain in complex with SMRT and BCoR located within the lateral groove with two key residues highlighted. Images produced using MacPyMOL. Adapted from (Ghetu *et al.* 2008)

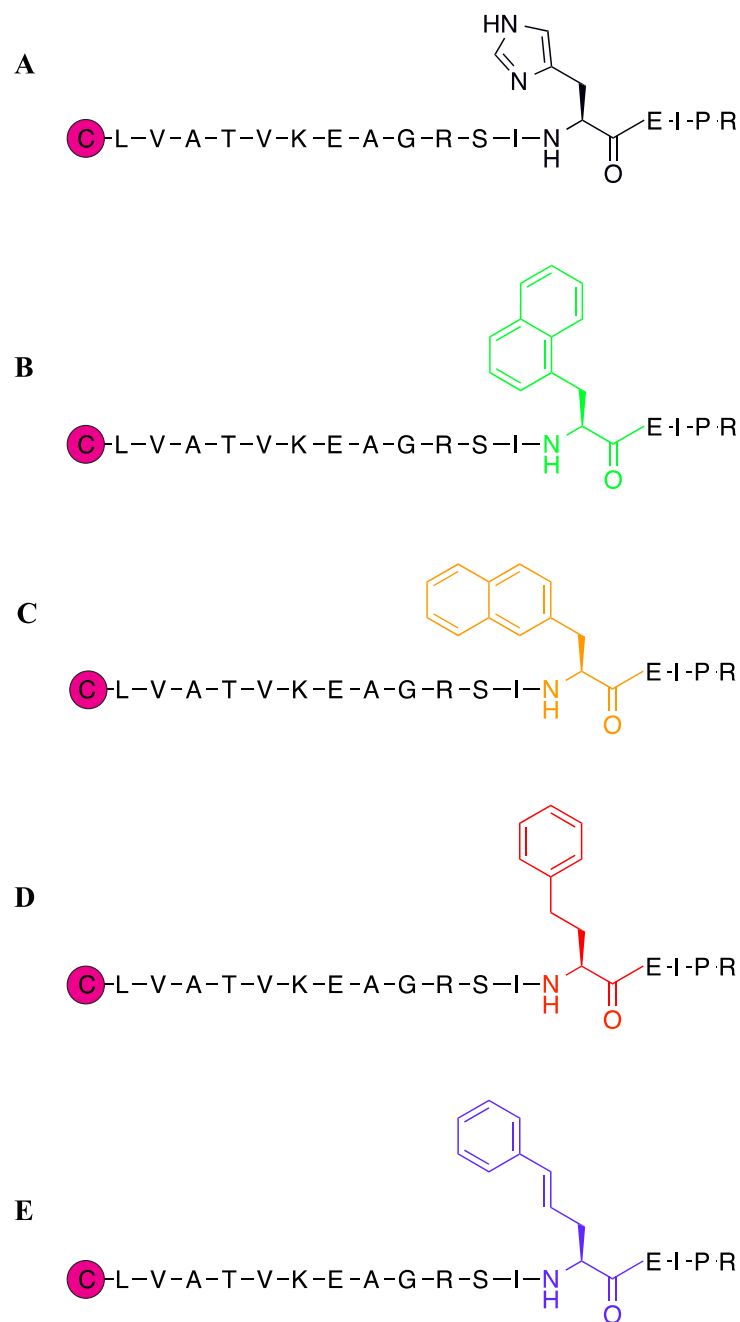


**Figure 5.4: SMRT-BBD peptides replacing H1426 for an artificial amino acid.**

Peptides based upon the SMRT-BBD sequence were synthesised with an N-terminal cysteine residue, which allowed coupling of a fluorophore for use in an FP assay. H1426 was replaced with an artificial amino acid. (A) Native SMRT, (B) 1-naphthyl, (C) 2-naphthyl, (D) homophenylalanine and (E) styryl. Peptides were synthesised by Dr. Andrew Jamieson in the chemistry department at the University of Leicester.

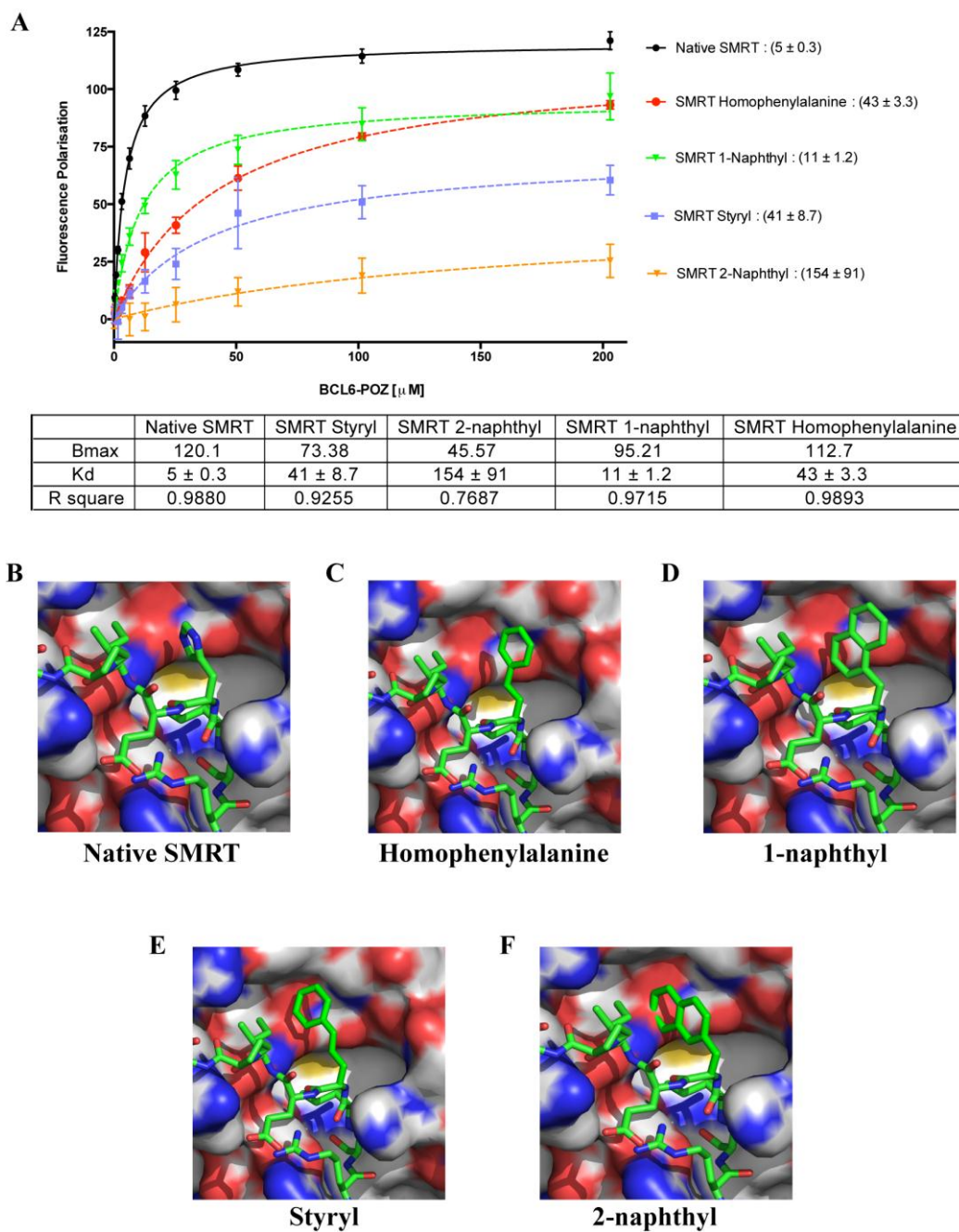


**Figure 5.5: SMRT peptide containing artificial amino acids in place of H1426 to explore binding to the BCL6 BTB-POZ domain.**

(A) Binding curves determined by fluorescence polarisation for native peptide, 1-naphthyl, 2-naphthyl, styryl and homophenylalanine substitutions of histidine 1426 (H1426) of SMRT binding to the BCL6 BTB-POZ domain. The Kd of each peptide in  $\mu\text{M}$  (mean  $\pm$  SEM) is presented to the right of the compound name and also within the table below. (B) to (F) represent each unnatural amino acid modelled onto the SMRT peptide at residue H1426. (B) Native SMRT, (C) Homophenylalanine, (D) 1-naphthyl, (E) Styryl and (F) 2-naphthyl. SEM calculated from  $n=3$ .

### 5.3 - Discussion

This chapter described the use of a cell viability assay using Cell Titre Glo, (CTG), in order to determine the effects of rifamycin SV and rifabutin on the cell line DG75-AB7 allowing a comparison between the effects observed in the presence and absence of BCL6. Competition assays were used to see whether rifamycin SV or rifabutin could compete with SMRT for the binding site on the BCL6 BTB-POZ domain. In addition, peptides based upon the SMRT-BBD were designed to bind with weaker affinity for the BCL6 BTB-POZ domain than the native SMRT-BBD to aid in the determination of a  $K_d$  value for rifabutin with BCL6. Furthermore, experiments were carried out to explore the consequences of substituting specific artificial amino acids in the SMRT-BBD peptides in place of H1426 on the basis of structural similarities observed between rifabutin, SMRT, 79-6 and BCoR.

After validating the interaction between rifabutin and the BTB-POZ domain of BCL6 by NMR and X-ray crystallography, the next step was to explore its potential effects on cell viability. In addition, despite rifamycin SV failing to form a complex with the BCL6 BTB-POZ domain during crystallisation trials, it was nevertheless observed to interact with the BCL6 BTB-POZ domain as shown by NMR (Figure 3.8), therefore, rifamycin SV was also investigated for its ability to possibly affect cell viability. DG75-AB7's provide a platform to compare cell viability when treated with rifamycin SV and rifabutin in the presence and absence of BCL6. Although rifamycin SV and rifabutin are both anti-microbials used in the treatment of tuberculosis, which is an intracellular pathogen that can only be killed by cell-permeant agents, very little is known about the effects of these compounds on mammalian cells. Kunin *et al* suggest that a peak serum concentration following oral dosing is  $0.5\mu\text{g/ml}$  ( $0.6\mu\text{M}$ ) (Kunin 1996). However, the intracellular concentration is likely to be higher due to the high lipid solubility of these compounds. At a concentration of  $1\mu\text{M}$  (approximately the therapeutic serum concentration) neither rifamycin SV nor rifabutin caused a change in cell viability when compared to untreated cells. However, at much higher concentrations, DG75-AB7 cells treated with rifabutin showed reduced cell viability. At these higher concentrations the combination of rifabutin plus DOX caused further loss of viability. As the addition of DOX to the DG75-AB7 cell line switches off BCL6

expression, a further decrease in viability compared to DOX treatment alone suggests that rifabutin may be interacting elsewhere causing off-target effects (Figure 5.1).

Technical difficulties arose when using rifamycin SV and rifabutin during cell culture experiments. The first was the lack of solubility of each compound. Precipitation of the compounds was visible upon addition to the cell suspension, which also became extremely viscous upon treatment. Precipitation of the compounds may have provided an inaccurate concentration between the concentration administered and the concentration of compound available to elicit an effect on cell viability. One possibility to establish this would have been to measure the intracellular-to-extracellular concentration of each compound by HPLC-MS/MS to precisely determine the intracellular concentration of each compound compared.

As described previously, the co-repressor SMRT binds to the BCL6 BTB-POZ domain with a  $K_d$  of between 3 and 5 $\mu$ M (Figures 5.2A and 5.5A). The affinity of rifabutin for BCL6 is ~1.4mM as determined by NMR (Figure 3.12). To investigate the ability of rifabutin and rifamycin SV to displace the SMRT-BBD and to determine an  $IC_{50}$ , as well as to determine the mechanism of binding in detail, an FP competition assay was developed. As a positive control for competition, the small molecule inhibitor, 79-6 with a binding affinity for BCL6 of 140 $\mu$ M was used (Cerchietti *et al.*, 2010). Competition was successfully achieved with 79-6 for SMRT binding to the BTB-POZ domain with an  $IC_{50}$  of 140 $\mu$ M (Figure 5.2B). Unfortunately, it was not possible to calculate an  $IC_{50}$  for either rifabutin or rifamycin SV (Figure 5.2C). Therefore, mutations and/or deletions of the SMRT-BBD were designed to generate a SMRT peptide with weaker affinity for BCL6 to potentially enable rifabutin to displace it.

Mutations and/or deletions were based upon Ahmad *et al.*, 2003, and were considered when forming a basis for designing peptides with weaker affinity for the BCL6 BTB-POZ domain. For example, deletion of residues 1414-1416 which make minor contributions to the strength of binding, the deletion of 1414-1420 leads to complete abrogation of complex formation and mutations of EIPR to AAAA leads to abolished binding (Ahmad *et al.*, 2003). However, peptides designed with mutations and/or deletions either maintained a  $K_d$  similar to the native SMRT-BBD or completely abrogated complex formation, therefore rendering them unsuitable for use in

determining an  $IC_{50}$  for rifabutin and rifamycin SV (Table 5.1 and Figure 5.2D). A possible reason as to why a  $K_d$  for rifamycin SV and rifabutin was unachievable by this method includes; the viscosity of the solution as it can impede the workings of the FP assay by affecting polarisation. Rifamycin SV, rifabutin and 79-6 were all solubilised in DMSO, a known solvent that can increase viscosity, however, the stock solution of 79-6 contained 5.6% DMSO and successfully competed out SMRT, whereas rifamycin SV and rifabutin stock solutions contained 4% DMSO and failed to show displacement of SMRT therefore DMSO has a negligible effect in this assay.

Another possible factor contributing to the viscosity of the solution could be due to the high concentration of compound used within the assay, as an increase in viscosity was repeatedly observed with an increase in concentration of compound. Rifabutin has ~10-fold less affinity for the BCL6 BTB-POZ domain than 79-6, (1.4mM compared to 140 $\mu$ M respectively), which could explain why 79-6 was able to displace SMRT-BBD but rifabutin and rifamycin SV could not. Therefore, although there is structural evidence for rifabutin binding to the co-repressor binding site of the BCL6 BTB-POZ domain, and by implication rifamycin SV binding to the same site, the interaction is weak and no effects on viability of a BCL6 dependent cell line could be detected at concentrations achievable in human serum.

Both SMRT and BCoR occupy a binding pocket within the lateral groove of the BCL6 BTB-POZ domain (Chapter 4). Whilst SMRT and NCoR bind to the BTB-POZ domain of BCL6 through an identical sequence, GRSIHEIPR, (residues 1422-1430 of SMRT and 1348-1356 of NCoR), the sequence used by BCoR, APSSWVVPG, shows no similarity to the SMRT-BBD. However both peptides bind in a similar manner to the BTB-POZ domain, Trp-509 of BCoR and His-1426 of SMRT make contacts with residues Met-51, Cys-53, Ser-54, Gly-55, Asn-21, Arg-24 and Arg-28 of BCL6 (Ghetu *et al.* 2008). The small molecule inhibitor, 79-6, utilises a subset of the interactions employed by the SMRT peptide for binding to the BTB-POZ domain. The crystal structure of rifabutin in complex with BCL6 shows that rifabutin occupies the same pocket as H1426 of SMRT and W509 of BCoR and 79-6 (Figures 4.8 and 5.3). The similarities in binding location and structure between rifabutin, 79-6, H1426 and W509 led to speculation about the importance of this region. The aim was to produce a peptide with higher affinity for BCL6 than the native SMRT-BBD in order to perturb

native SMRT and the recruitment of the co-repressor complex. To achieve this modified SMRT-BBD peptides were designed which incorporated different artificial amino acids in place of H1426. Homophenylalanine and styryl side chains were used in order to place aromatic rings in closer proximity to Tyr-58 than the native H1426, elucidating the importance of these aromatic rings in this region in relation to their influence on binding affinity for BCL6. However, all four substituted peptides led to a reduced binding affinity for the BCL6 BTB-POZ domain compared to native SMRT-BBD (Figure 5.5A). The modelling of the 2-naphthyl amino acid in place of H1426 shows a steric clash between the side chain and the BTB-POZ domain, which provides an explanation for the reduced binding affinity (Figure 5.5F). These experiments demonstrate the stringent requirements and key SMRT:BTB-POZ interactions that need to be targeted by compounds acting as lead molecules for the development of therapeutically useful BCL6 inhibitors.

## Chapter 6 - Discussion and future work

The focus of this thesis has been the detailed structural investigation of the binding of ansamycin antibiotics to the co-repressor binding site of the BCL6 BTB-POZ domain. BCL6 is a target for therapy in diffuse large B-cell lymphoma (Cerchietti *et al.* 2009; Cerchietti, Ghetu, *et al.* 2010a). BCL6 has also been shown to have a possible therapeutic role in breast cancer and autoimmunity (Logarajah *et al.* 2003; Walker *et al.* 2014). Peptides derived from the SMRT/NCoR BBD are effective in abrogating BTB-POZ domain functions and a small molecule inhibitor, 79-6, has similar effects. Work described here, together with previous work from others (Cerchietti, Ghetu, *et al.* 2010a) helps to define the BCL6 BTB-POZ domain co-repressor binding site as a druggable site.

BCL6 has roles in normal immunity and in lymphomagenesis. Studies in mouse models have shown that constitutive B-cell expression of BCL6 causes lymphomas with a similar histological appearance to human DLBCL. This supports genetic characterisation of human lymphomas demonstrating that defects in acetylation (Pasqualucci *et al.* 2011), ubiquitylation (Duan *et al.* 2012) and mutation of a regulatory site in the promoter (Wang *et al.* 2002; Pasqualucci *et al.* 2003) as well as chromosomal translocation (Ye, Rao, *et al.* 1993b) are all associated with DLBCL. The role of BCL6 in normal immunity is illustrated by mice bearing homozygous disruption of the endogenous BCL6 alleles, which are unable to form GCs and suffered from severe inflammatory disease (Ye *et al.* 1997; Dent *et al.* 1997) (possibly due to effects in macrophages) (Toney *et al.* 2000), leading to early death. Recently, BCL6 has been shown to have an essential role in differentiation of a subset of effector CD4<sup>+</sup> T-cells and follicular helper T-cells (Nurieva *et al.* 2009; Johnston *et al.* 2009). However, the mechanism of action of BCL6 in T-cells may be fundamentally different from that in B-cells: disruption of the BTB-POZ domain by "knock-in" of mutation in mice has no effect on T-cell development whilst abrogating germinal centre B-cell function (Huang *et al.* 2013). This observation strengthens the potential of BCL6 inhibitors as therapeutically useful compounds for the treatment of B-cell lymphomas without suppressing T-cell mediated immunity.

It has been demonstrated in this thesis that rifabutin, an ansamycin antibiotic, forms a complex with the BTB-POZ domain of the oncogenic transcriptional repressor BCL6. NMR and X-ray crystallography was used to characterise the BCL6-rifabutin complex (Figure 4.6, 4.7 and 4.8).

The peak displaying the greatest chemical shift perturbation was employed to estimate affinity of rifabutin for the BTB-POZ domain but the assignment of this peak remains unknown. The partial assignments (82 out of 121 residues) provided by Cerchietti *et al* were unable to aid in the identity of the peak due to the lack of alignment of the assignments with the spectrum. Initially, when the assignments were overlaid with the BTB-POZ domain spectrum, they appeared to reside diagonally to the right of the spectral peaks. This shift in alignment is indicative of a TROSY experiment (Pervushin *et al.* 1997). Cerchietti *et al* state that they used a TROSY experiment for assignment collection, however, this was also the case throughout this work for all 2D spectra during NMR experiments, therefore if both experiments were carried out using a TROSY then they would be expected to align.

It would, of course, have been useful to assign the complete BTB-POZ domain of BCL6, especially to identify the most perturbed peak, but because co-crystals of rifabutin and the BCL6 BTB-POZ domain were obtained it was now possible to determine, in detail, the orientation of the antibiotic and estimate the significant molecular interactions. Crystals of the complex diffracted to 2.3Å, with clear electron density readily identifiable for rifabutin. Unfortunately, a crystal structure of BCL6 in complex with rifamycin SV could not be obtained (Chapters 3 and 4). BCL6 was seeded with rifamycin SV and rifabutin at a molar ratio of 1:8. Therefore, to factor in the reduced affinity of rifamycin SV for BCL6 in comparison to rifabutin, a higher concentration of rifamycin SV could have been used when setting up the crystal trials to increase the chance of complex formation. The crystal structure of BCL6 has been previously solved in the apo form and in complex with SMRT, BCoR and 79-6. The BCL6-SMRT structure was used to solve BCL6 in complex with rifabutin by molecular replacement, which provided a much less time-consuming method when compared to NMR assignments. Molecular replacement proved successful in solving BCL6 in complex with rifabutin, therefore assignments of the BTB-POZ domain were no longer required.

The crystal structure showed clearly, the precise binding site of rifabutin to BCL6. This site is of extreme interest because it is also where the co-repressor SMRT binds in order to aid in the transcriptional repression of BCL6 downstream targets. Indeed the finding that 79-6, a compound discovered through computer assisted design binds to the same site as rifabutin, which was identified through an assay to inhibit BCL6 transcriptional activity strongly suggests that the co-repressor binding site is druggable.

The use of small molecules as potential inhibitors of BCL6 has been of great interest, as these may become lead molecules for drug discovery. Both the small molecule, 79-6, and SMRT peptide cause apoptosis of BCL6 dependent cell lines but as therapeutic inhibitors, both are associated with problems. Peptides are not suitable for oral administration whilst 79-6 lacks stability and is not highly membrane permeable. Rifabutin is a broad spectrum antibiotic used mainly in the treatment of tuberculosis. Rifabutin, as with other members of the ansamycin family are known to inhibit bacterial DNA dependent RNA polymerase (RNAP) by sterically blocking the extension of the RNA chain (Campbell *et al.* 2001). Rifabutin and other ansamycin antibiotics are also not likely to be good starting compounds for drug discovery because the medicinal chemistry will be very complicated. The rifamycin family of antibiotics differ predominantly in the nature of the side chain at positions C3 or C4 (Riva & Silvestri 1972). Rifamycin SV appeared to bind in the same location as rifabutin (according to the limited NMR data) but rifamycin SV may bind even more weakly than rifabutin. These compounds differ because rifabutin has bulky substituents involving both C3 and C4. Speculatively it may be that the interactions made by the side chain groups are important in defining the binding characteristics. The difference in tail architecture between rifamycin SV and rifabutin could also be one reason that rifabutin seems to bind with higher affinity to BCL6 than rifamycin SV. One approach to determine the relevance of the tails involved in the interaction with BCL6 would be to screen rifamycin family derivatives using NMR, and compare chemical shift perturbations.

In order to determine if rifabutin could be translated into a potential drug therapy for the treatment of lymphoma, in vitro cell-based assays and fluorescence polarisation were employed. Measurement of the chemical shift perturbation by NMR estimates the affinity of rifabutin for BCL6 at ~ 1.4mM, which is ~10 fold weaker than 79-6, with an affinity of 140µM for BCL6. Cerchietti *et al* carried out cell-based assays using

DLBCL lymph node biopsies, and treated with 79-6 at concentrations of 125 $\mu$ M and 250 $\mu$ M for 48 hours. The range of 79-6 concentrations tested, varied greatly between BCL6 dependent cell lines, from 24 $\mu$ M to 936 $\mu$ M in OCI-Ly7 and FARAGE respectively (Cerchietti *et al.*, 2010a). DG75-AB7 cells were treated with rifabutin and rifamycin SV at a concentration ranging between 1 $\mu$ M and 50 $\mu$ M. At 50 $\mu$ M both rifabutin and rifamycin SV were clearly having "off-target" effects, and therefore, the concentration was not increased further. However, if the affinity of rifabutin for BCL6 estimated by NMR is ~1mM then at 50 $\mu$ M the treatment concentration is ~20-fold below the binding affinity expected to be needed for an interaction. Kunin *et al* shows that the serum concentration of rifabutin is ~ 0.6 $\mu$ M after a standard single dose of 300mg. In experiments to measure cell viability, no effect was observed at 1  $\mu$ M a concentration close to an achievable serum concentration. Also, 79-6 was administered for 48 hours, whereas DG75-AB7 cells were treated for 24 hours. However, there were difficulties encountered in using these compounds for cell culture work. Precipitation observed upon treatment cast doubt on the true concentration of compound in solution able to enter the cells to elicit an effect.

Lack of data generated from the cell viability assay led to the development of a competition assay using fluorescence polarisation in order to obtain an IC<sub>50</sub> for rifabutin. 79-6 was used as a control for competition and to validate the experimental set up. Successful competition was observed between 79-6, SMRT and BCL6, with an IC<sub>50</sub> of ~ 140 $\mu$ M, in line with published literature. However, testing rifamycin SV and rifabutin in the same manner did not show competition between them and BCL6. One reason that competition was unable to be observed in this assay could be due to the large difference in affinity for BCL6 between rifabutin and 79-6. However, at 3mM, there is a slight indication of competition (Figure 5.2C). One amendment of carrying out this assay would have been to begin at a slightly higher concentration of rifabutin to fully investigate this observation. The main reason for beginning the competition at 3mM was due to the estimated Kd for BCL6, at 1.4mM, at which a starting point of 3mM should be sufficient. In addition, the sample became extremely viscous in the presence of such high concentrations of rifabutin. It is known that the viscosity of the solution can affect the polarisation in this type of assay.

A different approach was then taken to determine the IC<sub>50</sub> of rifabutin. Peptides were designed based upon the SMRT-BBD incorporating truncations and/or deletions of the 17-amino acid binding sequence, for the production of a peptide that has weaker affinity for BCL6 than the native SMRT to potentially enable rifabutin to compete for binding. However, these truncations and/or deletions showed an 'all or nothing' binding phenotype, therefore it was not possible to determine an IC<sub>50</sub> for rifabutin. Both rifabutin and 79-6 comprise of ring structures, and both are situated within a shallow pocket in close proximity to Tyr-58 of BCL6. In the apo structure this space is empty, but when bound to SMRT or BCoR it is occupied by H1426 and W509 respectively. SMRT and BCoR do not share any sequence similarity, therefore the presence of similar side chains suggested an important feature for binding. Structural features of all four were used as a basis for designing peptides that may have higher affinity for BCL6 than native SMRT by the incorporation of an unnatural amino acid in place of H1426 in the SMRT BBD. However, these peptides failed to achieve affinity higher than the native peptide.

The structural analysis of rifabutin binding to the BCL6 BTB-POZ domain provides important information about the pocket formed within the lateral groove and re-enforces the observation that the transcription factor, BCL6, can be therapeutically targeted. In addition, the residues lining the groove are unique to BCL6, suggesting that it might be possible to limit "off-target" effects, which if translated into clinical practice might limit toxicity due to the standard R-CHOP chemotherapy. There are other theoretical advantages to specific targeting of the BCL6 BTB-POZ domain. It has been shown that inhibition of the BCL6 BTB-POZ domain does not have an effect on plasmacytic differentiation, which is controlled through the RD2 domain (Huang *et al.* 2014), nor does it affect the ability for BCL6 to homodimerise and bind to its consensus DNA sequences within the promoters of its target genes. As mentioned above the BTB-POZ domain is also dispensable for T-cell function (Huang *et al.* 2013).

The work described here defines a druggable pocket in BCL6. There are two approaches to extending this work. One is to carry out structural studies employing further derivatives of rifamycin SV. This is likely to be a laborious and uncertain process. An alternative is to carry out large scale and systematic screens of compound libraries. Whilst this will also be complex any small compound "hits" are likely to be

more applicable for medicinal chemistry. The laboratory will be taking the latter route to try to develop inhibitors of co-repressor binding to the BCL6 BTB-POZ domain.

## **Appendices 1: – Publications**

# The Ansamycin Antibiotic, Rifamycin SV, Inhibits BCL6 Transcriptional Repression and Forms a Complex with the BCL6-BTB/POZ Domain

Sian E. Evans<sup>1,2</sup>, Benjamin T. Goult<sup>1</sup>, Louise Fairall<sup>1</sup>, Andrew G. Jamieson<sup>3</sup>, Paul Ko Ferrigno<sup>4✉</sup>, Robert Ford<sup>4✉</sup>, John W. R. Schwabe<sup>1</sup>, Simon D. Wagner<sup>2\*</sup>

**1** Department of Biochemistry, University of Leicester, Leicester, United Kingdom, **2** Department of Cancer Studies and Molecular Medicine and MRC Toxicology Unit, University of Leicester, Leicester, United Kingdom, **3** Department of Chemistry, University of Leicester, Leicester, United Kingdom, **4** Section of Experimental Therapeutics, Leeds Institute of Molecular Medicine, University of Leeds, Leeds, United Kingdom

## Abstract

BCL6 is a transcriptional repressor that is over-expressed due to chromosomal translocations, or other abnormalities, in ~40% of diffuse large B-cell lymphoma. BCL6 interacts with co-repressor, SMRT, and this is essential for its role in lymphomas. Peptide or small molecule inhibitors, which prevent the association of SMRT with BCL6, inhibit transcriptional repression and cause apoptosis of lymphoma cells *in vitro* and *in vivo*. In order to discover compounds, which have the potential to be developed into BCL6 inhibitors, we screened a natural product library. The ansamycin antibiotic, rifamycin SV, inhibited BCL6 transcriptional repression and NMR spectroscopy confirmed a direct interaction between rifamycin SV and BCL6. To further determine the characteristics of compounds binding to BCL6-POZ we analyzed four other members of this family and showed that rifabutin, bound most strongly. An X-ray crystal structure of the rifabutin-BCL6 complex revealed that rifabutin occupies a partly non-polar pocket making interactions with tyrosine58, asparagine21 and arginine24 of the BCL6-POZ domain. Importantly these residues are also important for the interaction of BCL6 with SMRT. This work demonstrates a unique approach to developing a structure activity relationship for a compound that will form the basis of a therapeutically useful BCL6 inhibitor.

**Citation:** Evans SE, Goult BT, Fairall L, Jamieson AG, Ko Ferrigno P, et al. (2014) The Ansamycin Antibiotic, Rifamycin SV, Inhibits BCL6 Transcriptional Repression and Forms a Complex with the BCL6-BTB/POZ Domain. PLoS ONE 9(3): e90889. doi:10.1371/journal.pone.0090889

**Editor:** Javier Marcelo Di Noia, Institut de Recherches Cliniques de Montréal (IRCM), Canada

**Received:** December 29, 2013; **Accepted:** February 5, 2014; **Published:** March 4, 2014

**Copyright:** © 2014 Evans et al. This is an open-access article distributed under the terms of the Creative Commons Attribution License, which permits unrestricted use, distribution, and reproduction in any medium, provided the original author and source are credited.

**Funding:** SEE is supported by a University of Leicester PhD Studentship (<http://www.le.ac.uk>). The work is supported by a Wellcome Trust Programme Grant WT091820 and Senior Investigator Grant WT100237 to JWRS (<http://www.wellcome.ac.uk>). The funders had no role in study design, data collection and analysis, decision to publish or preparation of the manuscript.

**Competing Interests:** Drs. Paul Ko Ferrigno and Rob Ford worked at the University of Leeds whilst carrying out the work described in the manuscript. They now both work for Avacta Life Sciences Ltd. This does not alter the authors' adherence to PLOS ONE policies on sharing data and materials.

\* E-mail: sw227@le.ac.uk

✉ Current address: Avacta Life Sciences, Ltd, Thorp Arch Estate, Wetherby, United Kingdom

## Introduction

BCL6 is a transcriptional repressor [1] that accomplishes its effects by binding to DNA through carboxy-terminal zinc fingers and recruitment of co-repressors to its mid-portion and amino-terminus (Figure 1A). Co-repressors NCoR (NCOR1), BCoR (BCOR) and SMRT (NCOR2), which are components of multi-protein complexes that include histone deacetylases, associate with the amino-terminal POZ domain [2–4]. SMRT and NCoR share an amino acid sequence (GRSIEHPR) that is required for binding to the BCL6-POZ domain and is functionally important [5] but in contrast BCoR binding is by means of a different primary sequence (APSSWVVP) [6]. The binding of co-repressor, SMRT, to the BCL6-POZ domain has been shown to be required for BCL6 function in B-cells, although it may be dispensable for its function in T-cells [7]. SMRT is a scaffold protein that mediates the recruitment of the HDAC3 repression complex to BCL6 and other repressive transcription factors [8].

BCL6 is expressed in normal germinal center B-cells [9] and is essential for high affinity antibody formation [10,11]. At a cellular level its role may be to allow proliferation and inhibit

differentiation to plasma cells [12]. It has been demonstrated that BCL6 promotes the proliferation of primary tonsillar B-cells [13] and prevents terminal differentiation to plasma cells in B-cell lines [12,14].

BCL6 is involved in chromosomal translocations in ~25% of all cases of diffuse large B-cell lymphoma (DLBCL) [15] and is, therefore, likely to have a major role in driving lymphomagenesis. This is supported by the finding that mice with constitutive B-cell expression of BCL6 develop lymphomas similar to human DLBCL [16]. Gene expression profiling has been utilized to subtype DLBCL into groups with differing clinical outcomes [17,18]. The majority of cases with BCL6 translocations are associated with poor prognosis activated B-cell (ABC) DLBCL [19] as defined by the “cell of origin” classification [18,20]. Other mechanisms causing constitutive expression of BCL6 have been described; mutations disrupting a negative regulatory site in the promoter region of the *BCL6* gene occur in 10 to 15% of DLBCL [21,22] and disruption of normal post-translational regulation of BCL6 by various mechanisms have also been reported and are likely to contribute to deregulated expression [23–25]. Overall

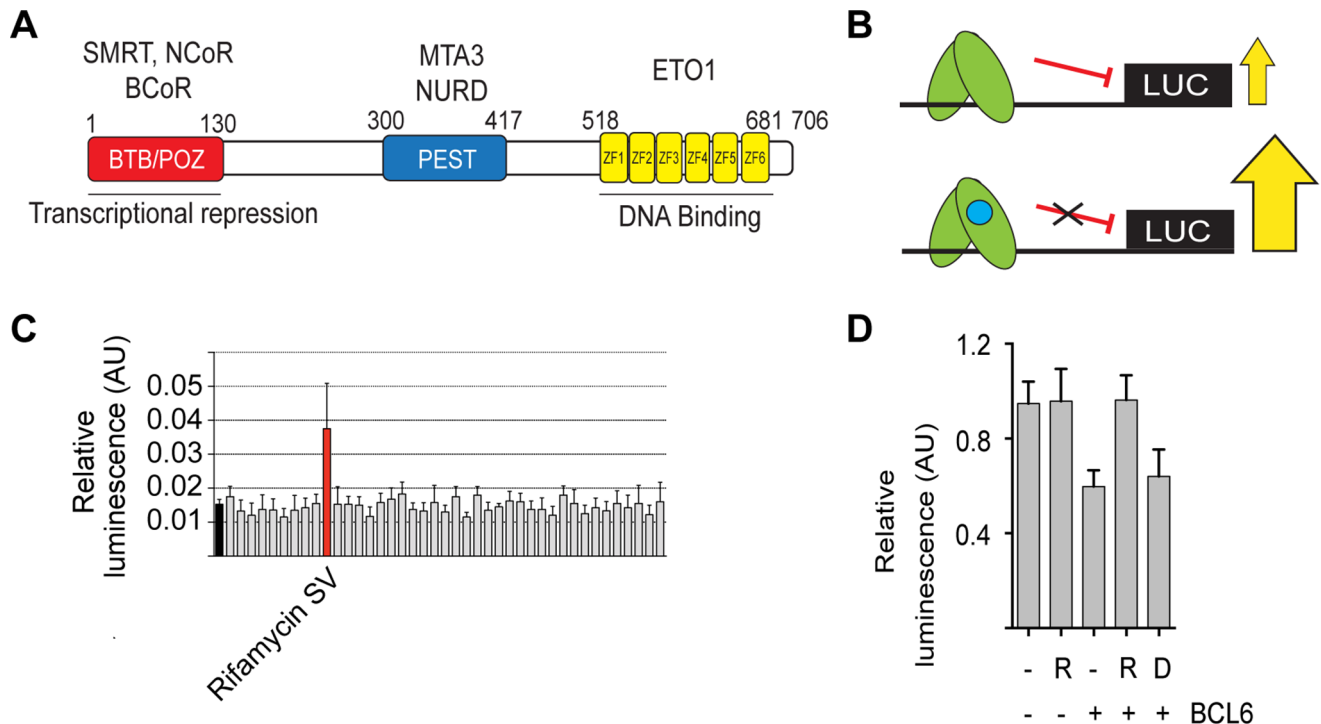


**Figure 1. A natural product screen to identify novel inhibitors of BCL6 transcriptional repression.** (A) Schematic of BCL6 showing amino-terminal POZ domain (red), carboxy terminal zinc fingers (yellow) and mid portion containing PEST domains (blue). Different proteins associate with the three portions of BCL6. NCoR, BCoR and SMRT associate with the POZ domain, MTA3 and NuRD with the mid portion and ETO1 with the zinc fingers. (B) Illustration of the screening strategy. BCL6 (green) is shown associating with its binding site cloned upstream of a luciferase reporter gene. Without any compound, or with an inactive compound i.e. one that does not bind BCL6, luciferase output is repressed but in the presence of active compound BCL6 mediated repression is prevented and output of luciferase increases. (C) Screening results for half a plate (40 compounds) from the natural product library. The black bar (furthest left) is the mean negative control i.e. transfected cells without test compound, and the black horizontal line the mean value across the entire screen. The red bar shows rifamycin SV. (D) The effect of rifamycin is due to inhibition of BCL6 transcriptional repression. HEK293T cells were co-transfected with a BCL6 expression construct and a luciferase reporter. Transcriptional repression due to BCL6 was relieved by rifamycin SV (R), but not by an agent that was ineffective in the screen (D). doi:10.1371/journal.pone.0090889.g001

BCL6 is an important oncogene in DLBCL but it is also expressed from an un-rearranged locus in follicular lymphoma, Burkitt's lymphoma and nodular lymphocyte predominant Hodgkin's lymphoma. Although its role has not been investigated in detail in these diseases it is also likely to contribute to cellular proliferation and survival.

A peptide corresponding to the region of SMRT interacting with the BCL6-POZ domain has been demonstrated to be functionally active *in vitro* and *in vivo* [26,27]. The peptide prevents normal germinal center formation in mice and when administered to BCL6 dependent cell lines or primary lymphoma cells causes apoptosis. A combination of computer assisted drug design and screens of small molecule libraries led to the identification of a compound, 79-6, that binds in the SMRT binding groove in the BCL6 POZ domain [28]. 79-6 is also functionally active *in vivo* and causes apoptosis of BCL6 dependent lymphoma cell lines. However, there are on-going efforts to carry out further small molecule library screens for BCL6 inhibitors.

Here we report the identification of a direct interaction between the BCL6 POZ domain and members of the ansamycin antibiotic family: rifamycin SV and rifabutin. This represents a novel non-bactericidal activity of the rifamycin family of antibiotics. Rifabutin was found to cause the largest chemical shift perturbations by NMR and a crystal structure of BCL6 in complex with rifabutin reveals new insights into the structure activity relation-

ships required for potential therapeutic agents to disrupt the SMRT/BCL6 interaction.

## Materials and Methods

### Luciferase reporter screening assay

A BCL6 reporter construct as previously described [12] was transfected into DG75 an EBV negative Burkitt's lymphoma cell line utilising Nucleofector program O-006 (Lonza Group Ltd, Basel, Switzerland). A natural product library (TimTec, Newark, DE, USA) was purchased unsolvated and solvated to a concentration of 10 mM with DMSO. After each compound was effectively solvated, 5  $\mu$ l was added to the corresponding wells in a daughter plate and diluted with 95  $\mu$ l of sterile water. From the daughter plate, 3  $\mu$ l of compound was pipetted into 22  $\mu$ l of complete RPMI 1640 in quadruplicate into each different assay plate. The compounds were diluted into each assay plate at a concentration of 20  $\mu$ M. One batch of DG-75 cells was transfected with BCL6 reporter construct with a standard amount of a construct expressing Renilla luciferase as a transfection control. The transfected cells were then incubated at 37°C for 16 to 20 hours. The assay plates were centrifuged and 50  $\mu$ l of the transfected cells were pipetted into the designated wells on the assay plate. The transfected cells were incubated for 12 hours with the compounds before harvesting and determination of luciferase activity.

HEK293T cells were seeded at  $2 \times 10^4$  cells/well in 96-well plates and following 24 hours in culture were co-transfected with a BCL6 reporter vector (100 ng), Renilla luciferase control vector (100 ng) and a full-length BCL6 expression plasmid (200 ng) using polyethylenimine (PEI) (Sigma, St. Louis, MO, USA). Compound (5  $\mu$ M) was added and cells were lysed, harvested and luciferase activity determined after 24 hours. Each condition was carried out in triplicate.

### Protein expression and purification

DNA encoding the POZ domain (residues 7 to 128) of human BCL6 (Figure 1A), with cysteine8 mutated to glutamine, cysteine67 mutated to arginine and cysteine84 mutated to asparagine, was cloned into a vector containing a 58-amino acid GB1 solubility enhancement tag, a  $6 \times$  histidine affinity tag and a TEV cleavage site (PROTEX, University of Leicester; (<http://www2.le.ac.uk/departments/biochemistry/research-groups/protex>)). Constructs were expressed in the *E. coli* strain Rosetta (DE3) (Novagen, Merck Chemicals Ltd., Beeston, UK) (Figures S1A and S1B). For preparation of  $^{15}$ N-labelled samples bacteria were cultured 2M9 minimal media containing 1 g of  $^{15}$ N-ammonium chloride per liter. For crystallisation and fluorescence polarisation *E. coli* were cultured in 2xYT medium. Bacteria were cultured at 37°C BCL6-POZ was purified using Ni-NTA resin and subsequent buffer exchange into 50 mM sodium phosphate pH 6, 300 mM NaCl, 5 mM DTT. Following TEV cleavage overnight at 4°C the sample was further purified by gel filtration using a Superdex S200 column (GE Healthcare, Amersham, UK). Protein concentrations were measured using Bio-Rad Protein Assay (Bio-Rad, Hercules, CA, USA).

### Peptide Synthesis and Fluorescence Polarization

Fmoc-protected amino acids were purchased from Novabiochem (Merck Chemicals Ltd, Nottingham, UK) or PolyPeptide Group (Strasbourg, France) (Fmoc-homophenylalanine, Fmoc-Styrylalanine, Fmoc-1-naphthylalanine & Fmoc-2-naphthylalanine) and were used as received. Peptides were synthesized on a CEM Liberty 1 automated microwave-assisted solid-phase peptide synthesizer (CEM Corporation, Buckingham, UK) using a 30 mL Teflon reactor vessel on 0.05 mmol scale using Fmoc-Arg(Pbf)-Wang resin (100–200 mesh) (substitution: 0.63 mmol/g). Peptide solutions were made in PBS containing 1 mM tris-(2-carboxyethylphosphine) and then coupled via the amino-terminal cysteine to the thiol-reactive BODIPY TMR dye (Invitrogen, Paisley, UK) in accordance with manufacturers instructions. Unreacted dye was removed by gel filtration using a PD-10 column (GE Healthcare). Fluorescence polarization experiments were performed in a black 96 well assay plate (Corning, Amsterdam, The Netherlands). Titrations were performed using a fixed concentration of SMRT peptide, with increasing concentration of the BCL6-POZ domain protein, in a final volume of 100  $\mu$ l of assay buffer (PBS, 0.05% (v/v) Triton X-100, 0.1 mg/mL BSA). The plate was mixed by shaking for 1 min and measurements were then taken using a Victor X5 plate reader (Perkin Elmer, Waltham, MA, USA) at room temperature with an excitation wavelength of 531 nm and an emission wavelength of 595 nm. Experiments were performed in triplicate and data were analysed using GraphPad Prism (version 6.0, GraphPad Software, Inc., San Diego, CA, USA).  $K_d$  values were calculated by nonlinear curve fitting using a one-site binding (hyperbola).

### NMR spectroscopy

All NMR experiments were performed at 303 K using Bruker AVANCE DRX 600 or AVANCE AVII 800 spectrometers both equipped with CryoProbes. Titrations were carried out using 280  $\mu$ M BCL6-POZ in 50 mM sodium phosphate pH 6, 300 mM NaCl, 5 mM DTT, 5% v/v D<sub>2</sub>O. Compounds were resuspended in deuterated DMSO (DMSO-d<sub>6</sub>). 2D  $^1\text{H}^{15}\text{N}$  heteronuclear single-quantum correlation (HSQC) spectra were acquired with transverse relaxation optimization (TROSY) [29] using 32 scans and 92 increments.  $^1\text{H}^{15}\text{N}$  HSQC spectra were collected on BCL6-POZ alone and then with increasing amount of compound. Data were analyzed using CCPN Analysis [30].

### Crystallization and X-ray structure determination

Crystals of the BCL6-POZ domain were obtained using the sitting drop vapor diffusion method at room temperature (Figure S1) BCL6-POZ was concentrated to 3.8 mg/ml and crystallised in the presence of rifabutin at a ratio of 1:8. In detail 1  $\mu$ l of BCL6-POZ in 50 mM sodium phosphate pH 6, 300 mM NaCl, 5 mM DTT (in the presence or absence of rifabutin) was mixed with 1  $\mu$ l reservoir solution (20% PEG 6000, 100 mM sodium citrate, pH 5). Crystals grew in the space group P1 21 1. Data were collected to 2.3 Å on the microfocus beam line I24 at the Diamond Light Source, Didcot, Oxfordshire. Data were processed and integrated using XDS, iMosflm, Pointless and Aimless [31,32]. The structure was solved using molecular replacement using Phaser [33] and the BCL6-POZ domain from the BCL6/SMRT structure (1R2B, [34]). Model fitting and refinement were performed using Coot and Refmac [35,36]. Statistics of the refinement are presented in Table 1. The  $R_{\text{free}}$  remained higher than expected probably due to the small size of the crystals and slightly streaky nature of the diffraction.

### Accession numbers

Coordinates and structure factors for the BCL6-POZ domain (residues 7–128) – Rifabutin complex have been deposited in the Protein Data Bank (ID code 4CP3).

## Results

### Natural Product Screen for inhibitors of the BCL6-SMRT interaction

Natural products form the basis for many drugs in clinical use. Despite their chemical complexity, they have other properties such as cell permeability and relatively high bioavailability that make them attractive starting materials for screens in drug discovery projects. We screened a commercial natural product library consisting of 480 compounds for ability to prevent BCL6 induced transcriptional repression in the Burkitt's lymphoma cell line DG75 (Figure 1B). Nine compounds modified transcriptional activity of a reporter construct bearing BCL6 binding sites in DG75 (3 compounds repressing and 6 compounds enhancing luciferase activity) (Figure 1C and Figures S2 and S3). However, the BCL6 DNA binding sequence shares sequence similarities to that of the STAT family of transcription factors [10] and our results might reflect inhibition of transcription factors other than BCL6. Therefore, to show directly that BCL6 transcription was inhibited we co-transfected a BCL6 expression construct and a luciferase reporter into HEK293T cells that do not express endogenous BCL6. Luciferase expression was repressed by BCL6 and this was relieved by the addition of rifamycin SV (labelled R) (Figure 1D), which was detected in the initial library screen (Figure 1C), but not by the other eight compounds.

**Table 1.** Data collection and refinement statistics (Molecular replacement).

<b>BCL6/Rifabutin</b>	
<b>Data Collection</b>	
Space Group	P 1 21 1
Cell dimensions	
<i>a,b,c</i> (Å)	35.17, 54.83, 58.16
$\alpha,\beta,\gamma$ (°)	90, 95.21, 90
Resolution (Å)	39.82–2.3 (2.38–2.3)
$R_{\text{merge}}$	10.8 (51.8)
$I/\sigma I$	9.8 (4.1)
Completeness (%)	97.13 (97)
Redundancy	3.0 (2.9)
<b>Refinement</b>	
Resolution (Å)	2.3
No. reflections	9168
$R_{\text{work}}/R_{\text{free}}$	20.2/26.9
No. Atoms	2053
Protein	1969
Ligand/ion	61
Water	23
B-factors	
Protein	27.9
Rifabutin	48
Water	24.6
R.M.S. deviations	
Bond lengths (Å)	0.013
Bond angles (°)	1.885

\*Highest resolution shell is shown in parenthesis.  
doi:10.1371/journal.pone.0090889.t001

### Rifamycin SV directly interacts with BCL6-POZ

In order to determine whether a direct interaction with BCL6 in solution was responsible for the observed effects on transcription, we utilized an NMR chemical shift perturbation assay. Work by others has demonstrated that the important interactions of BCL6 with co-repressors occur through the amino-terminal POZ domain, which also mediates homodimerisation [37]. The TROSY  $^1\text{H}^{15}\text{N}$  TROSY-HSQC NMR spectrum of the BCL6-POZ homodimer showed good dispersion and uniform line widths indicative of a stable well-folded protein (Figure S4). Addition of rifamycin SV (Figure 2A), resulted in a subset of peaks shifting in a concentration dependent manner (Figure 2B) supporting the hypothesis that rifamycin interacts directly with the BCL6-POZ domain. However, even at large excesses of rifamycin SV the chemical shift perturbations were relatively small and chemical shift changes continued to be detectable at high concentrations demonstrating that binding had still not reached saturation.

### Screening of rifamycin derivatives

Rifamycin SV belongs to a family of ansamycin antibiotics, which have related structures, comprising a naphthoquinone ring bridged by an aliphatic chain (Figure 2A and 2C). In order to determine whether other members of the family also bound to the BCL6-POZ domain we analysed the commercially available

compounds rifabutin, rifapentine, rifampicin and rifaximin as well as 3-formyl rifamycin, for interaction with the BCL6-POZ domain.

These derivatives all caused spectral changes of varying magnitude with the greatest shifts caused by rifabutin (Figure 2C and 2D). The estimated order of binding from weakest to strongest was: rifaximin, rifapentine, 3-formyl rifamycin, rifampicin, rifamycin SV and rifabutin. Comparison of the BCL6-POZ domain spectra on addition of rifamycin SV and rifabutin (Figures 2B and 2D) showed small differences in the observed shifts of some peaks suggesting minor differences in binding in solution. By plotting the chemical shift change ( $\delta\Delta$ ) of the most shifted peak, as a function of rifabutin concentration it was possible to estimate the  $K_d$  of the interaction as being in the order of  $\sim 1$  mM.

### Structure of the BCL6-POZ- Rifabutin complex

To explore further the atomic details of the interaction we crystallized the BCL6-POZ domain in complex with rifabutin. Complex crystals were readily obtained and easily identified due to the purple colour of rifabutin (Figure S1C). Molecular replacement with the BCL6-POZ domain (1R2B, [34]) as search molecule produced a clear electron density map with extra density readily identifiable for rifabutin (Figure 3, Table 1). Despite the BCL6-POZ domain being a symmetrical dimer [2,3] only one molecule of rifabutin is present per dimer. The rifabutin is located at the dimer interface and binds to the surface that overlaps the surface bound by the SMRT and NCoR peptides [2,34]. The naphthoquinone ring of rifabutin occupies the pocket, which is occupied by the residues histidine1426 of SMRT, histidine1352 of NCoR, or tryptophan509 of BCOR, in the three POZ domain co-repressor structures [6]. The most important interaction appears to be a  $\pi$ -stacking interaction with the aromatic ring of tyrosine58 of the BCL6-POZ domain. The aliphatic “handle” or macrocycle of rifabutin makes electrostatic interactions with asparagine21 and arginine24 (Figure 3).

A small molecule, 79–6, has been described previously and has been observed to bind in the same pocket at the BCL6:SMRT interface [28]. Comparison of the binding of SMRT peptide, 79–6 and rifabutin demonstrates remarkable similarities (Figure 4). Specifically apolar interactions with tyrosine58 and electrostatic interactions with asparagine21 and arginine24 are involved in the binding of all three molecules.

### SMRT peptide containing artificial amino acids to explore binding to BCL6-POZ domain

In order to explore the importance of histidine1426 of SMRT or histidine1352 of NCoR for binding to the pocket in the BCL6-POZ domain, which is also occupied by rifabutin and 79–6 we synthesised SMRT/NCoR peptides with artificial amino acids replacing the histidine (Figure S5). By fluorescence polarisation the  $K_d$  of binding of the BCL6-POZ domain to labelled wild-type SMRT peptide was determined to be 5  $\mu\text{M}$ . All the artificial amino acids that were employed in the study showed reduced binding, as compared to wild-type peptide, but there were considerable differences in affinity. Whilst the peptide bearing a 1-naphthyl residue had a binding affinity of 11  $\mu\text{M}$  the 2-naphthyl peptide had a much lower affinity of 154  $\mu\text{M}$  (Figure 5A). Homophenylalanine and styryl derivatives had intermediate affinities. Modelling of these artificial amino acids, such that they have the same orientation as tryptophan509 of BCOR and histidine1426 of SMRT [6], suggested explanations for this data (Figure 5B, 5C and 5D). Whilst 1-naphthyl is oriented within the pocket, 2-naphthyl clashes with the BCL6-POZ domain, which is likely to prevent significant binding. Homophenylalanine and

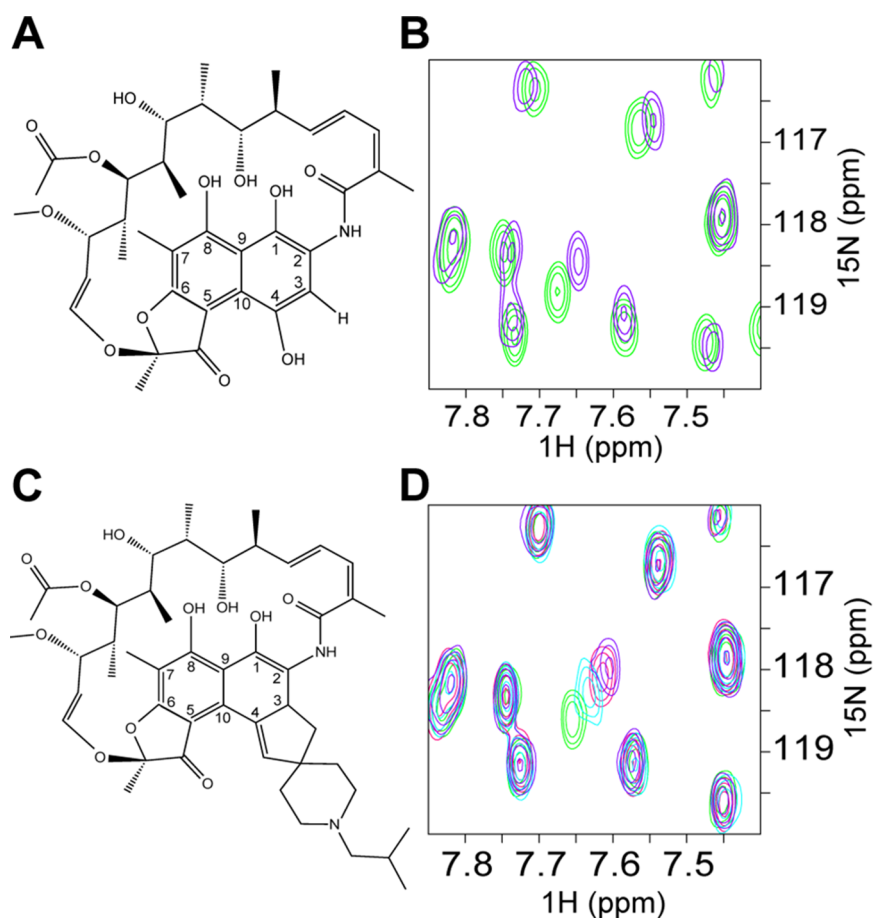


**Figure 2. Rifamycin SV and its derivative, rifabutin, bind directly to the BCL6-POZ domain.** Schematic diagram to compare the structures of (A) rifamycin SV and (C) rifabutin. These two compounds differ with respect to the side chains on C-3 and C-4. (B) and (D) TROSY  $^1\text{H},^{15}\text{N}$  HSQC spectra of 280  $\mu\text{M}$  BCL6-POZ domain. (B) Chemical shift changes due to rifamycin SV. An overlay of the spectra of BCL6-POZ domain alone (green) and in the presence of a 16:1 molar ratio of rifamycin (purple). (D) Chemical shift changes due to rifabutin with an overlay of the spectra of BCL6-POZ domain alone (green) and in the presence of 4:1 (light blue), 8:1 (red) and 16:1 (purple) molar ratios of rifabutin. doi:10.1371/journal.pone.0090889.g002

styryl side chains were employed to place aromatic rings, potentially capable of interacting with tyrosine58 closer to the BCL6-POZ domain than is histidine1426 in the wild-type structure. Binding affinity was again reduced demonstrating the stringent requirements for compounds that are to be lead molecules as BCL6 inhibitors.

## Discussion

There is interest in developing BCL6 inhibitors because this transcription factor is required for proliferation and survival of several types of non-Hodgkin's lymphoma and nodular lymphocyte predominant Hodgkin's lymphoma and proof of principle studies have demonstrated the efficacy of inhibiting BCL6 in diffuse large B-cell lymphoma [27,28]. The rifamycins and especially rifabutin are attractive starting materials for producing a clinically useful BCL6 inhibitor because of their high lipid solubility, extensive tissue penetrance and long half-life [38].

We have demonstrated that rifamycin SV and rifabutin, members of the ansamycin antibiotic family, that have clinical uses in the prevention or treatment of bacterial infections due to binding and inhibition of bacterial DNA-dependent RNA polymerase, are able to bind the BCL6-POZ domain.

This result is functionally significant as demonstrated by inhibition of BCL6 transcriptional repression by rifamycin SV. The luciferase reporter assay we employed produced 9 "hits" of which only rifamycin SV bound to BCL6. Three of the compounds appeared to enhance transcriptional repression i.e. reduced luciferase production, and for one of these compounds (Figure S2A) the explanation may be that it is a known inhibitor of firefly luciferase (Figure S3B) [39].

Rifamycin SV is derived from rifamycin B (the natural fermentation product of *Streptomyces mediterranei*) by removal of the glycolic group bound to C-4. The rifamycins are potent inhibitors of bacterial DNA dependent RNA polymerase [40] and are utilised in the treatment of tuberculosis. Another property of these compounds, their high lipid solubility, may help to penetrate the bacterial wall. Structurally, the rifamycins consist of a naphthoquinonic chromophore, which is spanned by an aliphatic bridge between the nitrogen on C-2 and the oxygen on C-12 of the naphthoquinone moiety (Figure 2A and 2C). The members of the family differ primarily in the side chains on C-3 and C-4. We demonstrate that rifamycins bind with different strengths to the BCL6 POZ domain. These agents largely differ in the side chain attachments to C-3 and C-4, which do not appear to make significant interactions with the protein in our crystal structure. One possibility is that the side-chains alter the

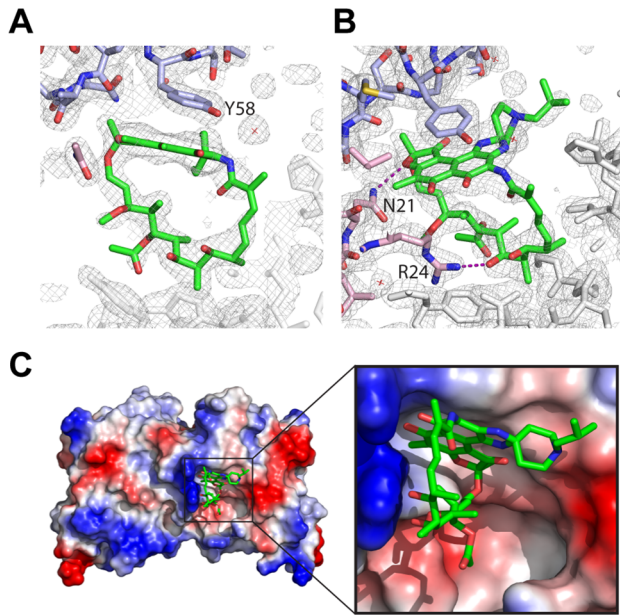


**Figure 3. Crystal structure of rifabutin and BCL6-POZ domain.**

Electron density corresponding to rifabutin, following refinement, in the context of surrounding electron density demonstrating the proximity of (A) tyrosine58 from one monomer of the POZ dimer and (B) asparagine21 and arginine24 from the other monomer. (C) Surface representation of BCL6-POZ with basic residues (including asparagine21 and arginine24) in blue and acidic residues in red. The naphthoquinone rings of rifabutin are in proximity to tyrosine58 whilst the aliphatic bridge is adjacent to the basic surface.  
doi:10.1371/journal.pone.0090889.g003

rigidity of the molecule to alter the fit in the lateral groove of the POZ domain dimer. Supporting the view that the C-3/C-4 side chains are important in modulating function, others have shown that rifamycin SV can inhibit amyloid fibril formation through disruption of interactions between fibril aromatic rings that are required for elongation whereas rifaximin does not have this effect [41].

SMRT and NCoR occupy a binding pocket that is present in the apo i.e. unliganded, form of BCL6. The co-repressor, BCOR, associates with BCL6 through interactions with the lateral groove as do SMRT and NCoR. Whilst SMRT and NCoR bind to the BCL6-POZ domain through identical sequences, GRSIHEIPR (residues 1422 to 1430 of SMRT and residues 1348 to 1356 of NCoR), there is no similarity to the BCL6 binding sequence of BCOR, APSSWVVPG. However, binding of peptides derived from SMRT and BCOR have been investigated in detail [6]. BCOR tryptophan509 and SMRT histidine1426 make similar contacts on the BCL6-POZ domain, namely with residues methionine51, cysteine53, serine54, glycine55, asparagine21, arginine24 and arginine28 [6]. The small molecule, 79–6, utilizes a subset of the interactions employed by the SMRT peptide for binding to the BCL6 POZ domain. Our X-ray crystallographic studies show that rifabutin occupies the pocket utilised by histidine in the SMRT and NCoR sequences and tryptophan in BCOR. The binding of rifabutin to the BCL6 POZ domain also appears very similar to that of the small molecule, 79–6, [28]. Collectively it seems likely that rifamycin SV and rifabutin can occupy a druggable pocket in the BCL6-POZ domain.

Macrocyclic compounds, of which rifamycin SV and rifabutin are examples, may have utility in perturbing protein-protein

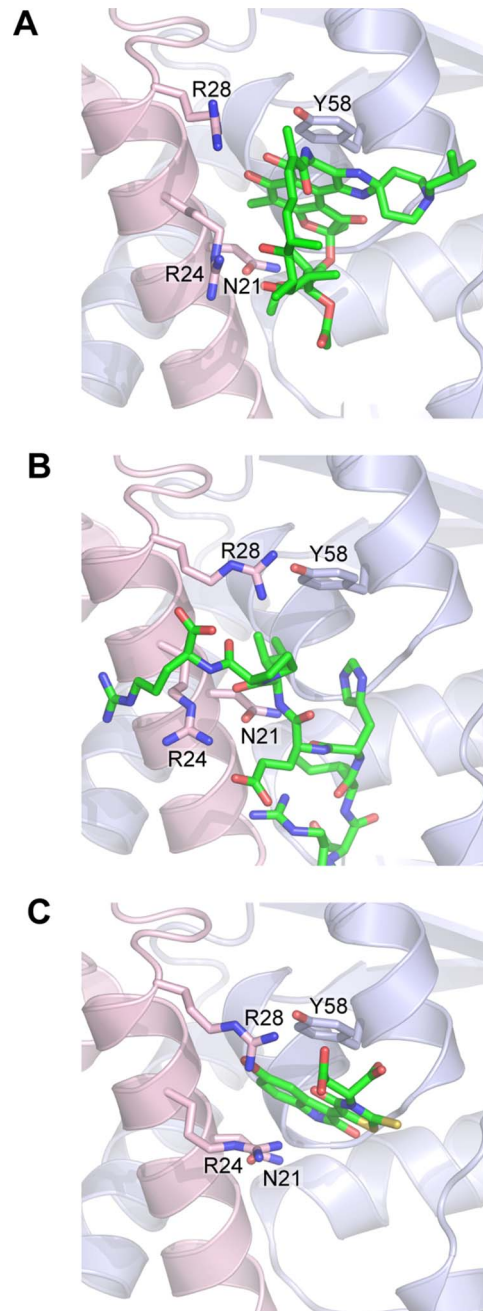


**Figure 4. BCL6-POZ domain in complex with rifabutin, 79–6 and the SMRT peptide.** A section of the BCL6-POZ domain structure is shown binding; (A) rifabutin, (B) the SMRT peptide and (C) 79–6.  
doi:10.1371/journal.pone.0090889.g004

interactions and are also highly membrane permeable. We suggest that the rifamycins will be interesting compounds from which to develop BCL6 inhibitors.

### Supporting Information

**Figure S1 Protein purification and crystallisation of BCL6.** (A) Coomassie stained polyacrylamide gel showing production of BCL6-POZ domain with a GB1 tag and TEV cleavage of the tag. (B) BCL6-POZ domain purified away from the GB1 tag by size exclusion gel filtration. Coomassie stained

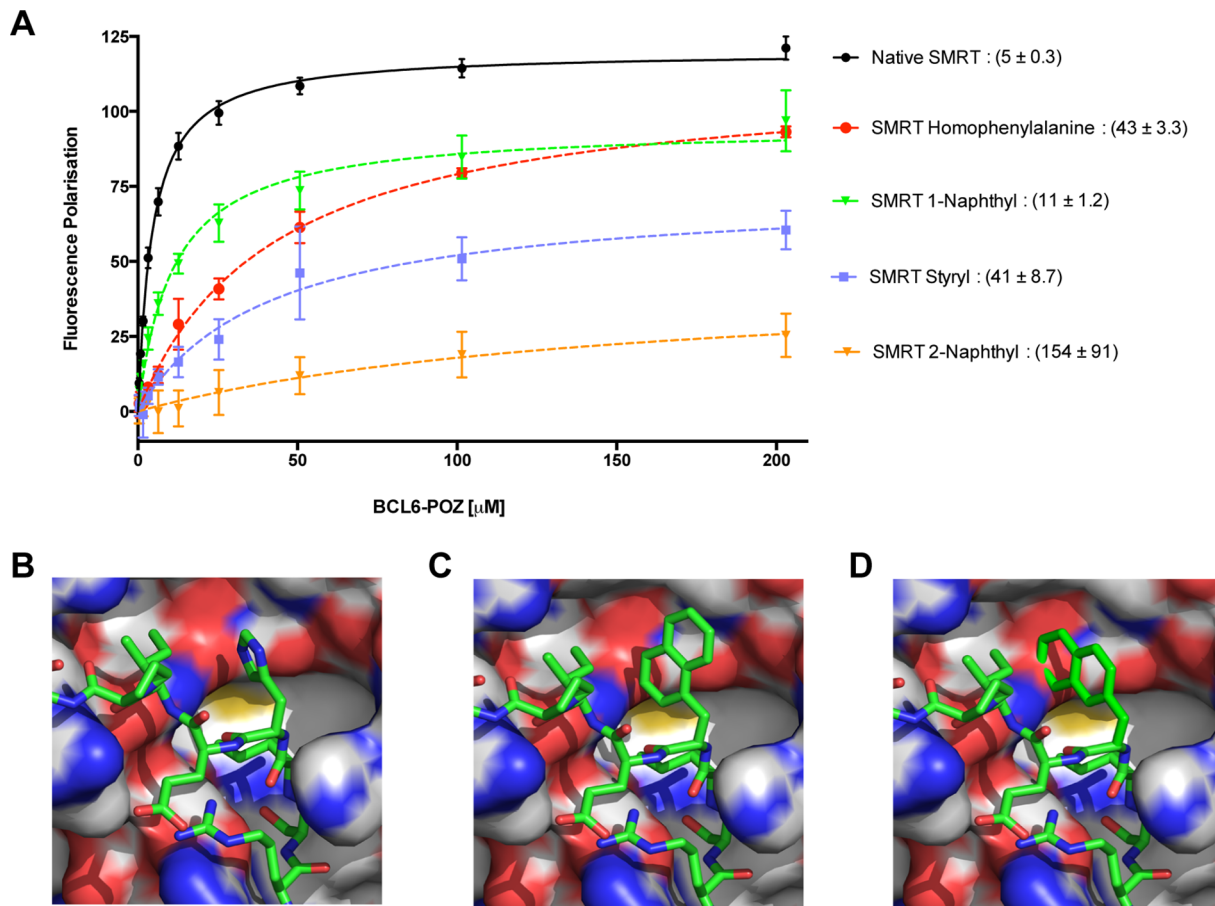


**Figure 5. Binding requirements of the SMRT peptide explored utilising artificial amino acids to replace histidine.** (A) Binding curves obtained by fluorescence polarisation for wild-type peptide and 1-naphthyl, 2-naphthyl, styryl and homophenylalanine substitutions of histidine1426 of SMRT. The  $K_d$  in  $\mu\text{M}$  (mean  $\pm$  SEM) is presented to the right of the compound name. (B) Structure of wild-type SMRT peptide bound to the BCL6-POZ domain. Molecular modelling of (C) 1-naphthyl SMRT peptide and (D) 2-naphthyl SMRT peptide. doi:10.1371/journal.pone.0090889.g005

polyacrylamide gel showing fractions collected. (C) BCL6-POZ crystal mounted in a loop at the Diamond Synchrotron beamline I24 (Red box  $25.9 \mu\text{m}^2$ ). The crystals are faintly lilac having taken up the coloured rifabutin.

(TIF)

**Figure S2 Natural product library screening.** Results for all 480 compounds are presented. Column to the left in orange is the mean negative control i.e. transfected cells without test compound, and the orange horizontal line the mean value across the entire screen. Compounds considered “its” are represented as red columns and comprise 6 that relieve BCL6 transcriptional repression and 3, which appear to enhance repression.

(TIF)

**Figure S3 Structures of the 9 compounds that alter BCL6 transcriptional repression.** The most widely used compound name is presented apart from one compound (A), which has no common name and for which the IUPAC nomenclature is stated. The chemical identifier (CID) from PubChem is also presented. (A to C) Three compounds that reduce luciferase activity. (D to I) Compounds that enhance luciferase activity, including (I) Rifamycin SV.

(TIF)

**Figure S4 TROSY  $^1\text{H}$ ,  $^{15}\text{N}$  HSQC NMR spectrum of the BCL6-POZ domain.**

(TIF)

**Figure S5 Sequences of SMRT peptides.** Sequences of SMRT peptides utilised in fluorescence polarisation experiments together with the structures of the artificial amino acids at the position of histidine1426 in the wild-type peptide. (A) wild-type SMRT, (B) 1-naphthyl-SMRT, (C) 2-naphthyl-SMRT, (D) homophenylalanine-SMRT and (E) styryl-SMRT.

(TIF)

## Acknowledgments

We thank the PROTEX facility at the University of Leicester for generating the BCL6 expression construct and the beamline staff at DIAMOND for help with data collection. 3-formyl-rifamycin was a gift from Professor Colin Fishwick, University of Leeds.

## Author Contributions

Conceived and designed the experiments: SEE BTG PKF RF JWRS SDW. Performed the experiments: SEE BTG LF RF. Analyzed the data: SEE BTG LF JWRS SDW. Contributed reagents/materials/analysis tools: AGJ. Wrote the paper: SEE BTG LF JWRS SDW.

## References

- Chang CC, Ye BH, Chaganti RS, Dalla-Favera R (1996) BCL-6, a POZ/zinc-finger protein, is a sequence-specific transcriptional repressor. *Proc Natl Acad Sci USA* 93: 6947–6952.
- Melnick A, Carlile G, Ahmad KF, Kiang C-L, Corcoran C, et al. (2002) Critical residues within the BTB domain of PLZF and Bcl-6 modulate interaction with corepressors. *Mol Cell Biol* 22: 1804–1818.
- Dhordain P, Albagli O, Lin RJ, Ansieau S, Quief S, et al. (1997) Corepressor SMRT binds the BTB/POZ repressing domain of the LAZ3/BCL6 oncoprotein. *Proc Natl Acad Sci USA* 94: 10762–10767.
- Dhordain P, Lin RJ, Quief S, Lantoine D, Kerckaert JP, et al. (1998) The LAZ3(BCL-6) oncoprotein recruits a SMRT/mSIN3A/histone deacetylase containing complex to mediate transcriptional repression. *Nucleic Acids Res* 26: 4645–4651.
- Barish GD, Yu RT, Karunasiri MS, Becerra D, Kim J, et al. (2012) The Bcl6-SMRT/NCOR Cistrome Represses Inflammation to Attenuate Atherosclerosis. *Cell Metabolism* 15: 554–562. doi:10.1016/j.cmet.2012.02.012.
- Ghetu AF, Corcoran CM, Cerchietti L, Bardwell VJ, Melnick A, et al. (2008) Structure of a BCOR corepressor peptide in complex with the BCL6 BTB domain dimer. *Mol Cell* 29: 384–391. doi:10.1016/j.molcel.2007.12.026.
- Huang C, Hatzi K, Melnick A (2013) Lineage-specific functions of Bcl-6 in immunity and inflammation are mediated by distinct biochemical mechanisms. *Nat Immunol*: 1–11. doi:10.1038/ni.2543.
- Oberoi J, Fairall L, Watson PJ, Yang J-C, Czinnerer Z, et al. (2011) Structural basis for the assembly of the SMRT/NCOR core transcriptional repression machinery. *Nat Struct Mol Biol* 18: 177–184. doi:10.1038/nsmb.1983.
- Allman D, Jain A, Dent A, Maile RR, Selvaggi T, et al. (1996) BCL-6 expression during B-cell activation. *Blood* 87: 5257–5268.
- Dent AL, Shaffer AL, Yu X, Allman D, Staudt LM (1997) Control of Inflammation, Cytokine Expression, and Germinal Center Formation by BCL-6. *Science* 276: 589–592. doi:10.1126/science.276.5312.589.
- Ye BH, Cattoretti G, Shen Q, Zhang J, Howe N, et al. (1997) The BCL-6 proto-oncogene controls germinal center formation and Th2-type inflammation. *Nat Genet* 16: 161–170.
- Reljic R, Wagner SD, Peakman LJ, Fearon DT (2000) Suppression of signal transducer and activator of transcription 3-dependent B lymphocyte terminal differentiation by BCL-6. *J Exp Med* 192: 1841–1848.
- Shvarts A, Brummelkamp TR, Scheeren F, Koh E, Daley GQ, et al. (2002) A senescence rescue screen identifies BCL6 as an inhibitor of anti-proliferative p19(ARF)-p53 signaling. *Genes Dev* 16: 681–686. doi:10.1101/gad.929302.
- Tunyaplin C, Shaffer AL, Angelin-Duclos CD, Yu X, Staudt LM, et al. (2004) Direct repression of prdm1 by Bcl-6 inhibits plasmacytic differentiation. *J Immunol* 173: 1158–1165.
- Offit K, Coco Lo F, Louie DC, Ye BH, Jhanwar SC, et al. (1994) Rearrangement of the bcl-6 gene as a prognostic marker in diffuse large-cell lymphoma. *N Engl J Med* 331: 74–80. doi:10.1056/NEJM199407143310202.
- Cattoretti G, Pasqualucci L, Ballon G, Tam W, Nandula SV, et al. (2005) Deregulated BCL6 expression recapitulates the pathogenesis of human diffuse large B cell lymphomas in mice. *Cancer Cell* 7: 445–455. doi:10.1016/j.ccr.2005.03.037.
- Shipp MA, Ross KN, Tamayo P, Weng AP, Kutok JL, et al. (2002) Diffuse large B-cell lymphoma outcome prediction by gene-expression profiling and supervised machine learning. *Nat Med* 8: 68–74. doi:10.1038/nm102-68.
- Alizadeh AA, Eisen MB, Ma C, Lossos IS, Rosenwald A, et al. (2000) Distinct types of diffuse large B-cell lymphoma identified by gene expression profiling. *Nature* 403: 503–511. doi:10.1038/35000501.
- Iqbal J, Greiner TC, Dave BJ, Smith L, Sanger WG, et al. (2007) Distinctive patterns of BCL6 molecular alterations and their functional consequences in different subgroups of diffuse large B-cell lymphoma. *Leukemia*. doi:10.1038/sj.leu.2404856.
- Lossos IS, Czerwinski DK, Alizadeh AA, Wechsler MA, Tibshirani R, et al. (2004) Prediction of Survival in Diffuse Large-B-Cell Lymphoma Based on the Expression of Six Genes. *N Engl J Med* 350: 1828–1837. doi:10.1056/NEJMoa032520.
- Pasqualucci L, Migliazza A, Basso K, Houldsworth J, Chaganti RSK, et al. (2003) Mutations of the BCL6 proto-oncogene disrupt its negative autoregulation in diffuse large B-cell lymphoma. *Blood* 101: 2914–2923. doi:10.1182/blood-2002-11-3387.
- Wang X, Li Z, Naganuma A, Ye BH (2002) Negative autoregulation of BCL-6 is bypassed by genetic alterations in diffuse large B cell lymphomas. *Proc Natl Acad Sci USA* 99: 15018–15023. doi:10.1073/pnas.232581199.
- Duan S, Cermak L, Pagan JK, Rossi M, Martinengo C, et al. (2011) FBXO11 targets BCL6 for degradation and is inactivated in diffuse large B-cell lymphomas. *Nature* 481: 90–93. doi:10.1038/nature10688.
- Cerchietti LC, Hatzi K, Caldas-Lopes E, Yang SN, Figueroa ME, et al. (2010) BCL6 repression of EP300 in human diffuse large B cell lymphoma cells provides a basis for rational combinatorial therapy. *J Clin Invest* 120: 4569–4582. doi:10.1172/JCI42869.
- Pasqualucci L, Dominguez-Sola D, Chiarenza A, Fabbri G, Grunn A, et al. (2011) Inactivating mutations of acetyltransferase genes in B-cell lymphoma. *Nature* 471: 189–195. doi:10.1038/nature09730.
- Polo JM, Dell'Oso T, Ranuncolo SM, Cerchietti L, Beck D, et al. (2004) Specific peptide interference reveals BCL6 transcriptional and oncogenic mechanisms in B-cell lymphoma cells. *Nat Med* 10: 1329–1335. doi:10.1038/nm1134.
- Cerchietti L, Yang S, Shaknovich R, Hatzi K, Polo J, et al. (2008) A peptidomimetic inhibitor of BCL6 with potent anti-lymphoma effects in vitro and in vivo. *Blood* 113: 3997–3405. doi:10.1182/blood-2008-07-168773.
- Cerchietti LC, Ghetu AF, Zhu X, Da Silva GF, Zhong S, et al. (2010) A small-molecule inhibitor of BCL6 kills DLBCL cells in vitro and in vivo. *Cancer Cell* 17: 400–411. doi:10.1016/j.ccr.2009.12.050.
- Pervushin K, Riek R, Wider G, Wüthrich K (1997) Attenuated T<sub>2</sub> relaxation by mutual cancellation of dipole-dipole coupling and chemical shift anisotropy indicates an avenue to NMR structures of very large biological macromolecules in solution. *Proceedings of the National Academy of Sciences* 94: 12366–12371.
- Vranken WF, Boucher W, Stevens TJ, Fogh RH, Pajon A, et al. (2005) The CCPN Data Model for NMR Spectroscopy: Development of a Software Pipeline. *Proteins* 59: 687–696.
- Leslie AGW (2006) The integration of macromolecular diffraction data. *Acta Crystallogr D Biol Crystallogr* 62: 48–57. doi:10.1107/S0907444905039107.
- Evans PR, Murshudov GN (2013) How good are my data and what is the resolution? *Acta Crystallogr D Biol Crystallogr* 69: 1204–1214. doi:10.1107/S0907444913000061.
- McCoy AJ, Grosse-Kunstleve RW, Adams PD, Winn MD, Storoni LC, et al. (2007) Phaser crystallographic software. *J Appl Crystallogr* 40: 658–674. doi:10.1107/S0021889807021206.
- Ahmad KF, Melnick A, Lax S, Bouchard D, Liu J, et al. (2003) Mechanism of SMRT corepressor recruitment by the BCL6 BTB domain. *Mol Cell* 12: 1551–1564.
- Collaborative Computational Project, Number 4 (1994) The CCP4 suite: programs for protein crystallography. *Acta Crystallogr D Biol Crystallogr* 50: 760–763. doi:10.1107/S0907444994003112.
- Emsley P, Lohkamp B, Scott WG, Cowtan K (2010) Features and development of Coot. *Acta Crystallogr D Biol Crystallogr* 66: 486–501. doi:10.1107/S0907444910007493.
- Dhordain P, Albagli O, Ansieau S, Koken MH, Dewindt C, et al. (1995) The BTB/POZ domain targets the LAZ3/BCL6 oncoprotein to nuclear dots and mediates homomerisation in vivo. *Oncogene* 11: 2689–2697.
- Kunin CM (1996) Antimicrobial activity of rifabutin. *Clin Infect Dis* 22 Suppl 1: S3–13–discussionS13–4.
- Auld DS, Southall NT, Jadhav A, Johnson RL, Diller DJ, et al. (2008) Characterisation of chemical libraries for luciferase inhibitory activity. *J Med Chem* 51: 2372–2386.
- Campbell EA, Korzhveva N, Mustaev A, Murakami K, Nair S, et al. (2001) Structural mechanism for rifampicin inhibition of bacterial RNA polymerase. *Cell* 104: 901–912.
- Woods LA, Platt GW, Hellewell AL, Hewitt EW, Homans SW, et al. (2011) Ligand binding to distinct states diverts aggregation of an amyloid-forming protein. *Nat Chem Biol* 7: 730–739. doi:10.1038/nchembio.635.

## References

- Abbas, A.K., Lichtman, A.H.H. & Pillai, S., 2012. *Basic Immunology*, Elsevier Health Sciences.
- Ahmad, K.F., Melnick, A., Lax, S., Bouchard, D., Liu, J., Kiang, C.L., Mayer, S., Takahashi, S., Licht, J.D., Prive, G.G. 2003. Mechanism of SMRT corepressor recruitment by the BCL6 BTB domain. *Molecular cell*, 12(6), pp.1551–1564.
- Ahmad, K.F., Engel, C.K., Prive, G.G., 1998. Crystal structure of the BTB domain from PLZF. *Proceedings of the National Academy of Sciences*, 95(21), pp.12123–12128.
- Albagli, O., Dhordain, P., Deweindt, C., Lecocq, G., Leprince, D. 1995. The BTB/POZ domain: a new protein-protein interaction motif common to DNA- and actin-binding proteins. *Cell growth & differentiation : the molecular biology journal of the American Association for Cancer Research*, 6(9), pp.1193–1198.
- Alizadeh, A.A., Eisen, M.B., Davis, R.E., Ma, C., Lossos, I.S., Rosenwald, A., Boldrick, J.C., Sabet, H., Tran, T., Yu, X., Powell, J.I., Yang, L., Marti, G.E., Moore, T., Hudson, J.Jr., Lu, L., Lewis, D.B., Tibshirani, R., Sherlock, G., Chan, W.C., Greiner, T.C., Weisenburger, D.D., Armitage, J.O., Warnke, R., Levy, R., Wilson, W., Grever, M.R., Byrd, J.C., Botstein, D., Brown, P.O., Staudt, L.M. 2000. Distinct types of diffuse large B-cell lymphoma identified by gene expression profiling. *Nature*, 403(6769), pp.503–511.
- Bardwell, V.J. & Treisman, R., 1994. The POZ domain: a conserved protein-protein interaction motif. *Genes & development*, 8(14), pp.1664–1677.
- Baron, B.W., Nucifora, G., McCabe, N., Espinosa, R 3<sup>rd</sup>, Le Beau, M.M., McKeithan, T.W. 1993. Identification of the gene associated with the recurring chromosomal translocations t(3;14)(q27;q32) and t(3;22)(q27;q11) in B-cell lymphomas. *Proceedings of the National Academy of Sciences*, 90(11), pp.5262–5266.
- Bastard, C., Tilly, H., Lenormand, B., Bigorgne, C., Boulet, D., Kunlin, A., Monconduit, M., Piquet, H. 1992. Translocations involving band 3q27 and Ig gene regions in non-Hodgkin's lymphoma. *Blood*, 79(10), pp.2527–2531.
- Beato, M. & Eisefeld, K., 1997. Transcription factor access to chromatin. *Nucleic Acids Research*, 25(18), pp.3559–3563.
- Bereshchenko, O.R., Gu, W. & Dalla-Favera, R., 2002. Acetylation inactivates the transcriptional repressor BCL6. *Nature genetics*, 32(4), pp.606–613.
- Bunting, K.L. & Melnick, A.M., 2013. New effector functions and regulatory mechanisms of BCL6 in normal and malignant lymphocytes. *Current opinion in immunology*, 25(3), pp.339–346.
- Butler, M.P., Lida, S., Capello, D., Rossi, D., Rao, P.H., Nallasivam, P., Louie, D.C., Chaganti, S., Au, T., Gascoyne, R.D., Gaidano, G., Chaganti, R.S., Dalla-Favera, R. 2002. Alternative translocation breakpoint cluster region 5' to BCL-6 in B-cell non-Hodgkin's lymphoma. *Cancer research*, 62(14), pp.4089–4094.

- Camp, R.L., Kraus, T.A., Birkeland, M.L., Pure, E. 1991. High levels of CD44 expression distinguish virgin from antigen-primed B cells. *The Journal of experimental medicine*, 173(3), pp.763–766.
- Campbell, E.A., Korzheva, N., Mustaev, A., Murakami, K., Nair, S., Goldfarb, A., Darst, S.A. 2001. Structural mechanism for rifampicin inhibition of bacterial rna polymerase. *Cell*, 104(6), pp.901–912.
- Cattoretti, G., Pasqualucci, L., Ballon, G., Tam, W., Nandula, S.V., Shen, Q., Mo, T., Murty, V.V., Dalla-Favera, R. 2005. Deregulated BCL6 expression recapitulates the pathogenesis of human diffuse large B cell lymphomas in mice. *Cancer Cell*, 7(5), pp.445–455.
- Cerchiatti, L.C., Yang, S.N., Shaknovich, R., Hatzi, K., Polo, J.M., Chadburn, A., Dowdy, S.F., Melnick, A. 2009. A peptomimetic inhibitor of BCL6 with potent antilymphoma effects in vitro and in vivo. *Blood*, 113(15), pp.3397–3405.
- Cerchiatti, L.C., Ghetu, A.F., Zhu, X., Da Silva, G.F., Zhong, S., Matthews, M., Bunting, K.L., Polo, J.M., Fares, C., Arrowsmith, C.H., Yang, S.N., Garcia, M., Coop, A., Mackerell, A.D Jr., Prive, G.G., Melnick, A. 2010a. A small-molecule inhibitor of BCL6 kills DLBCL cells in vitro and in vivo. *Cancer Cell*, 17(4), pp.400–411.
- Cerchiatti, L.C., Hatzi, K., Caldes-Lopes, E., Yang, S.N., Figueroa, M.E., Morin, R.D., Hirst, M., Mendez, L., Shaknovich, R., Cole, P.A., Bhalla, K., Gascoyne, R.D., Marra, M., Chiosis, G., Melnick, A. 2010b. BCL6 repression of EP300 in human diffuse large B cell lymphoma cells provides a basis for rational combinatorial therapy. *The Journal of clinical investigation*.
- Chang, C.C., Ye, B.H., Chaganti, R.S., Dalla-Favera, R. 1996. BCL-6, a POZ/zinc-finger protein, is a sequence-specific transcriptional repressor. *Proceedings of the National Academy of Sciences*, 93(14), pp.6947–6952.
- Chaplin, D.D., 2010. Overview of the immune response. *The Journal of allergy and clinical immunology*, 125(2 Suppl 2), pp.S3–23.
- Chattopadhyay, A., Tate, S.A., Beswick, R.W., Wagner, S.D, Ko Ferrigno, P. 2006. A peptide aptamer to antagonize BCL-6 function. *Oncogene*, 25(15), pp.2223–2233.
- Chen, J.D. & Evans, R.M., 1995. A transcriptional co-repressor that interacts with nuclear hormone receptors. *Nature*, 377(6548), pp.454–457.
- Chevallier, N., Corcoran, C.M., Lennon, C., Hyiek, E., Chadburn, A., Bardwell, V.J., Licht, J.D., Melnick, A. 2004. ETO protein of t(8;21) AML is a corepressor for Bcl-6 B-cell lymphoma oncoprotein. *Blood*, 103(4), pp.1454–1463.
- Coco, Lo, F., Ye, B.H., Lista, F., Corradini, P., Offit, K., Knowles, D.M., Chaganti, R.S., Dalla-Favera, R. 1994. Rearrangements of the BCL6 gene in diffuse large cell non-Hodgkin's lymphoma. *Blood*, 83(7), pp.1757–1759.
- Collaborative Computational Project, Number 4, 1994. The CCP4 suite: programs for protein crystallography. *Acta crystallographica. Section D, Biological*

*crystallography*, 50(Pt 5), pp.760–763.

- Craig, V.J., Arnold, I., Gerke, C., Huynh, M.Q., Wundisch, T., Neubauer, A., Renner, C., Falkow, S., Muller, A. 2010. Gastric MALT lymphoma B cells express polyreactive, somatically mutated immunoglobulins. *Blood*, 115(3), pp.581–591.
- Darnell, J.E., 2002. Transcription factors as targets for cancer therapy. *Nature Reviews Cancer*, 2(10), pp.740–749.
- De Ruijter, A.J.M., van Gennip, A.H., Caron, H.N., Kemp, S., van Kuilenburg, A.B. 2003. Histone deacetylases (HDACs): characterization of the classical HDAC family. *The Biochemical journal*, 370(Pt 3), pp.737–749.
- Dent, A.L., Shaffer, A.L., Yu, X., Allman, D., Staudt, L.M. 1997. Control of inflammation, cytokine expression, and germinal centre formation by BCL-6. *Science*, 276(5312), pp.589–592.
- Dent, A.L., Vasanwala, F.H. & Toney, L.M., 2002. Regulation of gene expression by the proto-oncogene BCL-6. *Critical reviews in oncology/hematology*, 41(1), pp.1–9.
- Dhordain, P., Albagli, O., Honore, N., Guidez, F., Lantoine, D., Schmid, M., The, H.D., Zelent, A., Koken, M.H. 2000. Colocalization and heteromerization between the two human oncogene POZ/zinc finger proteins, LAZ3 (BCL6) and PLZF. *Oncogene*, 19(54), pp.6240–6250.
- Dhordain, P., Albagli, O., Lin, R.J., Ansieau, S., Quief, S., Leutz, A., Kerckaert, J.P., Evans, R.M., Leprince, D. 1997. Corepressor SMRT binds the BTB/POZ repressing domain of the LAZ3/BCL6 oncoprotein. *Proceedings of the National Academy of Sciences*, 94(20), pp.10762–10767.
- Dhordain, P., Lin, R.J., Quief, S., Lantoine, D., Kerckaert, J.P., Evans, R.M., Albagli, O. 1998. The LAZ3(BCL-6) oncoprotein recruits a SMRT/mSIN3A/histone deacetylase containing complex to mediate transcriptional repression. *Nucleic Acids Research*, 26(20), pp.4645–4651.
- Duan, S., Cermak, L., Pagan, J.K., Rossi, M., Martinengo, C., di Celle, P.F., Chapuy, B., Shipp, M., Chiarle, R., Pagano, M. 2012. FBXO11 targets BCL6 for degradation and is inactivated in diffuse large B-cell lymphomas. *Nature*, 481(7379), pp.90–93.
- Duvic, M., Talpur, R., Ni, X., Zhang, C., Hazarika, P., Kelly, C., Chiao, J.H., Reilly, J.F., Ricker, J.L., Richon, V.M., Frankel, S.R. 2007. Phase 2 trial of oral vorinostat (suberoylanilide hydroxamic acid, SAHA) for refractory cutaneous T-cell lymphoma (CTCL). *Blood*, 109(1), pp.31–39.
- Emsley, P., Lohkamp, B., Scott, W.G., Cowtan, K. 2010. Features and development of Coot. *Acta crystallographica. Section D, Biological crystallography*, 66(Pt 4), pp.486–501.
- Evans, P. 2006. Scaling and assessment of data quality. *Acta crystallographica. Section D, Biological crystallography*, 62(Pt 1), pp.72–82.
- Evans, P.R., Murshudov, G.N., 2013. How good are my data and what is the resolution?

*Acta crystallographica. Section D, Biological crystallography*, 69(Pt 7), pp.1204–1214.

- Fernández, C., Wider, G. 2003. TROSY in NMR studies of the structure and function of large biological macromolecules. *Current opinion in structural biology*, 13(5), pp.570–580.
- Floss, H.G., Yu, T.W. 2005. Rifamycin-mode of action, resistance, and biosynthesis. *Chemical reviews*, 105(2), pp.621–632.
- Fujita, N., Jaye, D.L., Geigerman, C., Akyildiz, A., Mooney, M.R., Boss, J.M., Wade, P.A. 2004. MTA3 and the Mi-2/NuRD complex regulate cell fate during B lymphocyte differentiation. *Cell*, 119(1), pp.75–86.
- Fukuda, T., Yoshida, T., Okada, S., Hatano, M., Miki, T., Ishibashi, K., Okabe, S., Koseki, H., Hirosawa, S., Taniquchi, M., Miyasaka, N., Tokuhisa, T. 1997. Disruption of the Bcl6 gene results in an impaired germinal centre formation. *The Journal of experimental medicine*, 186(3), pp.439–448.
- Ghetu, A.F., Corcoran, C.M., Cerchietti, L., Bardwell, V.J., Melnick, A., Prive, G.G. 2008. Structure of a BCOR corepressor peptide in complex with the BCL6 BTB domain dimer. *Molecular cell*, 29(3), pp.384–391.
- Goodnow, C.C., Crosbie, J., Adelstein, S., Lavoie, T.B., Smith-Gill, S.J., Brink, R.A., Pritchard-Briscoe, H., Wotherspoon, J.S., Loblay, R.H., Raphael, K., Trent, R.J., Basten, A. 1988. Altered immunoglobulin expression and functional silencing of self-reactive B-lymphocytes in transgenic mice. *Nature*, 334(6184), pp.676–682.
- Gronenborn, A.M., Filpula, D.R., Essig, N.G., Achari, A., Whitlow, M., Wingfield, P.T., Clore, G.M. 1991. A novel, highly stable fold of the immunoglobulin binding domain of streptococcal protein G. *Science*, 253(5020), pp.657–661.
- Gu, W., Roeder, R.G., 1997. Activation of p53 sequence-specific DNA binding by acetylation of the p53 C-terminal domain. *Cell*, 90(4), pp.595–606.
- Gupta, S., Jiang, M., Anthony, A., Pernis, A.B. 1999. Lineage-specific modulation of interleukin 4 signaling by interferon regulatory factor 4. *The Journal of experimental medicine*, 190(12), pp.1837–1848.
- Harris, M.B., Chang, C.C., Berton, M.T., Danial, N.N., Zhang, J., Kuehner, D., Ye, B.H., Kvatyuk, M., Pandolfi, P.P., Cattoretti, G., Dalla-Favera, Rothman, P.B. 1999. Transcriptional repression of Stat6-dependent interleukin-4-induced genes by BCL-6: specific regulation of iepsilon transcription and immunoglobulin E switching. *Molecular and cellular biology*, 19(10), pp.7264–7275.
- HMRN - 2014, Incidence. Available at <http://www.hmrn.org> [Accessed September 12, 2014].
- Hörlein, A.J., Naar, A.M., Heinzl, T., Torchia, J., Gloss, B., Kurokawa, R., Ryan, A., Kamei, Y., Soderstrom, M., Glass, C.K., Rosenfeld, M.G. 1995. Ligand-independent repression by the thyroid hormone receptor mediated by a nuclear receptor co-repressor. *Nature*, 377(6548), pp.397–404.

- Huang, C., Gonzalez, D.G., Cote, C.M., Jiang, Y., Hatzi, K., Teater, M., Dai, K., Hla, T., Haberman, A.M., Malnick, A. 2014. The BCL6 RD2 Domain Governs Commitment of Activated B Cells to Form Germinal Centres. *Cell reports*.
- Huang, C., Hatzi, K., Melnick, A., 2013. Lineage-specific functions of Bcl-6 in immunity and inflammation are mediated by distinct biochemical mechanisms. *Nature immunology*, 14(4), pp.380–388.
- Huth, J.R., Bewley, C.A., Jackson, B.M., Hinnebusch, A.G., Clore, G.M., Gronenborn, A.M. 1997. Design of an expression system for detecting folded protein domains and mapping macromolecular interactions by NMR. *Protein science : a publication of the Protein Society*, 6(11), pp.2359–2364.
- Huynh, K.D., Bardwell, V.J., 1998. The BCL-6 POZ domain and other POZ domains interact with the co-repressors N-CoR and SMRT. *Oncogene*, 17(19), pp.2473–2484.
- Huynh, K.D., Fischle, W., Verdin, E., bardwell, V.J. 2000. BCoR, a novel corepressor involved in BCL-6 repression. *Genes & development*, 14(14), pp.1810–1823.
- Johnston, R.J., Poholek, A.C., DiToro, D., Yusef, I., Eto, D., Barnett, B., Dent, A.L., Craft, J., Crotty, S. 2009. Bcl6 and Blimp-1 Are Reciprocal and Antagonistic Regulators of T Follicular Helper Cell Differentiation. *Science (New York, NY)*, 325(5943), pp.1006–1010.
- Jones, I.C., Sharman, G.J., Pidgeon, J. 2005. <sup>1</sup>H and <sup>13</sup>C NMR data to aid the identification and quantification of residual solvents by NMR spectroscopy. *Magnetic resonance in chemistry : MRC*, 43(6), pp.497–509.
- Kelly, A.E., Ou, H.D., Withers, R., Dotsch, V. 2002. Low-conductivity buffers for high-sensitivity NMR measurements. *Journal of the American Chemical Society*, 124(40), pp.12013–12019.
- Kerckaert, J.P., Deweindt, C., Tilly, H., Quief, S., Lecocq, G., Bastard, C. 1993. LAZ3, a novel zinc-finger encoding gene, is disrupted by recurring chromosome 3q27 translocations in human lymphomas. *Nature genetics*, 5(1), pp.66–70.
- Klein, U., Dalla-Favera, R. 2008. Germinal centres: role in B-cell physiology and malignancy. *Nature reviews.Immunology*, 8(1), pp.22–33.
- Koehler, A.N. 2010. A complex task? Direct modulation of transcription factors with small molecules. *Current opinion in chemical biology*, 14(3), pp.331–340.
- Kortylewski, M., Kujawski, M., Wang, T., Wei, S., Zhang, S., Pilon-Thomas, S., Niu, G., Kay, H., Mule, J., Kerr, W.G., Jove, R., Pardoll, D., Yu, H. 2005. Inhibiting Stat3 signaling in the hematopoietic system elicits multicomponent antitumor immunity. *Nature medicine*, 11(12), pp.1314–1321.
- Krzysiek, R., Lefevre, E.A., Zou, W., Foussat, A., Bernard, J., Portier, A., Galanaud, P., Richard, Y. 1999. Antigen receptor engagement selectively induces macrophage inflammatory protein-1 alpha (MIP-1 alpha) and MIP-1 beta chemokine production in human B cells. *Journal of immunology (Baltimore, Md. : 1950)*, 162(8),

pp.4455–4463.

- Kunin, C.M., 1996. Antimicrobial Activity of Rifabutin. *Clinical Infectious Diseases*, 22(Supplement 1), pp.S3–S14.
- Kuppers, R., Zhao, M., Hansmann, M.L., Rajewsky, K. 1993. Tracing B cell development in human germinal centres by molecular analysis of single cells picked from histological sections. *The EMBO journal*, 12(13), pp.4955–4967.
- Kuppers, R., Klein, U., Hansmann, M.L., Rajewsky, K. 1999. Cellular origin of human B-cell lymphomas. *New England Journal of Medicine*, 341(20), pp.1520–1529.
- Küppers, R., 2005. Mechanisms of B-cell lymphoma pathogenesis. *Nature Reviews Cancer*, 5(4), pp.251–262.
- Legube, G., Trouche, D. 2003. Regulating histone acetyltransferases and deacetylases. *EMBO reports*, 4(10), pp.944–947.
- Lemercier, C., Brocard, M.P., Puvion-Dutilleul, F., Kao, H.Y., Albagli, O., Khochbin, S. 2002. Class II histone deacetylases are directly recruited by BCL6 transcriptional repressor. *The Journal of biological chemistry*, 277(24), pp.22045–22052.
- Leslie, A.G.W. 2006. The integration of macromolecular diffraction data. *Acta crystallographica. Section D, Biological crystallography*, 62(Pt 1), pp.48–57.
- Li, J., Wang, J., Wang, J., Nawaz, Z., Liu, J.M., Qin, J., Wong, J. 2000. Both corepressor proteins SMRT and N-CoR exist in large protein complexes containing HDAC3. *The EMBO journal*, 19(16), pp.4342–4350.
- Lin, R.J., Nagy, L., Inoue, S., Shao, W., Miller, W.H. Jr., Evans, R.M. 1998. Role of the histone deacetylase complex in acute promyelocytic leukaemia. *Nature*, 391(6669), pp.811–814.
- Liu, Y.J., Arpin, C., de Bouteiller, O., Guret, C., Banchereau, J., Martinez-Valdez, H., Lebecque, S. 1996. Sequential triggering of apoptosis, somatic mutation and isotype switch during germinal centre development. *Seminars in immunology*, 8(3), pp.169–177.
- Logarajah, S., Hunter, P., Kramen, M., Steele, D., Lakhani, S., Bobrow, L., Venkitaraman, A., Wagner, S. 2003. BCL-6 is expressed in breast cancer and prevents mammary epithelial differentiation. *Oncogene*, 22(36), pp.5572–5578.
- López-Cabrera, M., Munoz, E., Blazquez, M.V., Ursa, M.A., Santis, A.G., Sanchez-Madrid, F. 1995. Transcriptional regulation of the gene encoding the human C-type lectin leukocyte receptor AIM/CD69 and functional characterization of its tumor necrosis factor-alpha-responsive elements. *The Journal of biological chemistry*, 270(37), pp.21545–21551.
- MacLennan, I.C., 1994. Germinal centres. *Annual Review of Immunology*, 12, pp.117–139.
- Majmudar, C.Y., Mapp, A.K., 2005. Chemical approaches to transcriptional regulation.

*Current opinion in chemical biology*, 9(5), pp.467–474.

- Markiewski, M.M., Lambris, J.D., 2007. The role of complement in inflammatory diseases from behind the scenes into the spotlight. *The American journal of pathology*, 171(3), pp.715–727.
- Marks, P.A., Breslow, R., 2007. Dimethyl sulfoxide to vorinostat: development of this histone deacetylase inhibitor as an anticancer drug. *Nature biotechnology*, 25(1), pp.84–90.
- Masclé, X., Albagli, O., Lermercier, C. 2003. Point mutations in BCL6 DNA-binding domain reveal distinct roles for the six zinc fingers. *Biochemical and biophysical research communications*, 300(2), pp.391–396.
- McCoy, A.J., Grosse-Kunstleve, R.W., Adams, P.D., Winn, M.D., Storoni, L.C., Read, R.J. 2007. Phaser crystallographic software. *Journal of applied crystallography*, 40(Pt 4), pp.658–674.
- Mendez, L.M., Polo, J.M., Yu, J.J., Krupski, M., Ding, B.B., melnick, A., Ye, B.H. 2008. CtBP is an essential corepressor for BCL6 autoregulation. *Molecular and cellular biology*, 28(7), pp.2175–2186.
- Murshudov, G.N., Skubak, P., Lebedev, A.A., Pannu, N.S., Steiner, R.A., Nicholls, R.A., Winn, M.D., Long, F., Vagin, A.A. 2011. REFMAC5 for the refinement of macromolecular crystal structures. *Acta crystallographica. Section D, Biological crystallography*, 67(Pt 4), pp.355–367.
- Niu, H., Ye, B.H., Dalla-Favera, R., 1998. Antigen receptor signaling induces MAP kinase-mediated phosphorylation and degradation of the BCL-6 transcription factor. *Genes & development*, 12(13), pp.1953–1961.
- Nurieva, R.I., Chung, Y., Martinez, G.J., Yang, X.O., Tanaka, S., Matskevitch, T.D., Wang, Y.E., Dong, C. 2009. Bcl6 mediates the development of T follicular helper cells. *Science*, 325(5943), pp.1001–1005.
- Oberoi, J., Fairall, L., Watson, P.J., Yang, J.C., Czimmerer, Z., Kampmann, T., Goult, B.T., Greenwood, J.A., Goosh, J.T., Kallenberger, B.C., Nagy, L., Neuhaus, D., Schwabe, J.W. 2011. Structural basis for the assembly of the SMRT/NCOR core transcriptional repression machinery. *Nature structural & molecular biology*, 18(2), pp.177–184.
- Offit, K., Jhanwar, S., Ebrahim, S.A., Filippa, D., Clarkson, B.D., Chaganti, R.S. 1989. t(3;22)(q27;q11): a novel translocation associated with diffuse non-Hodgkin's lymphoma. *Blood*, 74(6), pp.1876–1879.
- Papadopoulou, V., Postigo, A., Sanchez-Tillo, E., Porter, A.C., Wagner, S.D. 2010. ZEB1 and CtBP form a repressive complex at a distal promoter element of the BCL6 locus. *The Biochemical journal*, 427(3), pp.541–550.
- Parekh, S., Polo, J.M., Shaknovich, R., Juszczynski, P., Lev, P., Ranuncolo, S.M., Yin, Y., Klein, U., Cattoretti, G., Dalla-Favera, R., Shipp, M.A., Melnick, A. 2007. BCL6 programs lymphoma cells for survival and differentiation through distinct

biochemical mechanisms. *Blood*, 110(6), pp.2067–2074.

- Pasqualucci, L., Dominguez-Sola, D., Chiarenza, A., Fabbri, G., Grunn, A., Trifonov, V., Kasper, L.H., Lerach, S., Tang, H., Ma, J., Rossi, D., Chadburn, A., Murty, V.V., Mullighan, C.G., Gaidano, G., Rabadan, R., Brindle, P.K., Dalla-Favera, R. 2011. Inactivating mutations of acetyltransferase genes in B-cell lymphoma. *Nature*, 471(7337), pp.189–195.
- Pasqualucci, L., Migliazza, A., Basso, K., Houldsworth, J., Chaganti, R.S., Dalla-Favera, R. 2003. Mutations of the BCL6 proto-oncogene disrupt its negative autoregulation in diffuse large B-cell lymphoma. *Blood*, 101(8), pp.2914–2923.
- Perez-Torrado, R., Yamada, D., Defossez, P.A. 2006. Born to bind: the BTB protein-protein interaction domain. *BioEssays : news and reviews in molecular, cellular and developmental biology*, 28(12), pp.1194–1202.
- Pervushin, K., Riek, R., Wider, G., Wuthrich, K. 1997. Attenuated T2 relaxation by mutual cancellation of dipole-dipole coupling and chemical shift anisotropy indicates an avenue to NMR structures of very large biological macromolecules in solution. *Proceedings of the National Academy of Sciences*, 94(23), pp.12366–12371.
- Phan, R.T., Dalla-Favera, R. 2004. The BCL6 proto-oncogene suppresses p53 expression in germinal-centre B cells. *Nature*, 432(7017), pp.635–639.
- Phan, R.T., Saito, M., Basso, K., Niu, H., Dalla-favera, R. 2005. BCL6 interacts with the transcription factor Miz-1 to suppress the cyclin-dependent kinase inhibitor p21 and cell cycle arrest in germinal centre B cells. *Nature immunology*, 6(10), pp.1054–1060.
- Polo, J.M., Dell'Oso, T., Ranuncolo, S.M., Cerchiatti, L., Beck, D., Da Silva, G.F., Prive, G.G., Licht, J.D., Melnick, A. 2004. Specific peptide interference reveals BCL6 transcriptional and oncogenic mechanisms in B-cell lymphoma cells. *Nature medicine*, 10(12), pp.1329–1335.
- Polo, J.M., Juszczynski, P., Monti, S., Cerchiatti, L., Ye, K., Grealley, J.M., Shipp, M., Melnick, A. 2007. Transcriptional signature with differential expression of BCL6 target genes accurately identifies BCL6-dependent diffuse large B cell lymphomas. *Proceedings of the National Academy of Sciences*, 104(9), pp.3207–3212.
- Privé, G.G., Melnick, A. 2006. Specific peptides for the therapeutic targeting of oncogenes. *Current opinion in genetics & development*, 16(1), pp.71–77.
- Raghunathan, K., Harris, P.T., Arvidson, D.N. 2010. Trial by fire: are the crystals macromolecules? *Acta crystallographica. Section F, Structural biology and crystallization communications*, 66(Pt 5), pp.615–620.
- Ranuncolo, S.M., Polo, J.M., Dierov, J., Singer, M., Kuo, T., Grealley, J., Green, R., Carroll, M., Melnick, A. 2007. Bcl-6 mediates the germinal centre B cell phenotype and lymphomagenesis through transcriptional repression of the DNA-damage sensor ATR. *Nature immunology*, 8(7), pp.705–714.

- Ranuncolo, S.M., Polo, J.M., Melnick, A., 2008. BCL6 represses CHEK1 and suppresses DNA damage pathways in normal and malignant B-cells. *Blood cells, molecules & diseases*, 41(1), pp.95–99.
- Redell, M.S., Tweardy, D.J., 2006. Targeting transcription factors in cancer: Challenges and evolving strategies. *Drug Discovery Today: Technologies*, 3(3), pp.261–267.
- Reljic, R., Wagner, S.D., Peakman, L.J., Fearon, D.T. 2000. Suppression of signal transducer and activator of transcription 3-dependent B lymphocyte terminal differentiation by BCL-6. *The Journal of experimental medicine*, 192(12), pp.1841–1848.
- Riva, S., Silvestri, L.G., 1972. Rifamycins: a general view. *Annual review of microbiology*, 26, pp.199–224.
- Saito, M., Gao, J., Basso, K., Kitagawa, Y., Smith, P.M., Bhagat, G., Pernis, A., Pasqualucci, L., Dalla-Favera, R. 2007. A signaling pathway mediating downregulation of BCL6 in germinal centre B cells is blocked by BCL6 gene alterations in B cell lymphoma. *Cancer Cell*, 12(3), pp.280–292.
- Savage, K.J., Monti, S., Kutok, J.L., Cattoretti, G., Neuberg, D., De Leval, L., Kurtin, P., Dal Cin, P., Ladd, C., Feuerhake, F., Aquiar, R.C., Li, S., Salles, G., Berger, F., Jing, W., Pinkus, G.S., Habermann, T., Dalla-Favera, Harris, n.L., Aster, J.C., Golub, T.R., Shipp, M.A. 2003. The molecular signature of mediastinal large B-cell lymphoma differs from that of other diffuse large B-cell lymphomas and shares features with classical Hodgkin lymphoma. *Blood*, 102(12), pp.3871–3879.
- Schindler, C., Darnell, J.E. 1995. Transcriptional responses to polypeptide ligands: the JAK-STAT pathway. *Annual review of biochemistry*, 64, pp.621–651.
- Seyfert, V.L., Allman, D., He, Y., Staudt, L.M. 1996. Transcriptional repression by the proto-oncogene BCL-6. *Oncogene*, 12(11), pp.2331–2342.
- Shaffer, A.L., Yu, X., He, Y., Boldrick, J., Chan, E.P., Staudt, L.M. 2000. BCL-6 represses genes that function in lymphocyte differentiation, inflammation, and cell cycle control. *Immunity*, 13(2), pp.199–212.
- Shankland, K.R., Armitage, J.O., Hancock, B.W., 2012. Non-Hodgkin lymphoma. *Lancet*, 380(9844), pp.848–857.
- Sjöberg, A.P., Trouw, L.A., Blom, A.M., 2009. Complement activation and inhibition: a delicate balance. *Trends in immunology*, 30(2), pp.83–90.
- Solvason, N., Wu, W.W., Kabra, N., Wu, X., Lees, E., Howard, M.C. 1996. Induction of cell cycle regulatory proteins in anti-immunoglobulin-stimulated mature B lymphocytes. *The Journal of experimental medicine*, 184(2), pp.407–417.
- Sommer, L.A.M., Meier, M.A., Dames, S.A., 2012. A fast and simple method for probing the interaction of peptides and proteins with lipids and membrane-mimetics using GB1 fusion proteins and NMR spectroscopy. *Protein Science*, 21(10), pp.1566–1570.

- Spanogiannopoulos, P., Waglechner, N., Koteva, K., Wright, G.D. 2014. A rifamycin inactivating phosphotransferase family shared by environmental and pathogenic bacteria. *Proceedings of the National Academy of Sciences of the United States of America*, 111(19), pp.7102–7107.
- Stadler, L.K.J., Hoffman, T., Tomlinson, D.C., Song, Q., Lee, T., Busby, M., Nyathi, Y., Gendra, E., Tiede, C., Flanagan, K., Cockell, S.J., Wipat, A., Harwood, C., Wagner, S.D., Knowles, M.A., Davis, J.J., Keegan, N., Ferrigno, P.K. 2011. Structure-function studies of an engineered scaffold protein derived from Stefin A. II: Development and applications of the SQT variant. *Protein engineering, design & selection : PEDS*, 24(9), pp.751–763.
- Stadler, L.K.J., Tomlinson, D.C., Lee, T., Knowles, M.A., Ko Ferrigno, P. 2014. The use of a neutral peptide aptamer scaffold to anchor BH3 peptides constitutes a viable approach to studying their function. *Cell death & disease*, 5, p.e1037.
- Stead, M.A., Rosbrook, G.O., Hadden, J.M., Trinh, C.H., Carr, S.B., Wright, S.C. 2008a. Structure of the wild-type human BCL6 POZ domain. *Acta crystallographica. Section F, Structural biology and crystallization communications*, 64(Pt 12), pp.1101–1104.
- Stogios, P.J., Downs, G.S., Jauhal, J.J., Nandra, S.K., Prive, G.G. 2005. Sequence and structural analysis of BTB domain proteins. *Genome biology*, 6(10), R82.
- Stogios, P.J., Chen, L., Prive, G.G., 2006. Crystal structure of the BTB domain from the LRF/ZBTB7 transcriptional regulator. *Protein Science*, 16(2), pp.336–342.
- Toney, L.M., Cattoretti, G., Graf, J.A., Merghoub, T., Pandolfi, P.P., Dalla-favera, R., Ye, B.H., Dent, A.L. 2000. BCL-6 regulates chemokine gene transcription in macrophages. *Nature immunology*, 1(3), pp.214–220.
- Tunyaplin, C., Shaffer, A.L., Angelin-Duclos, C.D., Yu, X., Staudt, L.M., Calame, K.L. 2004. Direct Repression of *prdm1* by Bcl-6 Inhibits Plasmacytic Differentiation. *The Journal of Immunology*, 173(2), pp.1158–1165
- Turkson, J., Zhang, S., Palmer, J., Kay, H., Stanko, J., Mora, L.B., Sebt, S., Yu, H., Jove, R. 2004. Inhibition of constitutive signal transducer and activator of transcription 3 activation by novel platinum complexes with potent antitumor activity. *Molecular cancer therapeutics*, 3(12), pp.1533–1542.
- Villa, R., Morey, L., Raker, V.A., Buschbeck, M., Gutierrez, A., De Santis, F., Corsaro, M., Varas, F., Bossi, D., Minucci, S., Pelicci, P.G., Di Croce, L. 2006. The methyl-CpG binding protein MBD1 is required for PML-RAR $\alpha$  function. *Proceedings of the National Academy of Sciences*, 103(5), pp.1400–1405.
- Villagra, A., Sotomayor, E.M., Seto, E., 2010. Histone deacetylases and the immunological network: implications in cancer and inflammation. *Oncogene*, 29(2), pp.157–173.
- Vranken, W.F., Boucher, W., Stevens, T.J., Fogh, R.H., Pajon, A., Llinas, M., Ulrich, E.L., Markley, J.L., Ionides, J., Laue, E.D. 2005. The CCPN data model for NMR spectroscopy: development of a software pipeline. *Proteins*, 59(4), pp.687–696.

- Walker, S.R., Liu, S., Xiang, M., Nicolais, M., Hatzi, K., Giannopoulou, E., Elemento, O., Cerchietti, L., Melnick, A., Frank, D.A. 2014. The transcriptional modulator BCL6 as a molecular target for breast cancer therapy. *Oncogene*.
- Walker, S.R., Nelson, E.A., Frank, D.A., 2007. STAT5 represses BCL6 expression by binding to a regulatory region frequently mutated in lymphomas. *Oncogene*, 26(2), pp.224–233.
- Wallace, A.C., Laskowski, R.A., Thornton, J.M., 1995. LIGPLOT: a program to generate schematic diagrams of protein-ligand interactions. *Protein engineering*, 8(2), pp.127–134.
- Wang, X., Li, Z., Naganuma, A., Ye, B.H. 2002. Negative autoregulation of BCL-6 is bypassed by genetic alterations in diffuse large B cell lymphomas. *Proceedings of the National Academy of Sciences*, 99(23), pp.15018–15023.
- Watson, P.J., Fairall, L., Schwabe, J. 2012. Nuclear hormone receptor co-repressors: Structure and function. *Molecular and cellular endocrinology*.
- Wehrli, W., Staehelin, M. 1971. Actions of the rifamycins. *Bacteriological reviews*, 35(3), pp.290–309.
- White, R.J., Martinelli, E., Lancini, G. 1974. Ansamycin biogenesis: studies on a novel rifamycin isolated from a mutant strain of *Nocardia mediterranei*. *Proceedings of the National Academy of Sciences*, 71(8), pp.3260–3264.
- Wider, G. 2005. NMR techniques used with very large biological macromolecules in solution. *Methods in enzymology*, 394, pp.382–398.
- Wolffe, A.P. 1994. Transcription: in tune with the histones. *Cell*, 77(1), pp.13–16.
- Wong, C.W., Privalsky, M.L. 1998. Components of the SMRT corepressor complex exhibit distinctive interactions with the POZ domain oncoproteins PLZF, PLZF-RARalpha, and BCL-6. *The Journal of biological chemistry*, 273(42), pp.27695–27702.
- Ye, B.H., Chaganti, S., Chang, C.C., Niu, H., Corradini, P., Chaganti, R.S., Dalla-Favera, R. 1995. Chromosomal translocations cause deregulated BCL6 expression by promoter substitution in B cell lymphoma. *The EMBO journal*, 14(24), pp.6209–6217.
- Ye, B.H., Cattoretti, G., Shen, Q., Zhang, J., Hawe, N., de Waard, R., Leung, C., Nouri-Shirazi, M., Orazi, A., Chaganti, R.S., Rothman, P., Stall, A.M., Pandolfi, P.P., Dalla-Favera, R. 1997. The BCL-6 proto-oncogene controls germinal-centre formation and Th2-type inflammation. *Nature genetics*, 16(2), pp.161–170.
- Ye, B.H., Lista, F., Lo Coco, F., Knowles, D.M., Offit, K., Chaganti, R.S., Dalla-Favera, R. 1993a. Alterations of a zinc finger-encoding gene, BCL-6, in diffuse large-cell lymphoma. *Science*, 262(5134), pp.747–750.
- Ye, B.H., Rao, P.H., Chaganti, R.S., Dalla-Favera, R. 1993b. Cloning of bcl-6, the locus involved in chromosome translocations affecting band 3q27 in B-cell lymphoma.

*Cancer research*, 53(12), pp.2732–2735.

Zhang, Jing., Zhong, Q. 2014. Histone deacetylase inhibitors and cell death. *Cellular and molecular life sciences : CMLS*, 71(20), pp.3885–3901.

Zhang, J., Kalkum, M., Chait, B.T., Roeder, R.G. 2002. The N-CoR-HDAC3 nuclear receptor corepressor complex inhibits the JNK pathway through the integral subunit GPS2. *Molecular cell*, 9(3), pp.611–623.

Zollman, S., Godt, D., Prive, G.g., Couderc, J.L., Iaski, F.A. 1994. The BTB domain, found primarily in zinc finger proteins, defines an evolutionarily conserved family that includes several developmentally regulated genes in *Drosophila*. *Proceedings of the National Academy of Sciences*, 91(22), pp.10717–10721.